Appendix A.16:

Hunt Ln – CPT 4674

Table 1: Site Description for Hunt Lane (CPT 4674 – CC LIQ 12).

Attribute	Yes/No			Description/Date	Symbol in Figure 1
	10-m Buffer	20-m Buffer	50-m Buffer		
Near a body of surface water or other free face features?	No	No	No	The site is situated to the S of the Avon River; its center is 184 m away from the nearest free-face feature, which is ~1.5 m high and oriented in the E-W direction.	NA
Lateral spreading observed during the CES?	No	No	No	Lateral spreading was not observed by the mapping team.[1]	NA
Nearby buildings or structures?	Yes	Yes	Yes	Building coverage of the 10-m, 20-m, and 50-m buffers is 29%, 27%, and 37%, respectively. Buildings are in the NE, NW, and SW quadrants of the 10-m buffer and in all quadrants of the 20-m and 50-m buffers.	White Fill + Brown Outline
Sloping land?	No	No	No	Flat land, residential area.	NA
Step changes in the ground surface?	No	No	No	NA	NA
Retaining walls?	No	No	No	NA	NA
Vegetation?	Yes	Yes	Yes	Trees and bushes cover 9% of the 10-m buffer, 21% of the 20-m buffer and 29% of the 50-m buffer. They are in all quadrants of the three buffers.	White Fill + Green Outline
Anthropogenic changes to the site between the LiDAR surveys?	No	No	No	Removal of five buildings outside of the NW and SE quadrants of the 50-m buffer between Dec 2012 and Feb 2014. One building was built at the same SE property by Aug 2014. Two buildings outside of the E and NW portions of the 50-m buffer were removed between Aug 2014 and Sep 2015. Two new buildings were added at these properties by Feb 2016. Earthwork was performed in the SW quadrant of the 20- and 50-m buffers between Feb 2014 and Aug 2014.	Building Removal from 2012 to 2015: Orange Crossline
Other important factors?	Yes	Yes	Yes	Low-motor-vehicle-volume roadway occupies 19% of the 10-m buffer and 18% of the 20-m buffer, affecting the E half of the 10-m buffer and the NE, SE, and SW quadrants of the 20-m buffer. The 50-m buffer is affected by this roadway and low-motor-vehicle-volume driveway that altogether occupy 5% of its area, affecting all its quadrants. Trampoline is in the SW portion of the 50-m buffer.	Road: Gray Fill + Red Outline; Driveway: White Fill + Gray Outline; Trampoline: White Fill + Purple Outline

Note: Buffer is the area within a circle of a specified radius with CPT investigations done at its center (172.692150°, -43.503948°).

[1] Canterbury Geotechnical Database. (2012). "Observed Ground Crack Locations", Map Layer CGD0400 - 23 July 2012, retrieved July 09, 2018 from https://canterburygeotechnicaldatabase.projectorbit.com/

Figure 1: Site plan with areas where LiDAR survey data is considered.

Note 1: Three patches (outlined in red) in the free field were initially selected for settlement assessment as areas free of vegetation and structures. Further analyses such as proximity of a patch to a CPT, proximity of a patch to a property subjected to addition and/or demolition of a structure, front yard/backyard alterations (e.g., ploughing, rubble, scrap), aerial distribution of sediment ejecta, and density of LiDAR points for 2003 resulted in Patches A and B being selected for detailed settlement assessment and the third patch being discarded in detailed settlement assessment. In addition, since significant amounts of ejecta were observed on roads in the CES, the entire portion of the road within the 50-m buffer was considered for settlement assessment. Roads as hard, relatively flat surfaces provide many ground-classified points. Therefore, it is very useful to compare settlement estimates on roads with settlement estimates for the unpaved patches.

Table 2: LiDAR flight error adjustments, global adjustments for the difference between average LiDAR point elevations and benchmark survey elevations, and vertical tectonic movement adjustments.

	Adjustments (mm)		
Earthquake Event(s)	LiDAR Flight Error	Global Offset[2]	Tectonic Vertical Movement
Sep-10	0	-3	0
Feb-11	0	16	-40
Jun-11	0	38	-45
Dec-11	0	-65	3
CES	0	-14	-82
Post Sep 2010 LiDAR survey affected by ejecta?*			Yes

Notes: The negative sign indicates the subtraction from the ground surface subsidence, while the positive sign indicates the addition to the ground surface subsidence; * indicates the presence of the blind sand boil within Patch B at the time of all post Feb-11 LiDAR surveys but Oct-15 LiDAR survey hence requires the addition of 20-mm ground surface subsidence for the Feb-11 EQ and the CES for Patch B.

Table 3a: LiDAR Measurement Error for Patch A.

Surveys	Buffer	Area Averaged Difference Indicating Repeat Measurement Error (mm)	$\sigma^*_{\text{individual LiDAR points}}$ (mm)	%Reduction in σ due to Area Averaging of LiDAR Points
Post Feb 2011: Mar 2011 and May 2011	10-m	58	59	[98,98]
	20-m	58		
	50-m	58		
Post Dec 2011: Feb 2012 and Oct 2015	10-m	5	70	[7,7]
	20-m	5		
	50-m	5		

*Standard deviation.

[2] Russell, J., & van Ballegooy, S. (2015). *Canterbury Earthquake Sequence: Increased liquefaction vulnerability assessment methodology*. New Zealand: Tonkin & Taylor Ltd.

Table 3b: LiDAR Measurement Error for Patch B.

Surveys	Buffer	Area Averaged Difference Indicating Repeat Measurement Error (mm)	$\sigma^*_{individual\ LiDAR\ points}$ (mm)	%Reduction in σ due to Area Averaging of LiDAR Points
Post Feb 2011: Mar 2011 and May 2011	10-m	NA	59	[107,107]
	20-m	63		
	50-m	63		
Post Dec 2011: Feb 2012 and Oct 2015	10-m	NA	70	[NA,NA]
	20-m	NA		
	50-m	NA		

*Standard deviation; Oct-2015 LiDAR survey was not considered due to the earthwork that was done between Feb 2014 and Aug 2014 within Patch B.

Table 3c: LiDAR Measurement Error for Road.

Surveys	Buffer	Area Averaged Difference Indicating Repeat Measurement Error (mm)	$\sigma^*_{individual\ LiDAR\ points}$ (mm)	%Reduction in σ due to Area Averaging of LiDAR Points
Post Feb 2011: Mar 2011 and May 2011	10-m	54	59	[85,92]
	20-m	50		
	50-m	49		
Post Dec 2011: Feb 2012 and Oct 2015	10-m	30	70	[43,50]
	20-m	35		
	50-m	35		

*Standard deviation.

Table 4a: Ground surface subsidence adjustments for Patch A due to LiDAR measurement error.

Earthquake Event(s)	$\sigma_{pre\text{-}EQ\ LiDAR\ survey}$ (mm)	$\sigma_{post\text{-}EQ\ LiDAR\ survey}$ (mm)	σ_{total} (mm)	Area Average Adjusted σ (mm)**
Sep-10	158	56	134	±132
Feb-11	56	59	59	±58
Jun-11	59	61	62	±61
Dec-11	61	70	87	±85
CES	158	70	124	±122

**Based on the highest %Reduction in Table 3a.

Table 4b: Ground surface subsidence adjustments for Patch B due to LiDAR measurement error.

Earthquake Event(s)	$\sigma_{\text{pre-EQ LiDAR survey}}$ (mm)	$\sigma_{\text{post-EQ LiDAR survey}}$ (mm)	σ_{total} (mm)	Area Average Adjusted σ (mm)**
Sep-10	158	56	134	±143
Feb-11	56	59	59	±63
Jun-11	59	61	62	±66
Dec-11	61	70	87	±92
CES	158	70	124	±133

**Based on the highest %Reduction in Table 3b.

Table 4c: Ground surface subsidence adjustments for Road due to LiDAR measurement error.

Earthquake Event(s)	$\sigma_{\text{pre-EQ LiDAR survey}}$ (mm)	$\sigma_{\text{post-EQ LiDAR survey}}$ (mm)	σ_{total} (mm)	Area Average Adjusted σ (mm)**
Sep-10	158	56	134	±123
Feb-11	56	59	59	±54
Jun-11	59	61	62	±57
Dec-11	61	70	87	±79
CES	158	70	124	±114

**Based on the highest %Reduction in Table 3c.

Table 5a: Raw liquefaction-related ground surface subsidence for Patch A using original LiDAR points.

	Average Ground Surface Subsidence (mm)		
Earthquake Event(s)	10-m Buffer	20-m Buffer	50-m Buffer
Sep-10	126	126	126
Feb-11	168	168	168
Jun-11	102	102	102
Dec-11	70	70	70
CES	466	466	466

Table 5b: Raw liquefaction-related ground surface subsidence for Patch B using original LiDAR points.

	Average Ground Surface Subsidence (mm)		
Earthquake Event(s)	10-m Buffer	20-m Buffer	50-m Buffer
Sep-10	NA	12	12
Feb-11	NA	150	150
Jun-11	NA	90	90
Dec-11	NA	62	62
CES	NA	314	314

Table 5c: Raw liquefaction-related ground surface subsidence for Road using original LiDAR points.

	Average Ground Surface Subsidence (mm)		
Earthquake Event(s)	10-m Buffer	20-m Buffer	50-m Buffer
Sep-10	9	68	34
Feb-11	98	120	142
Jun-11	92	106	111
Dec-11	45	40	37
CES	244	334	324

Table 6a: Corrected liquefaction-related ground surface subsidence for Patch A using original LiDAR points with the calculated adjustments in Table 2.

	Average Calculated Ground Surface Subsidence (mm)		
Earthquake Event(s)	10-m Buffer	20-m Buffer	50-m Buffer
Sep-10	123±125	123±125	123±125
Feb-11	144±50	144±50	144±50
Jun-11	95±50	95±50	95±50
Dec-11	8±75	8±75	8±75
CES	370±125	370±125	370±125

Notes: Plus/minus values are same as those in Table 4a, but rounded to the nearest 25; Positive overall values indicate ground surface subsidence, while negative overall values indicate ground surface uplift.

Table 6b: Corrected liquefaction-related ground surface subsidence for Patch B using original LiDAR points with the calculated adjustments in Table 2.

	Average Calculated Ground Surface Subsidence (mm)		
Earthquake Event(s)	10-m Buffer	20-m Buffer	50-m Buffer
Sep-10	NA	9±150	9±150
Feb-11	NA	146±75	146±75
Jun-11	NA	83±75	83±75
Dec-11	NA	0±100	0±100
CES	NA	237±125	237±125

Notes: Plus/minus values are same as those in Table 4b, but rounded to the nearest 25; Positive overall values indicate ground surface subsidence, while negative overall values indicate ground surface uplift.

Table 6c: Corrected liquefaction-related ground surface subsidence for Road using original LiDAR points with the calculated adjustments in Table 2.

	Average Calculated Ground Surface Subsidence (mm)		
Earthquake Event(s)	10-m Buffer	20-m Buffer	50-m Buffer
Sep-10	6±125	65±125	31±125
Feb-11	74±50	96±50	118±50
Jun-11	85±50	99±50	104±50
Dec-11	-17±75	-22±75	-26±75
CES	148±125	239±125	227±125

Notes: Plus/minus values are same as those in Table 4c, but rounded to the nearest 25; Positive overall values indicate ground surface subsidence, while negative overall values indicate ground surface uplift.

Table 7a: Corrected liquefaction-related ground surface subsidence for Patch A using LiDAR DEMs.

	Estimated Ground Surface Subsidence (mm)								
	10-m Buffer			20-m Buffer			50-m Buffer		
Earthquake Event(s)	16th %ile	50th %ile	84th %ile	16th %ile	50th %ile	84th %ile	16th %ile	50th %ile	84th %ile
Sep-10	50	100	100	50	100	100	50	100	100
Feb-11	150	150	150	150	150	150	150	150	150
Jun-11	50	50	100	50	50	100	50	50	100
Dec-11	100	100	100	100	100	100	100	100	100
CES	400	450	450	400	450	450	400	450	450

Note: These percentiles are not the exact statistical measures; they indicate the spatial variability of ground surface subsidence.

Table 7b: Corrected liquefaction-related ground surface subsidence for Patch B using LiDAR DEMs.

	Estimated Ground Surface Subsidence (mm)								
	10-m Buffer			20-m Buffer			50-m Buffer		
Earthquake Event(s)	16th %ile	50th %ile	84th %ile	16th %ile	50th %ile	84th %ile	16th %ile	50th %ile	84th %ile
Sep-10	NA	NA	NA	50	50	100	50	50	100
Feb-11	NA	NA	NA	100	150	150	100	150	150
Jun-11	NA	NA	NA	50	50	50	50	50	50
Dec-11	NA	NA	NA	50	100	150	50	100	150
CES	NA	NA	NA	350	350	400	350	350	400

Note: These percentiles are not the exact statistical measures; they indicate the spatial variability of ground surface subsidence.

Table 7c: Corrected liquefaction-related ground surface subsidence for PFY using LiDAR DEMs.

	Estimated Ground Surface Subsidence (mm)								
	10-m Buffer			20-m Buffer			50-m Buffer		
Earthquake Event(s)	16th %ile	50th %ile	84th %ile	16th %ile	50th %ile	84th %ile	16th %ile	50th %ile	84th %ile
Sep-10	50	50	100	50	50	100	50	50	100
Feb-11	100	100	150	100	100	250	100	150	250
Jun-11	50	50	50	50	50	50	50	50	50
Dec-11	50	50	50	50	50	50	50	50	150
CES	350	350	350	350	350	450	350	350	500

Note: These percentiles are not the exact statistical measures; they indicate the spatial variability of ground surface subsidence.

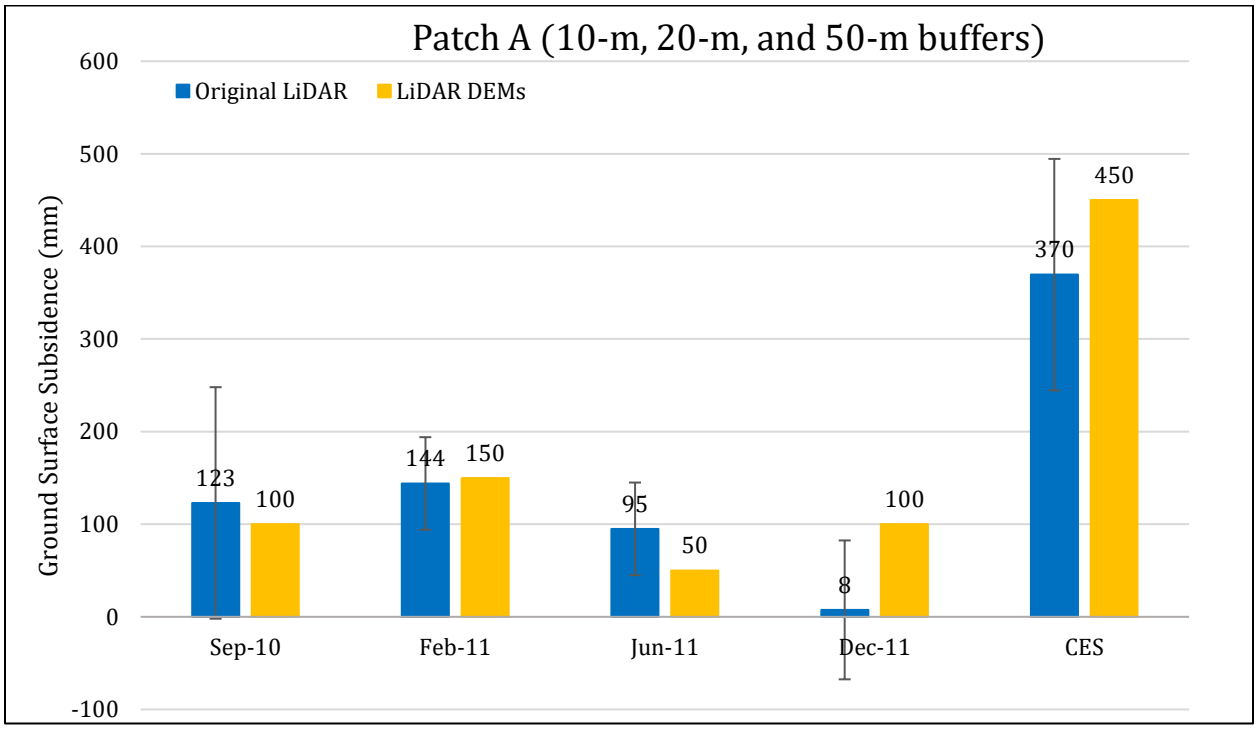

Figure 2: Comparison between ground surface subsidence determined from original LiDAR survey points and ground surface subsidence (50th %ile) estimated using LiDAR DEMs for Patch A.

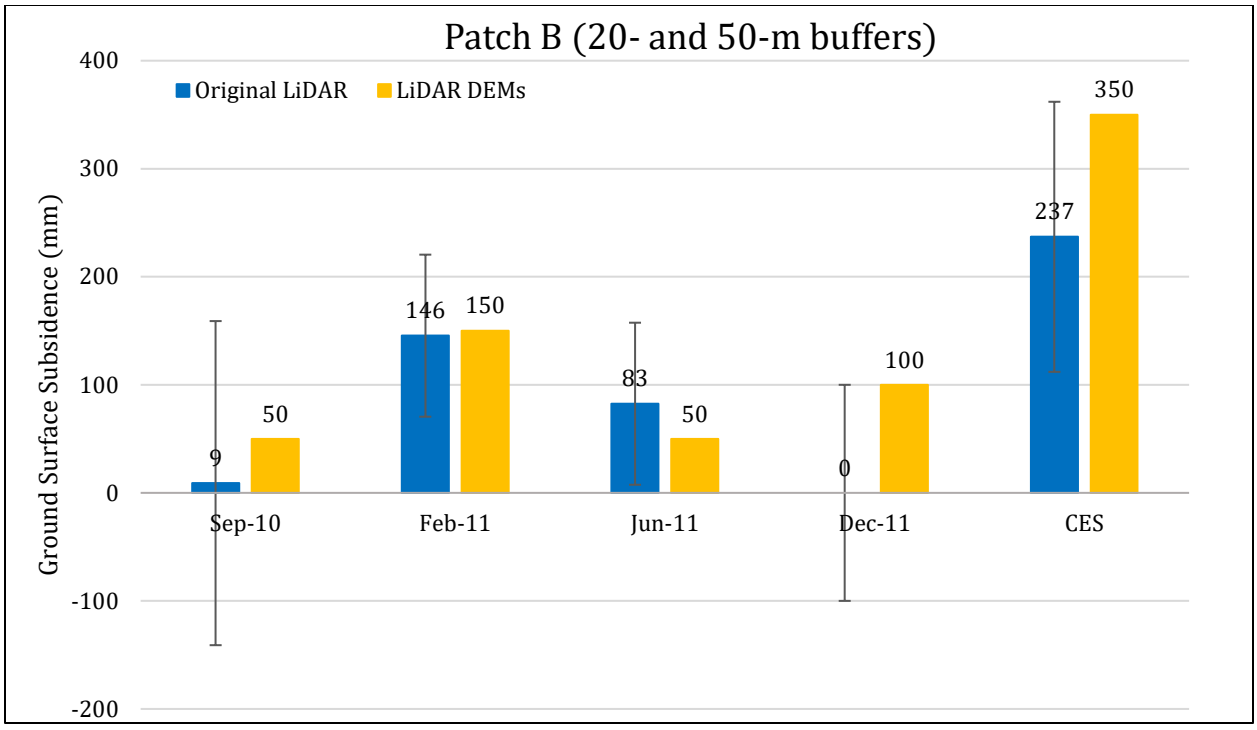

Figure 3: Comparison between ground surface subsidence determined from original LiDAR survey points and ground surface subsidence (50th %ile) estimated using LiDAR DEMs for Patch B.

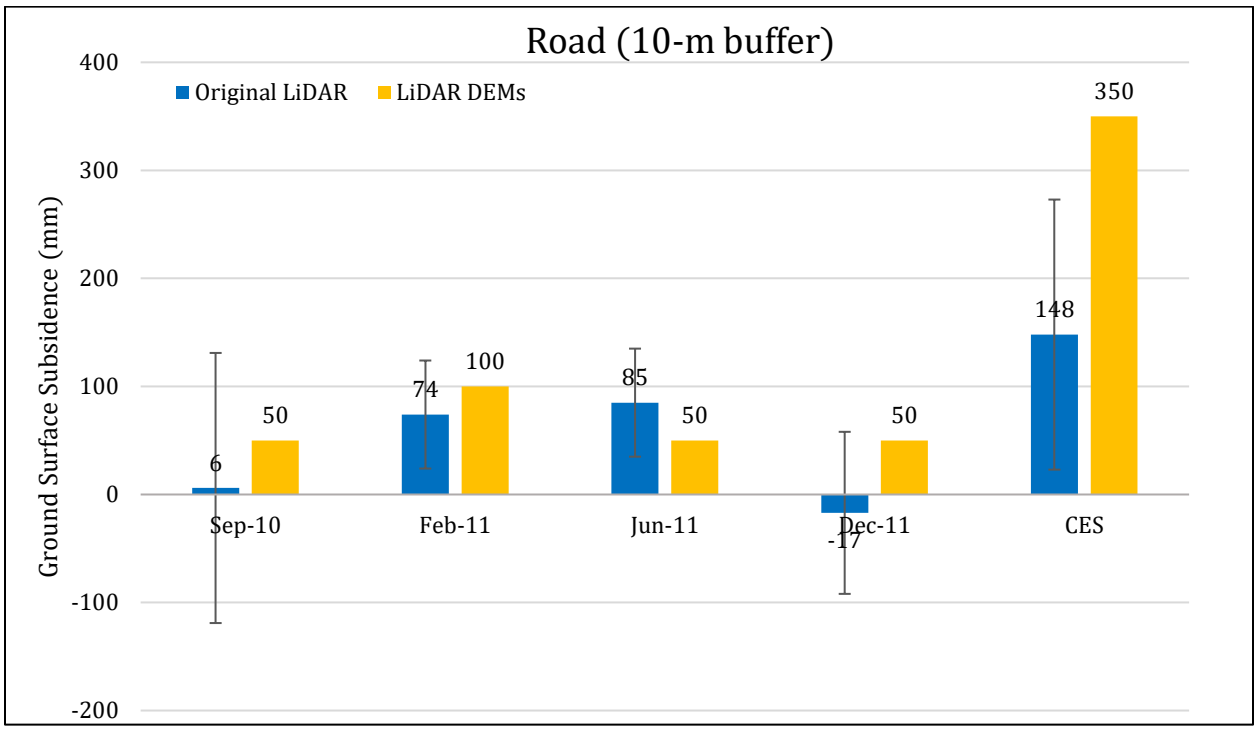

Figure 4: Comparison between ground surface subsidence determined from original LiDAR survey points and ground surface subsidence (50th %ile) estimated using LiDAR DEMs for Road for the 10-m buffer.

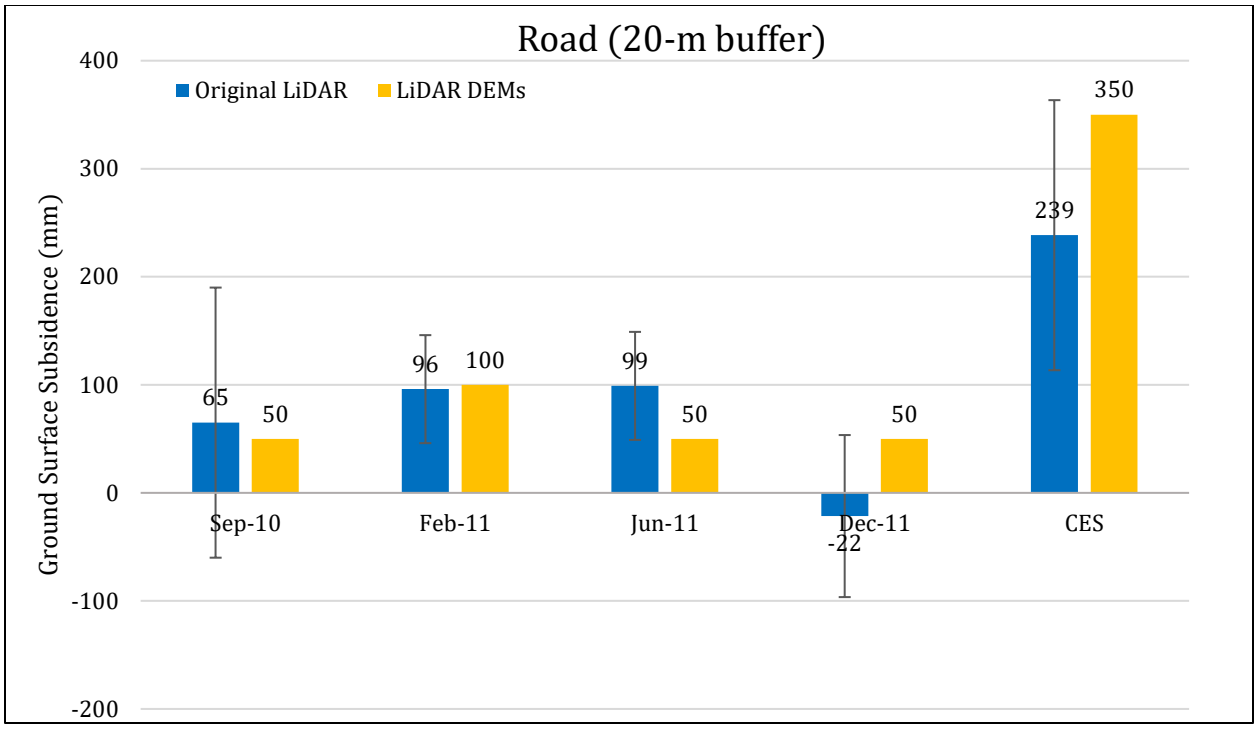

Figure 5: Comparison between ground surface subsidence determined from original LiDAR survey points and ground surface subsidence (50th %ile) estimated using LiDAR DEMs for Road for the 20-m buffer.

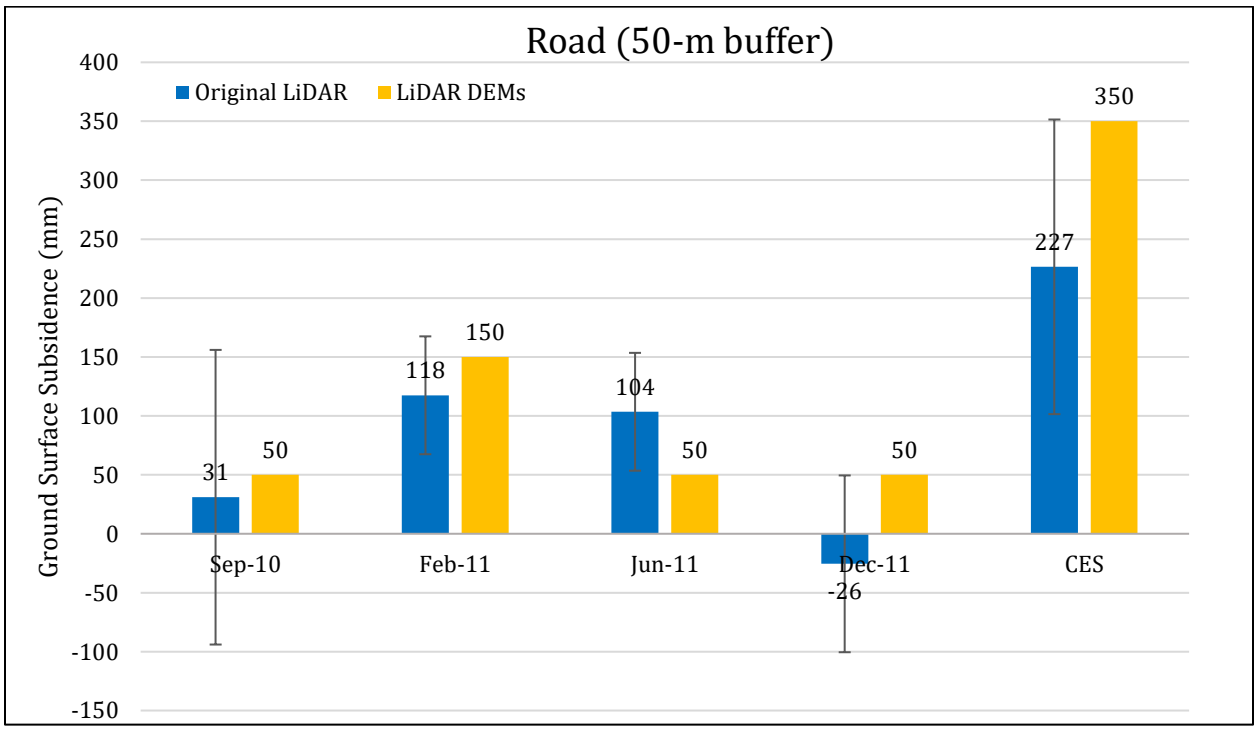

Figure 6: Comparison between ground surface subsidence determined from original LiDAR survey points and ground surface subsidence (50th %ile) estimated using LiDAR DEMs for Road for the 50-m buffer.

Note 2: The ground surface subsidence values determined from original LiDAR survey points are similar to the ground surface subsidence values estimated using LiDAR DEMs for all earthquake events.

Table 8a: Ejecta-Induced settlement for the top 20 m of the soil profile for Patch A for the 50th %ile PGA, P_L=50%, and C_{FC}=0.13 using BI-2014, ZRB-2002, and I_C cutoff of 2.6.

Earthquake Event(s)	M_W	PGA (g)	Depth to Groundwater (m)	S_T(mm)	S_{V1D} (mm)	$S_{E,L}$ (mm)
Sep-10	7.1	0.18	2.2	123±125	8±20	115±127
Feb-11	6.2	0.36	1.8	144±50	105±50	39±71
Jun-11	6.2	0.25	1.2	95±50	46±25	49±56
Dec-11	6.1	0.30	1.5	8±75	68±50	-60±90

Notes: S_T = Total settlement (Table 6); S_{V1D} = Average vertical settlement due to volumetric compression using Boulanger and Idriss (2014) (BI-2014) and Zhang et al. (2002) (ZRB-2002) procedures and de Greef and Lengkeek (2018) thin-layer correction; $S_{E,L}$ = Ejecta-induced settlement as the difference between the LiDAR-based S_T and S_{V1D}; NA = Not available.

Table 8b: Ejecta-Induced settlement for the top 20 m of the soil profile for Patch B for the 50th %ile PGA, P_L=50%, and C_{FC}=0.13 using BI-2014, ZRB-2002, and I_C cutoff of 2.6.

Earthquake Event(s)	M_W	PGA (g)	Depth to Groundwater (m)	S_T(mm)	S_{V1D} (mm)	$S_{E,L}$ (mm)
Sep-10	7.1	0.18	2.2	9±150	9±20	0±151
Feb-11	6.2	0.36	1.8	146±75	74±50	72±90
Jun-11	6.2	0.25	1.2	83±75	43±25	40±79
Dec-11	6.1	0.30	1.5	0±100	55±50	-55±112

Notes: S_T = Total settlement (Table 6); S_{V1D} = Average vertical settlement due to volumetric compression using Boulanger and Idriss (2014) (BI-2014) and Zhang et al. (2002) (ZRB-2002) procedures and de Greef and Lengkeek (2018) thin-layer correction; $S_{E,L}$ = Ejecta-induced settlement as the difference between the LiDAR-based S_T and S_{V1D}; NA = Not available.

Table 8c: Ejecta-Induced settlement for the top 20 m of the soil profile for Road within the 50-m buffer for the 50th %ile PGA, P_L=50%, and C_{FC}=0.13 using BI-2014, ZRB-2002, and I_C cutoff of 2.6.

Earthquake Event(s)	M_W	PGA (g)	Depth to Groundwater (m)	S_T(mm)	S_{V1D} (mm)	$S_{E,L}$ (mm)
Sep-10	7.1	0.18	2.2	31±125	11±20	20±102
Feb-11	6.2	0.36	1.8	118±50	105±50	13±71
Jun-11	6.2	0.25	1.2	104±50	57±25	47±56
Dec-11	6.1	0.30	1.5	-26±75	76±50	-102±90

Notes: S_T = Total settlement (Table 6); S_{V1D} = Average vertical settlement due to volumetric compression using Boulanger and Idriss (2014) (BI-2014) and Zhang et al. (2002) (ZRB-2002) procedures and de Greef and Lengkeek (2018) thin-layer correction; $S_{E,L}$ = Ejecta-induced settlement as the difference between the LiDAR-based S_T and S_{V1D}; NA = Not available.

Note 3: The uncertainty for volumetric settlement was derived based on the sensitivity of volumetric settlement to PGA, C_{FC}, and P_L for each earthquake event for VsVp 57203 *Shirley Intermediate School* and CC LIQ 1 – CPT 5586 – *Vivian St* sites. Taking the 50th percentile as the baseline case, the minimum and maximum values corresponding to the difference between the 25th percentile and the 50th percentile and the 75th percentile and the 50th percentile were determined. The arithmetic mean of the range of the minimum and maximum difference was evaluated for each patch at the two sites. The maximum arithmetic mean for each earthquake event was rounded to the nearest five and used as the uncertainty value. Accordingly, the 1-D volumetric settlement uncertainties of ±20, ±50, ±25, and ±50 mm for the Sep-10, Feb-11, Jun-11, and Dec-11 earthquake events, respectively, were used for all sites in this study.

Table 9a: Coverage area and height of ejecta estimates for Patch A using aerial and/or ground photographs and engineering judgement.

Earthquake Event	$H_{E,thick}$ (mm)	$A_{E,thick}$ (m^2)	$H_{E,thin}$ (mm)	$A_{E,thin}$ (m^2)	A_T (m^2)
Sep-10	0	0	0	0	18.5
Feb-11	200-300	8.1	40-60	2.6	18.5
Jun-11	NA	NA	NA	NA	18.5
Dec-11	0	0	10-30	4.3	18.5

Note: $A_{E,thick/thin}$ = Coverage area of thick/thin ejecta layers; $H_{E,thick/thin}$ = Lower-upper estimate of height of thick/thin ejecta layers; Thin and thick layers correspond to light gray and dark gray colors of ejecta observed in aerial photographs; A_T= Total assessment area of a buffer being considered; * indicates reduction in A_T due to the presence of objects within the assessment area.

Table 9b: Coverage area and height of ejecta estimates for Patch B using aerial and/or ground photographs and engineering judgement.

Earthquake Event	$H_{E,thin}$ (mm)	$A_{E,thin}$ (m^2)	$H_{E,thick}$ (mm)	$A_{E,thick}$ (m^2)	A_T (m^2)
Sep-10	0	0	0	0	69.4
Feb-11	40-60	32.5	0	0	69.4
Jun-11	10-20	22.7	0	0	69.4
Dec-11	10-30	5.2	0	0	69.4

Note: $A_{E,thick/thin}$ = Coverage area of thick/thin ejecta layers; $H_{E,thick/thin}$ = Lower-upper estimate of height of thick/thin ejecta layers; Thin and thick layers correspond to light gray and dark gray colors of ejecta observed in aerial photographs; A_T = Total assessment area of a buffer being considered; Blind sand boil (i.e., the mound formed by the liquefied soil trapped underneath the topsoil) with the height of 350 mm and the area of 3.5 m^2 formed as a result of the Feb-11 EQ but was not accounted for in the analysis because the soil was not ejected onto the ground surface.

Table 9c: Coverage area and height of ejecta estimates for Road within the 50-m buffer using aerial and/or ground photographs and engineering judgement.

EQ Event	$H_{E,thin1}$ (mm)	$A_{E,thin1}$ (m^2)	$H_{E,thin2}$ (mm)	$A_{E,thin2}$ (m^2)	$H_{E,thick1}$ (mm)	$A_{E,thick1}$ (m^2)	$H_{E,thick2}$ (mm)	$A_{E,thick2}$ (m^2)	A_T (m^2)
Sep-10	0	0	0	0	0	0	0	0	410
Feb-11	2-4	196	40-70	166	150-250	20.9	200-300	15	401*
Jun-11	3-6	325	10-20	33.3	20-40	51.9	0	0	410
Dec-11	3-6	13.2	20-40	35.0	40-80	4.8	50-100	5.4	421

Note: $A_{E,thick/thin}$ = Coverage area of thick/thin ejecta layers; $H_{E,thick/thin}$ = Lower-upper estimate of height of thick/thin ejecta layers; Thin and thick layers correspond to light gray and dark gray colors of ejecta observed in aerial photographs; A_T= Total assessment area of a buffer being considered; * indicates reduction in A_T due to the presence of objects within the assessment area.

Note 4: The values in Table 9 correspond to the coverage area of ejecta outlined in aerial photographs (Figures 88 through 94) and the lower and upper estimates of ejecta height based on geometry, ground photographs (Figures 100 and 101), EQC LDAT property inspection notes (Figures 95 through 99) and reports from Aug 2011. The ejecta-induced settlement using photographs and engineering judgment, $S_{E,P}$, is estimated as

$$S_{E,P} = \frac{\sum_{i=1}^{a} A_{E,thick,i} * H_{E,thick,i} + \sum_{j=1}^{b} A_{E,thin,j} * H_{E,thin,j}}{A_T} = \frac{\sum_{i=1}^{a} V_{E,thick,i} + \sum_{j=1}^{b} V_{E,thin,j}}{A_T}$$

where

- $A_{E,thick,i}$ and $H_{E,thick,i}$ are the area and the height of a thick ejecta layer, respectively;
- $A_{E,thin,j}$ and $H_{E,thin,j}$ are the area and the height of a thin ejecta layer, respectively;
- A_T is the total assessment area for a buffer being considered (Figure 1).

Table 10: Ejecta-induced settlement estimates based on aerial and/or ground photographs.

Earthquake Event	Patch A (10-, 20-, and 50-m buffers)		Patch B (20- and 50-m buffers)		Road (50-m buffer)	
	$S_{E,P,lower}$ (mm)	$S_{E,P,upper}$ (mm)	$S_{E,P,lower}$ (mm)	$S_{E,P,lower}$ (mm)	$S_{E,P,lower}$ (mm)	$S_{E,P,lower}$ (mm)
Sep-10	0	0	0	0	0	0
Feb-11	93	140	19	28	33	55
Jun-11	NA	NA	3	7	6	12
Dec-11	2	7	1	2	3	6

Note: $S_{E,P,lower}$ and $S_{E,P,upper}$ correspond to lower and upper estimates of $S_{E,P}$, respectively; NA = Not available due to the lack of physical evidence.

Table 11: Best final estimates of ejecta-induced settlement.

EQ Event	Patch A (10-, 20-, and 50-m buffers)			Patch B (20- and 50-m buffers)			Road (50-m buffer)		
	$S_{E,L}$ (mm)	$S_{E,P}$ (mm)	$S_{E,final}$ (mm)	$S_{E,L}$ (mm)	$S_{E,P}$ (mm)	$S_{E,final}$ (mm)	$S_{E,L}$ (mm)	$S_{E,P}$ (mm)	$S_{E,final}$ (mm)
Sep-10	115±127	0	0	0±151	0	0	20±102	0	0
Feb-11	39±71	117±23	90±30	72±90	24±4	40±30	13±71	44±11	35±25
Jun-11	49±56	NA	NA	40±79	5±2	15±25	47±56	9±3	20±20
Dec-11	-60±90	4.5±2.5	5±5	-55±112	1.5±0.5	<5	-102±90	4.5±1.5	5±5

Notes: $S_{E,L}$ = Ejecta-induced settlement based on LiDAR data reported in Table 8; $S_{E,P}$ = Median ejecta-induced settlement for the range of values reported in Table 10; $S_{E,final}$ = Best final estimate of ejecta-induced settlement rounded to the nearest 5; Final plus/minus values are also rounded to the nearest 5; NA = Not available due to the absence of physical evidence.

Note 5:

- For Patch A, $S_{E,final}$ for the Sep-10 and Dec-11 EQs is based solely on $S_{E,P}$, while $S_{E,final}$ for the Feb-11 EQ is a weighted average of $S_{E,L}$ and $S_{E,P}$ with respective weight coefficients of 1/3 and 2/3. For the Jun-11 EQ, $S_{E,final}$ for Patch A is not available due to the lack of physical evidence.
- For Patch B, $S_{E,final}$ is equal to $S_{E,P}$ for the Sep-10 and Dec-11 EQs. For the Feb-11 and Jun-11 EQs, $S_{E,final}$ is a weighted average of $S_{E,L}$ and $S_{E,P}$ with weights of 1/3 and 2/3, respectively.
- $S_{E,final}$ for Road is based solely on $S_{E,P}$ for the Sep-10 and Dec-11 EQs. $S_{E,final}$ for the Feb-11 and Jun-11 EQs is a weighted average of $S_{E,L}$ and $S_{E,P}$ with respective weight coefficients of 1/3 and 2/3.
- The uncertainty associated with $S_{E,final}$ is also a weighted average of uncertainties associated with $S_{E,L}$ and $S_{E,P}$ with the same corresponding weights.
- The weights are based on the LiDAR error bands, LPI prediction error (Maurer et al. 2014[3]), presence of ejecta at the time of LiDAR surveys, and completeness of visual evidence (i.e.,

[3] Maurer, B. W., Green, R. A., Cubrinovski, M., & Bradley, B. A. (2014). Evaluation of the Liquefaction Potential Index for Assessing Liquefaction Hazard in Christchurch, New Zealand. *Journal of Geotechnical and Geoenvironmental Engineering*, 140(7), 04014032-1-11. doi:10.1061/(asce)gt.1943-5606.0001117

ground and aerial photographs and EQC LDAT property inspection reports for the site). The Hunt Lane site is not in the apparent zone of higher/lower ground surface subsidence for any earthquake event. The site is in the zone of accurate LPI prediction to slight-moderate LPI overprediction of liquefaction severity for both the Sep-10 and Feb-11 EQ. The LDAT property inspection report is available for Patches A and B. There are several ground photographs of the road.

<u>Summary 1</u>:

- **The best estimate of the ejecta-induced free-field ground settlement at the Hunt Lane site for the SEP 2010, JUN 2011, and DEC 2011 earthquake is 0 mm, 15±25 mm (range = 0-40 mm, mean = 15 mm), and 5±5 mm, respectively. During the FEB 2011 earthquake, about 70% of the unobstructed area of the site experienced the ejecta-induced ground settlement in a range from 40±30 mm to 90±30 mm.**
- **The best estimate of the ejecta-induced free-field ground settlement of the road at the Hunt Lane site for the SEP 2010, FEB 2011, JUN 2011, and DEC 2011 earthquake is 0 mm, 35±25 mm, 20±20 mm, and 5±5 mm, respectively.**

Note 6: CPT 4674 was initially named as CC LIQ 12.

Figure 7: Location of the site.

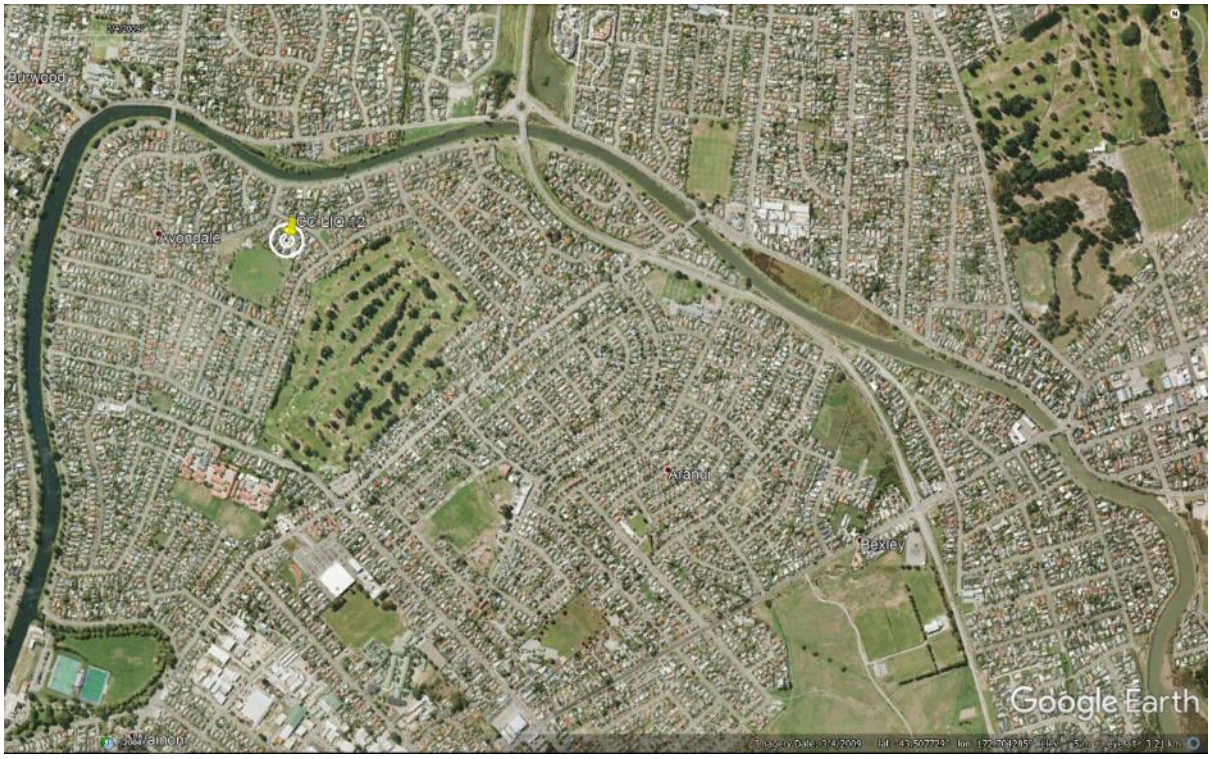

Figure 8: Position of the site relative to nearby buildings, vegetation, and free-face features.

Figure 9: Street view of the site showing flat land.

Figure 10: Satellite image of the site taken in Dec 2004.

Figure 11: Satellite image of the site taken in Mar 2009.

Figure 12: Satellite image of the site taken on 3 Sep 2010.

Figure 13: Satellite image of the site taken on 5 Sep 2010.

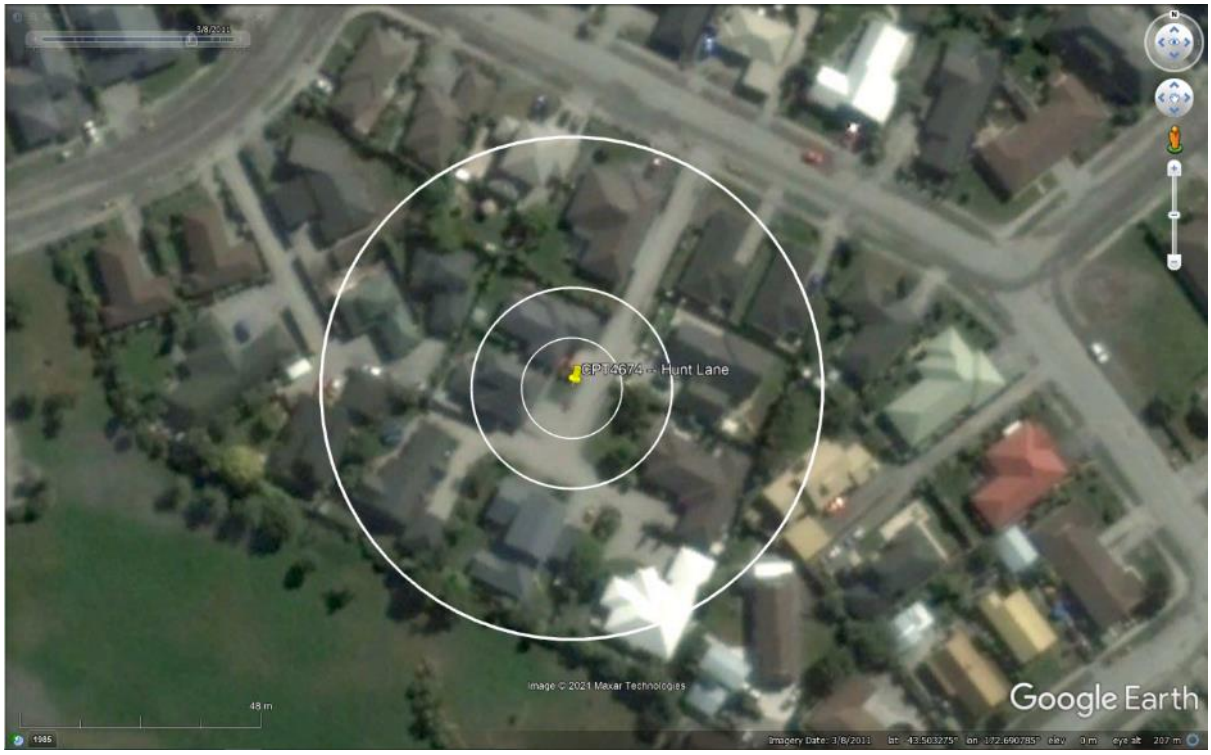

Figure 14: Satellite image of the site taken on 8 Mar 2011.

Figure 15: Satellite image of the site taken in Apr 2012.

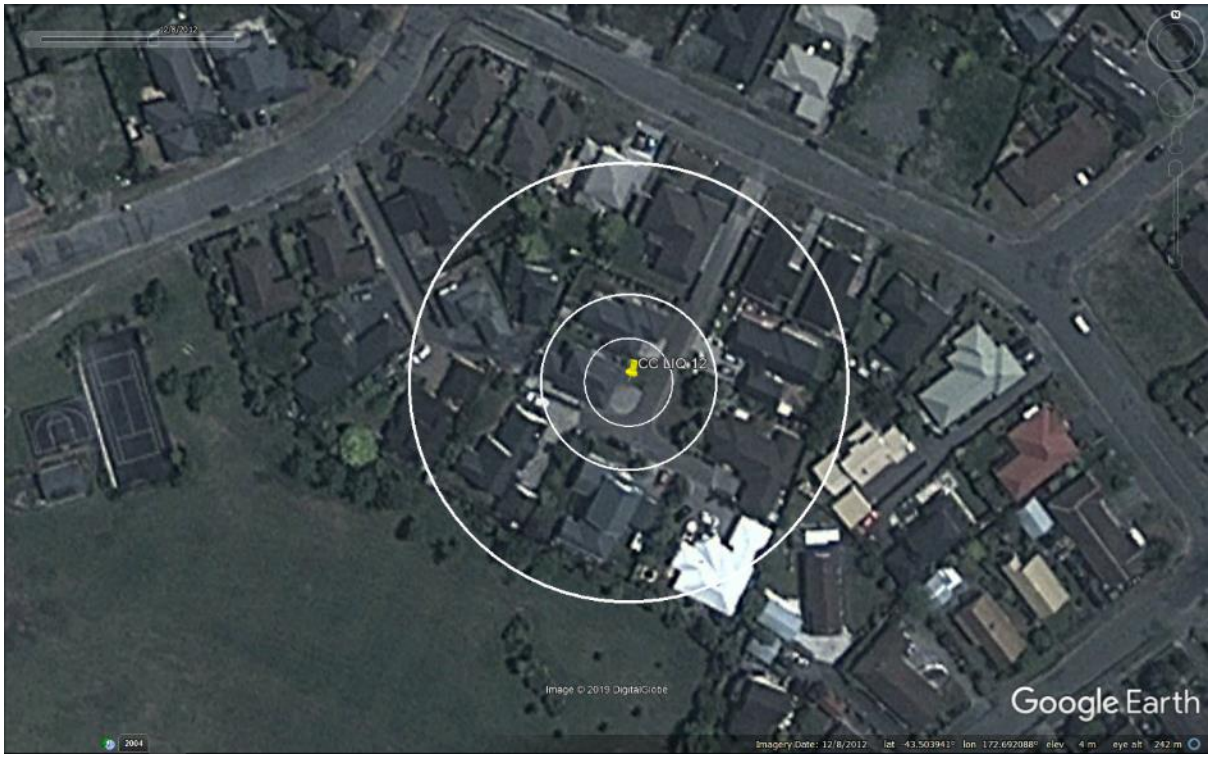

Figure 16: Satellite image of the site taken in Dec 2012.

Figure 17: Satellite image of the site taken in Jan 2013.

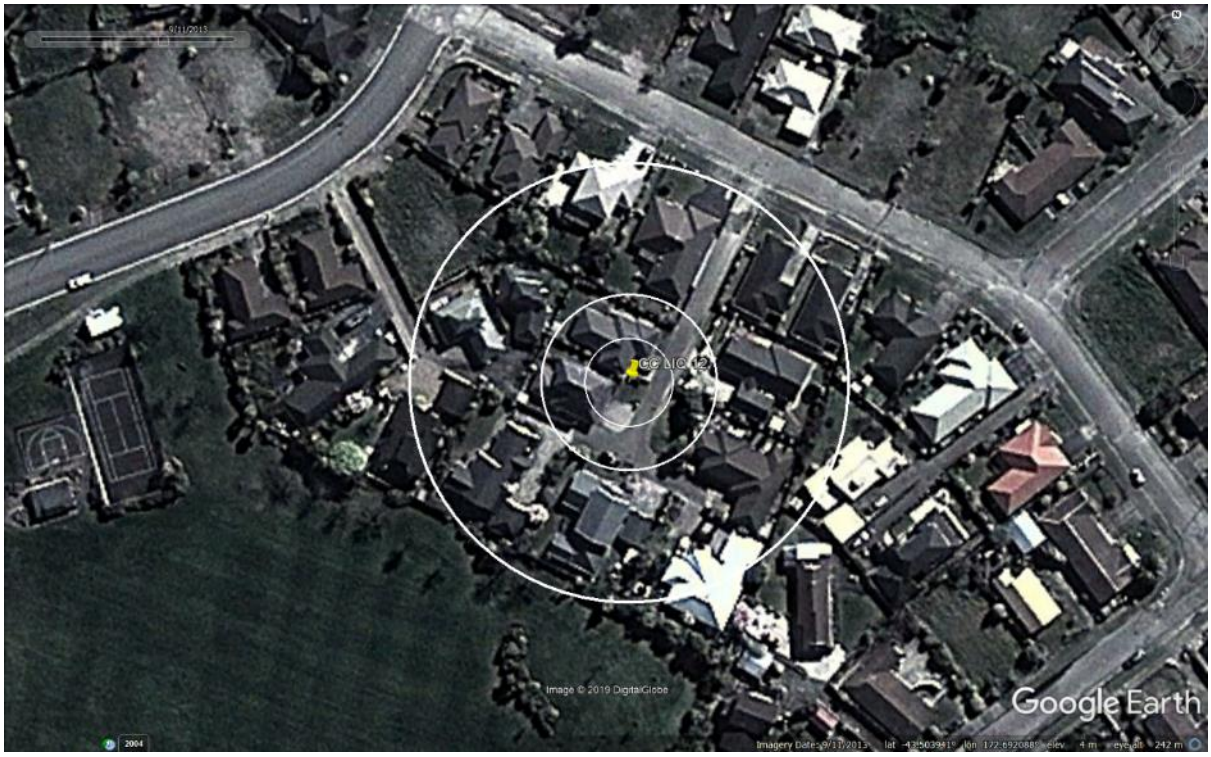

Figure 18: Satellite image of the site taken in Sep 2013.

Figure 19: Satellite image of the site taken in Feb 2014.

Figure 20: Satellite image of the site taken in Aug 2014.

Figure 21: Satellite image of the site taken in Jan 2015.

Figure 22: Satellite image of the site taken in Jun 2015.

Figure 23: Satellite image of the site taken in Jul 2015.

Figure 24: Satellite image of the site taken in Sep 2015.

Figure 25: Satellite image of the site taken in Feb 2016.

Figure 26: Aerial photograph of the site taken on Sep 4, 2010.

Figure 27: Aerial photograph of the site taken on Feb 24, 2011.

Figure 28: Aerial photograph of the site taken on June 14-15, 2011.

Figure 29: Aerial photograph of the site taken on June 16, 2011.

Figure 30: Aerial photograph of the site taken on Dec 24, 2011.

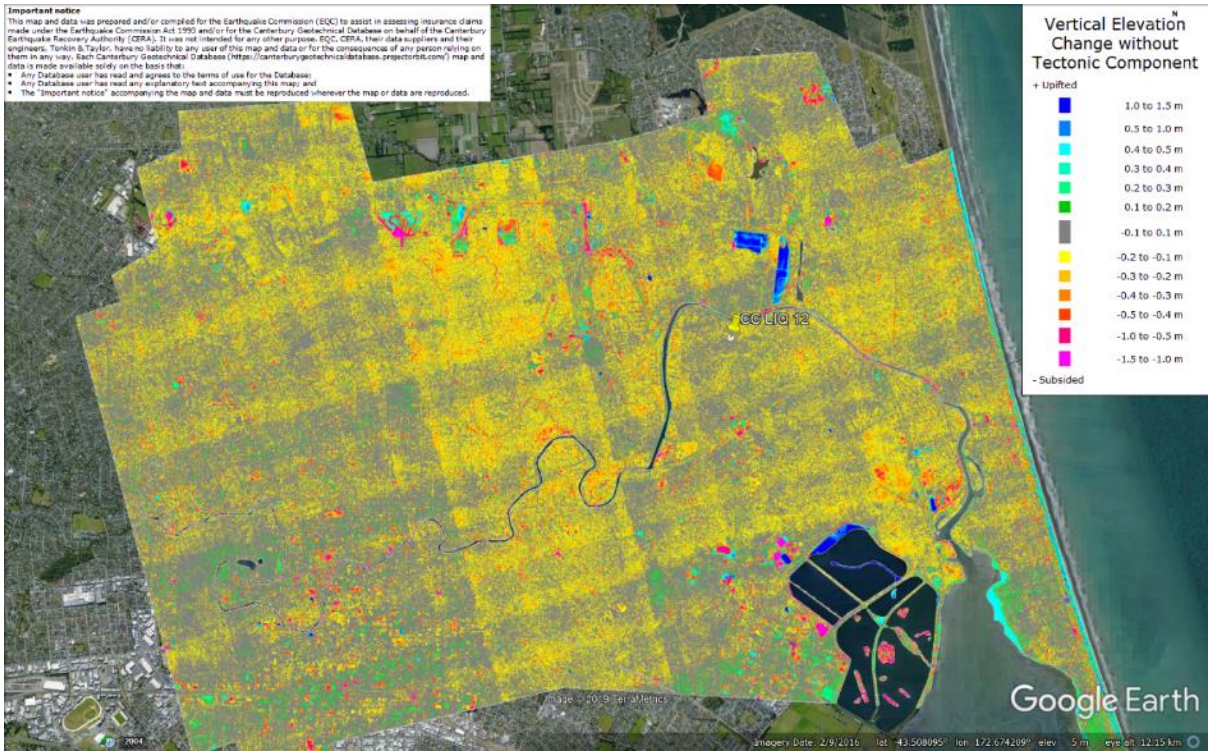

Figure 31: Vertical Ground Movements (Surface – Tectonic) for Sep 2010 Earthquake – the site is not in the apparent zone of overestimated ground surface subsidence.

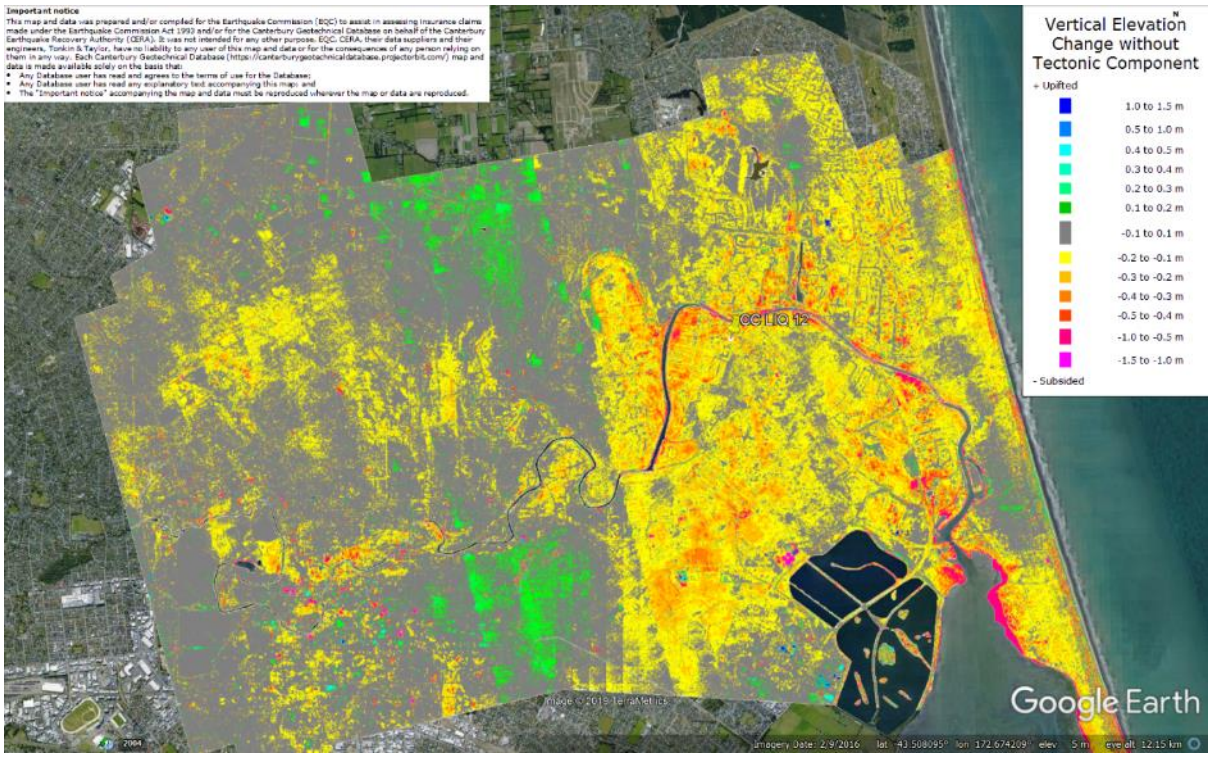

Figure 32: Vertical Ground Movements (Surface – Tectonic) for Feb 2011 Earthquake – the site is not in the apparent zone of underestimated ground surface subsidence.

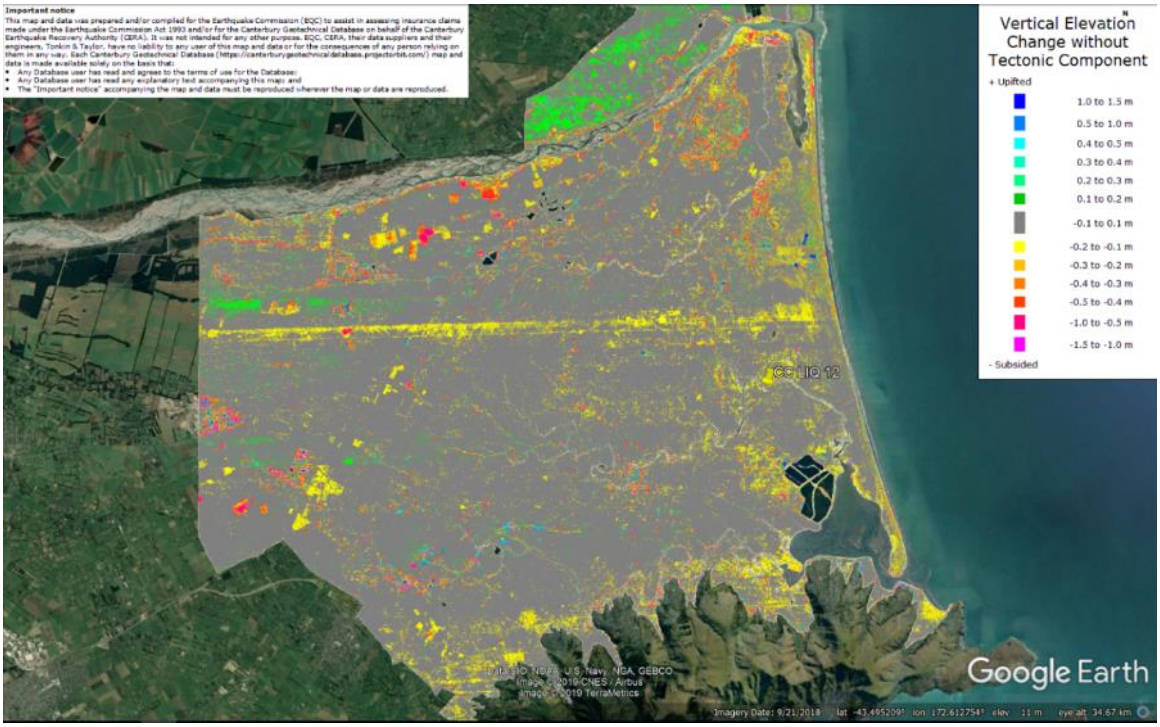

Figure 33: Vertical Ground Movements (Surface – Tectonic) for June 2011 Earthquake – the site is not in the apparent zone of overestimated or underestimated ground surface subsidence.

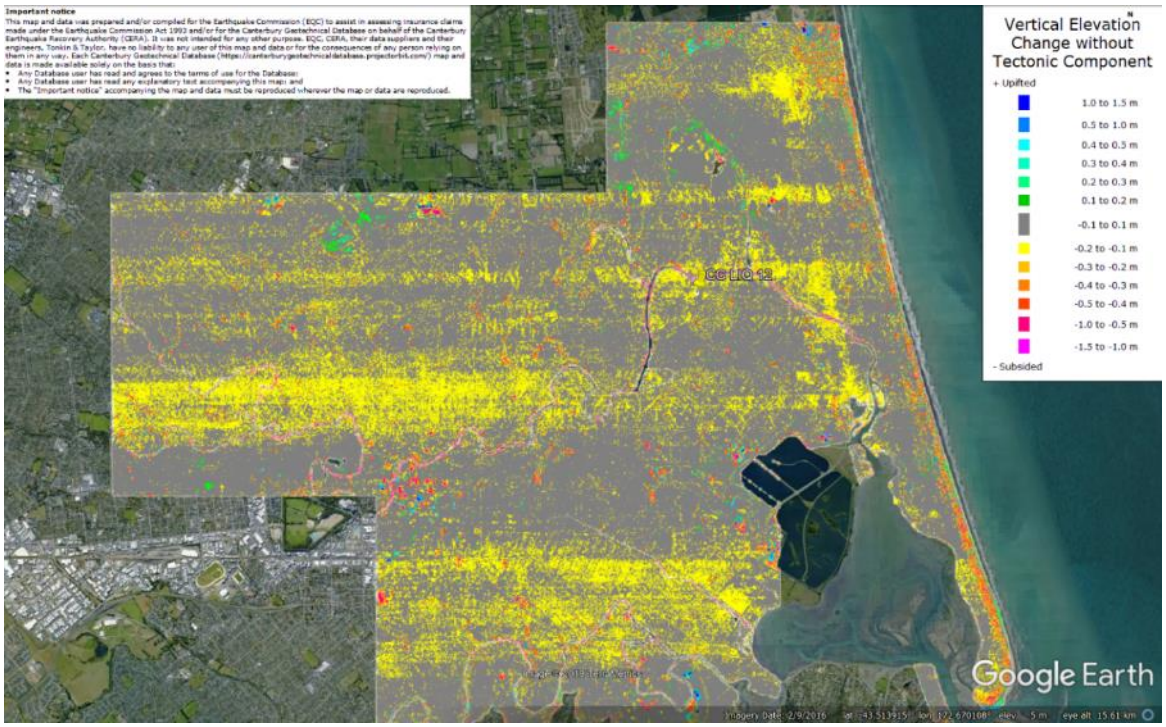

Figure 34: Vertical Ground Movements (Surface – Tectonic) for Dec 2011 Earthquake – the site is not in the apparent zone of overestimated or underestimated ground surface subsidence.

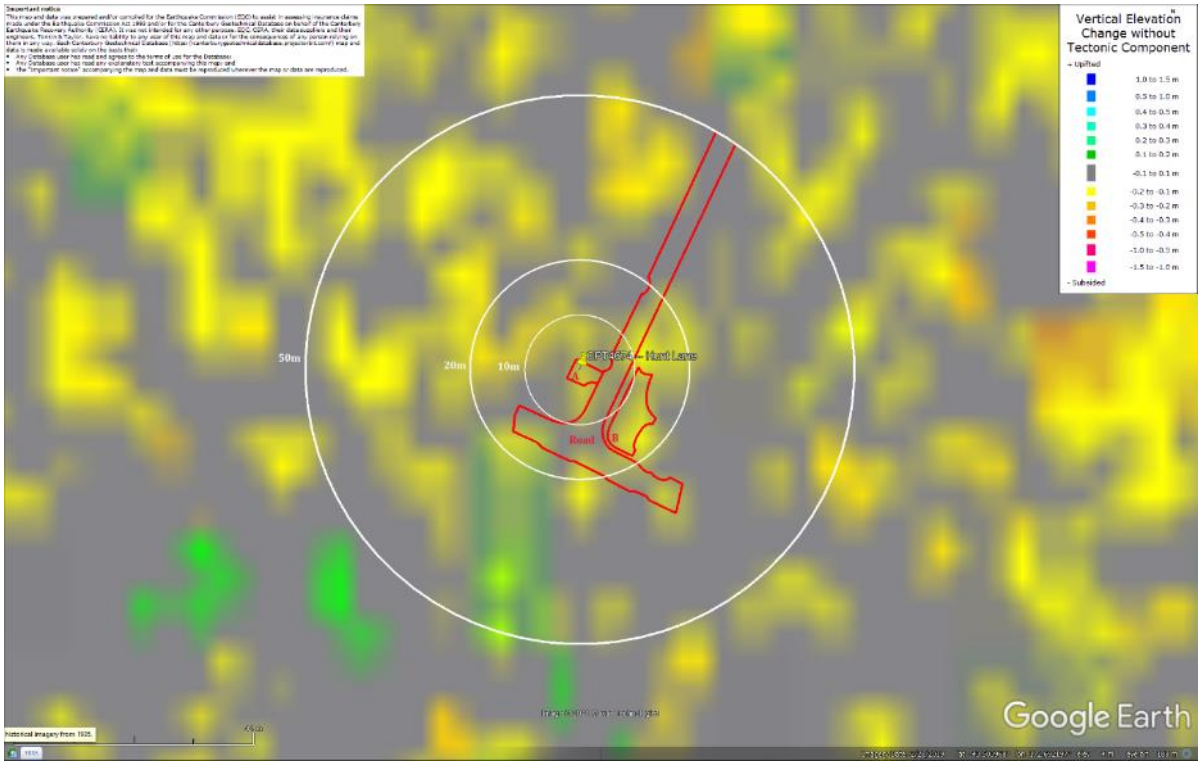

Figure 35: Ground surface subsidence without tectonic component for Sep 2010 Earthquake according to the LiDAR DEM.

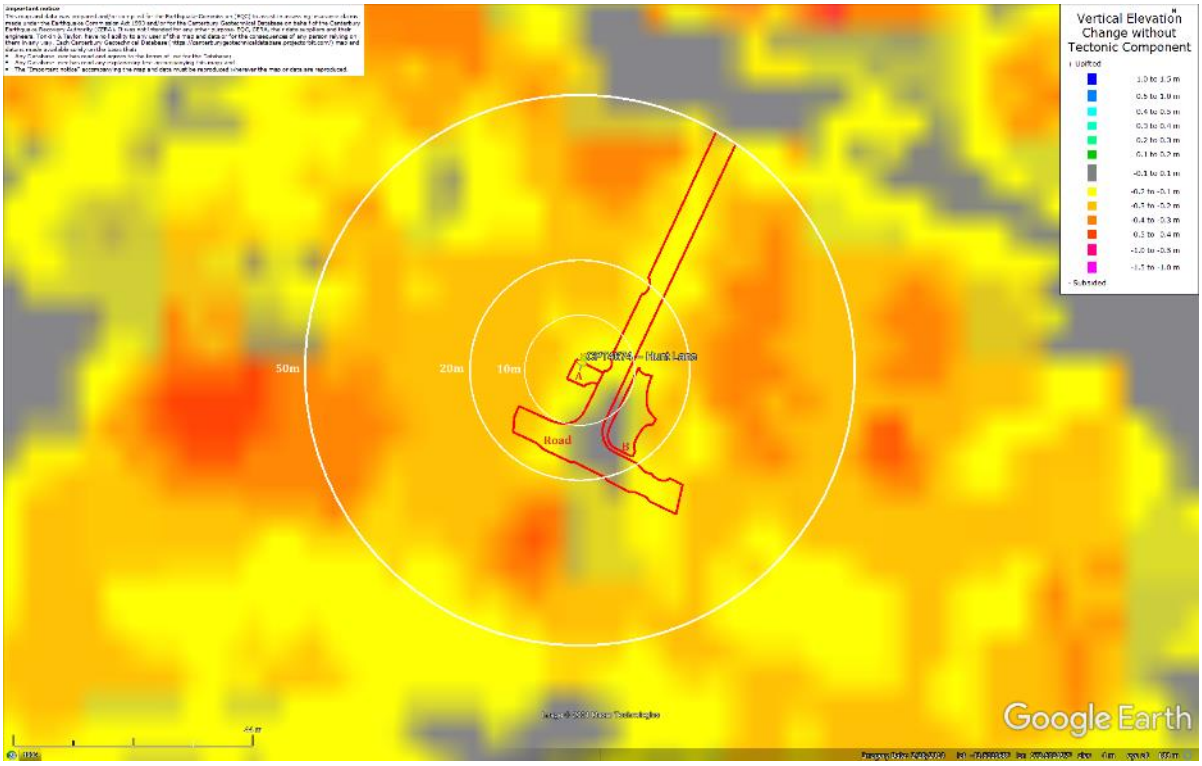

Figure 36: Ground surface subsidence without tectonic component for Feb 2011 Earthquake according to the LiDAR DEM.

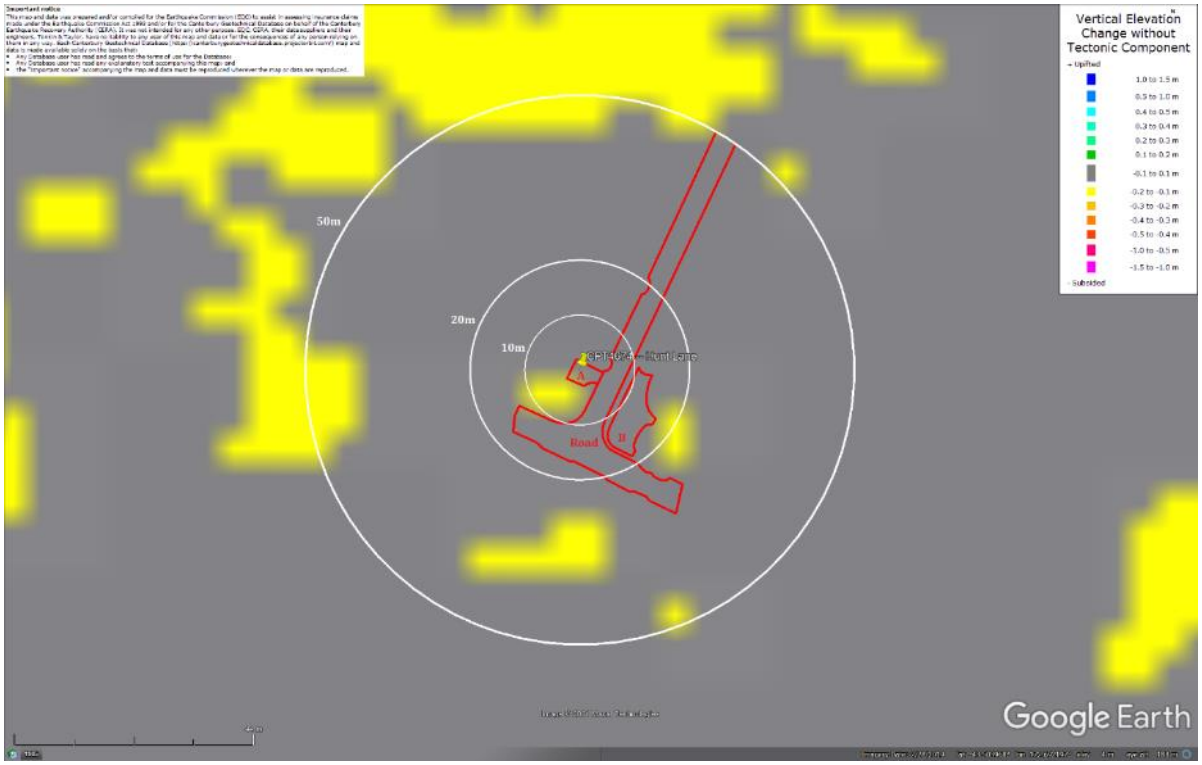

Figure 37: Ground surface subsidence without tectonic component for Jun 2011 Earthquake according to the LiDAR DEM.

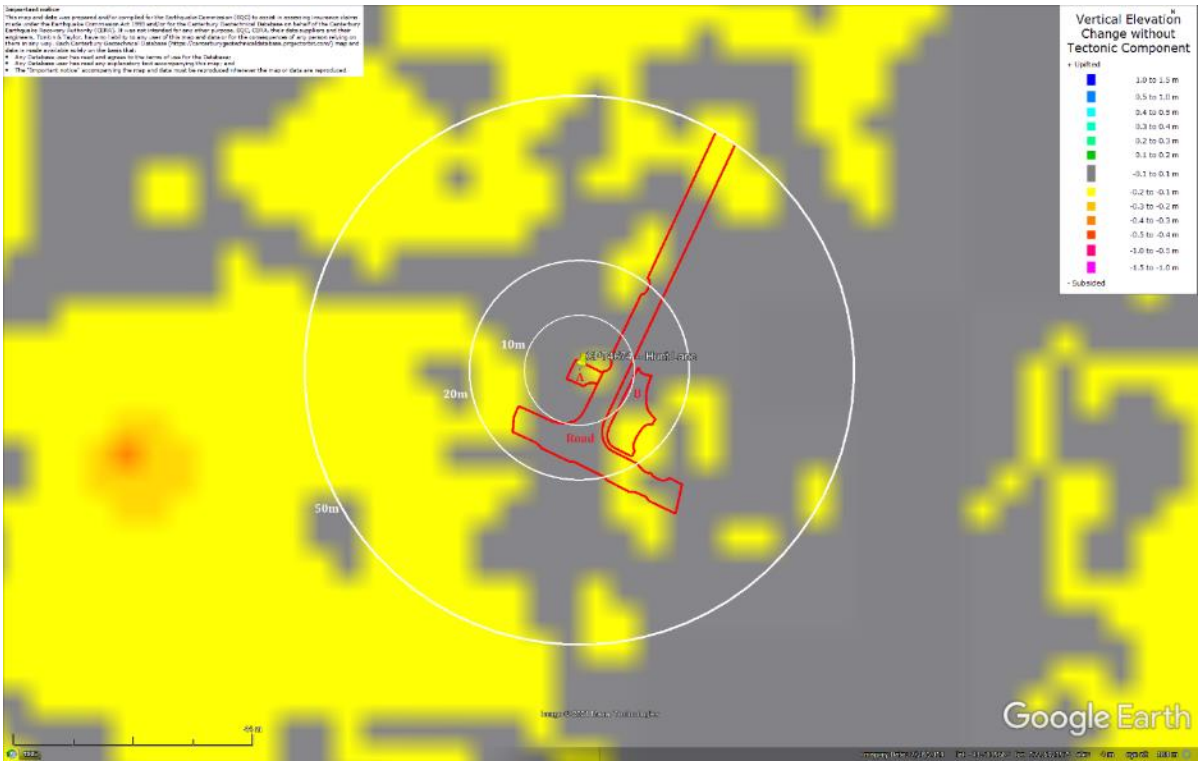

Figure 38: Ground surface subsidence without tectonic component for Dec 2011 Earthquake according to the LiDAR DEM.

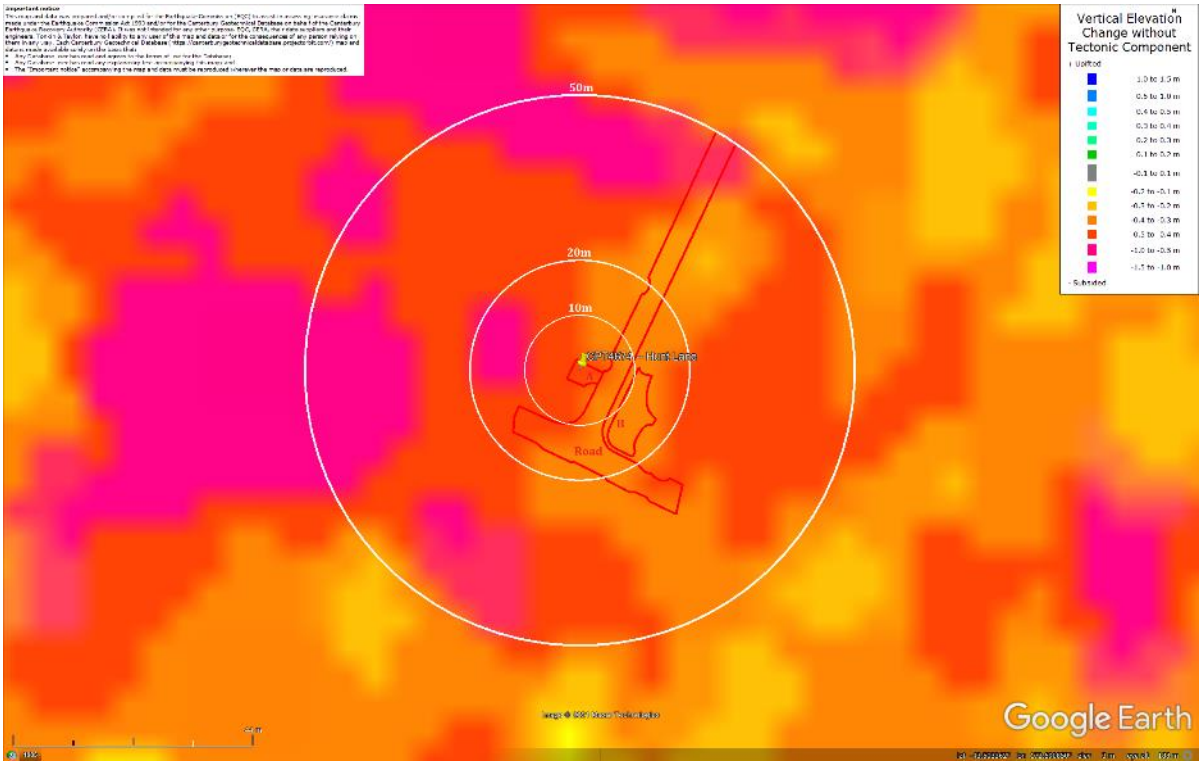

Figure 39: Ground surface subsidence without tectonic component for Canterbury Earthquake Sequence according to the LiDAR DEM.

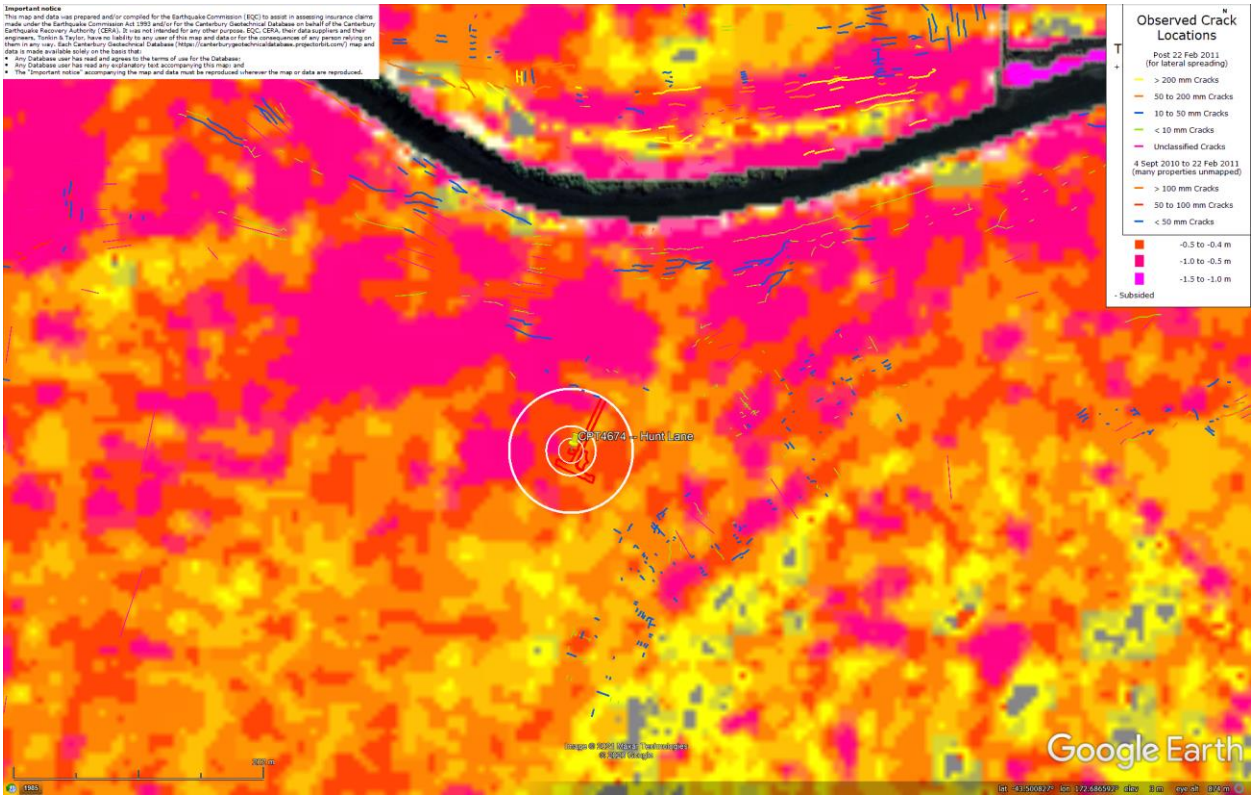

Figure 40: Absence of ground cracks indicates no lateral spreading for Canterbury Earthquake Sequence.

Figure 41: Vertical tectonic movements for Sep 2010 Earthquake.

Figure 42: Vertical tectonic movements for Feb 2011 Earthquake.

Figure 43: Vertical tectonic movements for June 2011 Earthquake.

Figure 44: Vertical tectonic movements for Dec 2011 Earthquake.

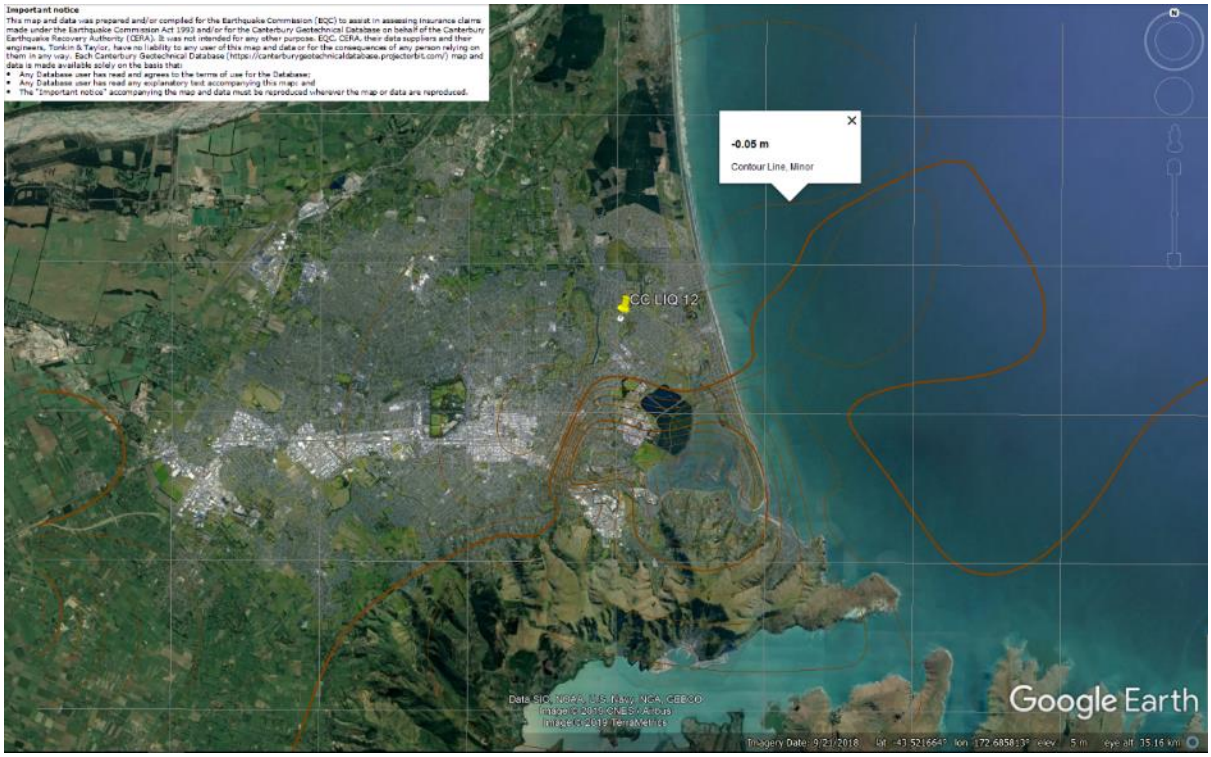

Figure 45: Vertical tectonic movements for Canterbury Earthquake Sequence.

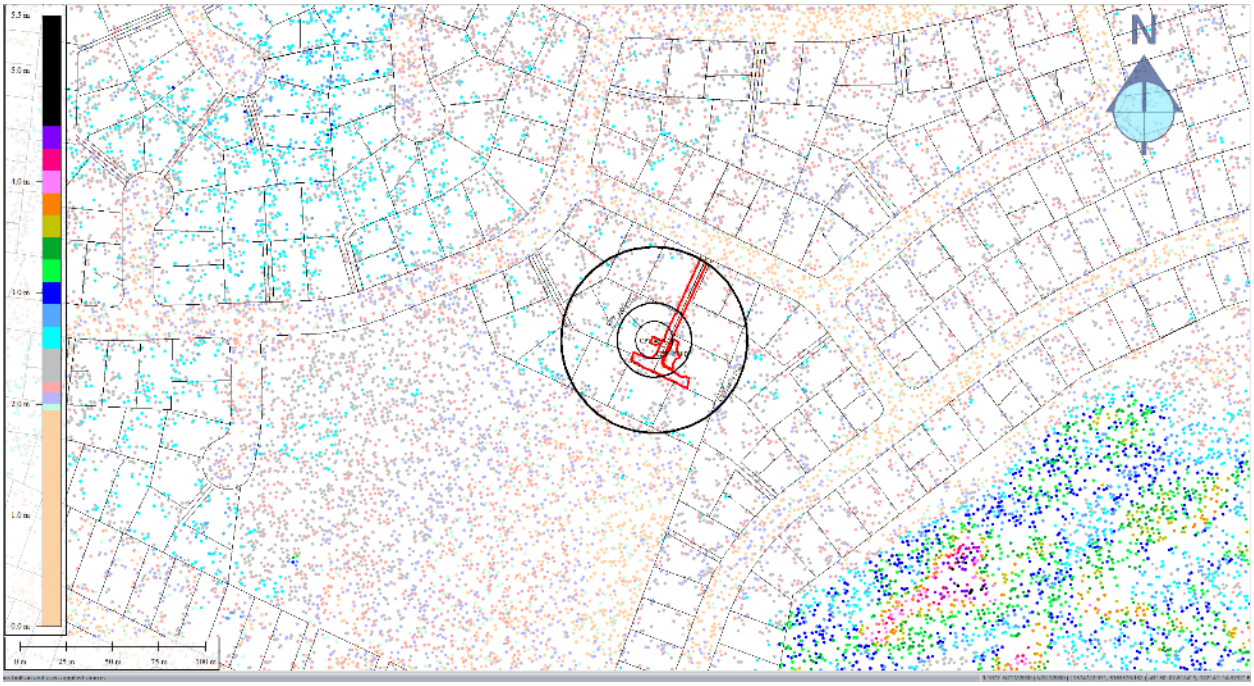

Figure 46: Jul 2003 LiDAR survey.

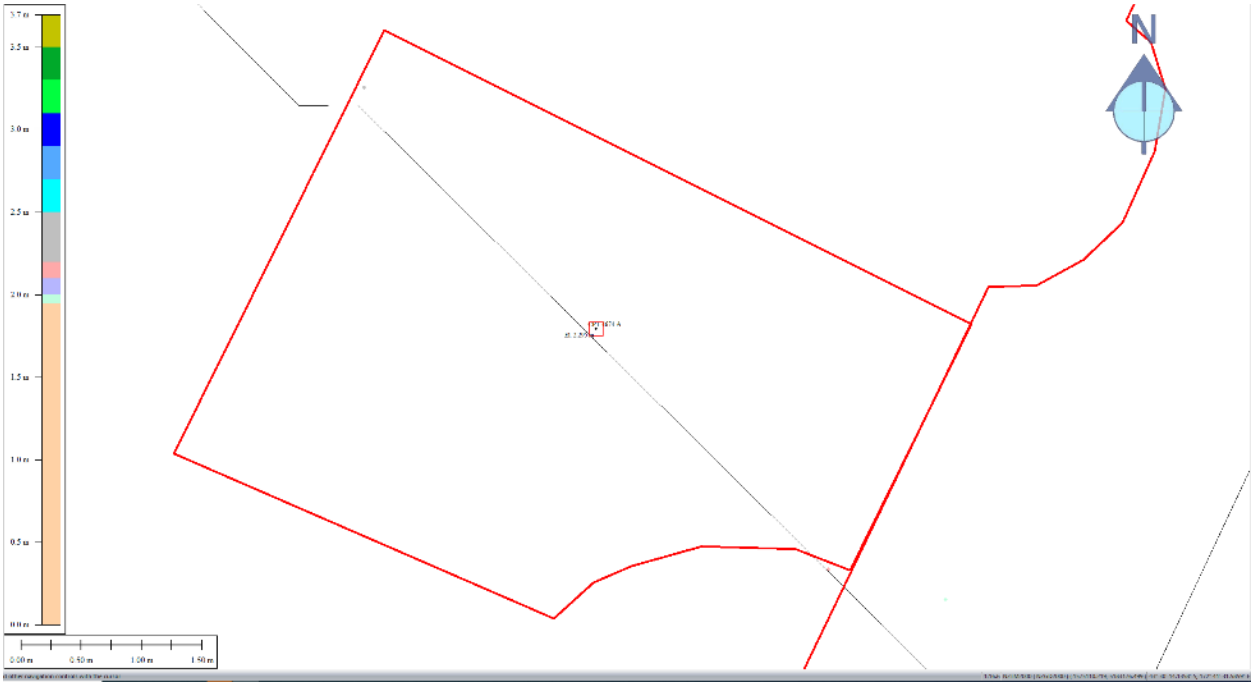

Figure 47: Ground surface elevation for Patch A for Jul 2003 LiDAR survey.

Figure 48: Ground surface elevation for Patch B for Jul 2003 LiDAR survey.

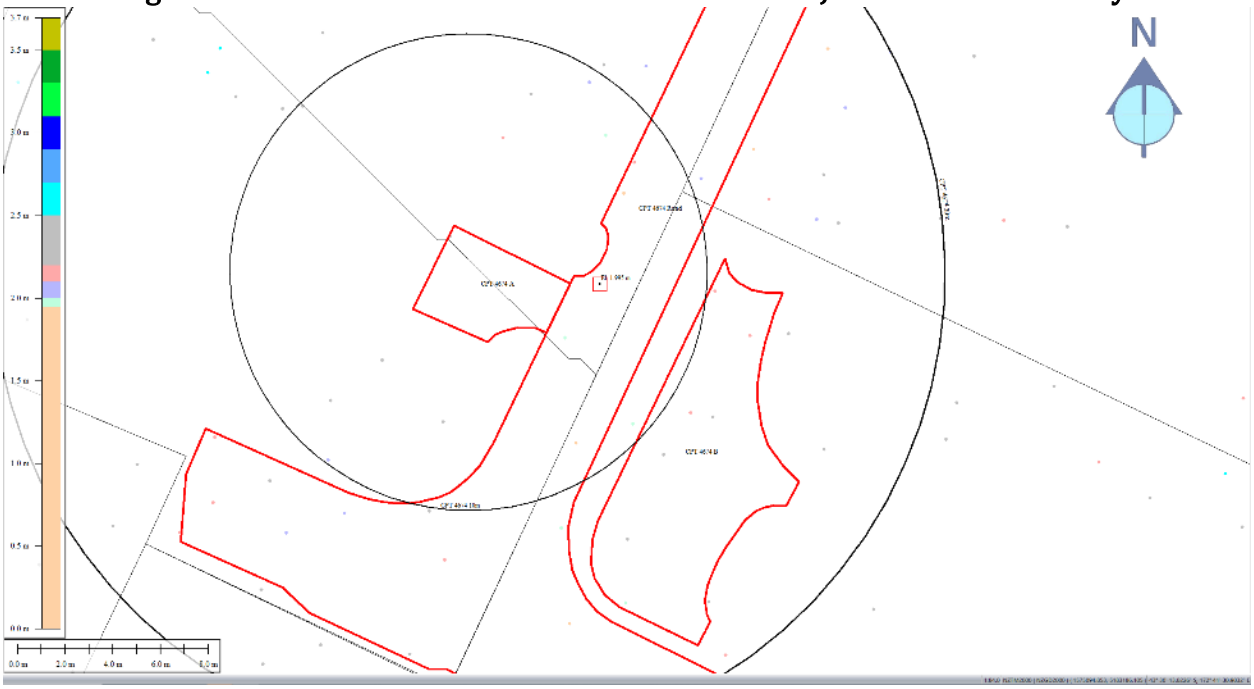

Figure 49: Ground surface elevation averaged over the 10-m buffer for Road for Jul 2003 LiDAR survey.

Figure 50: Ground surface elevation averaged over the 20-m buffer for Road for Jul 2003 LiDAR survey.

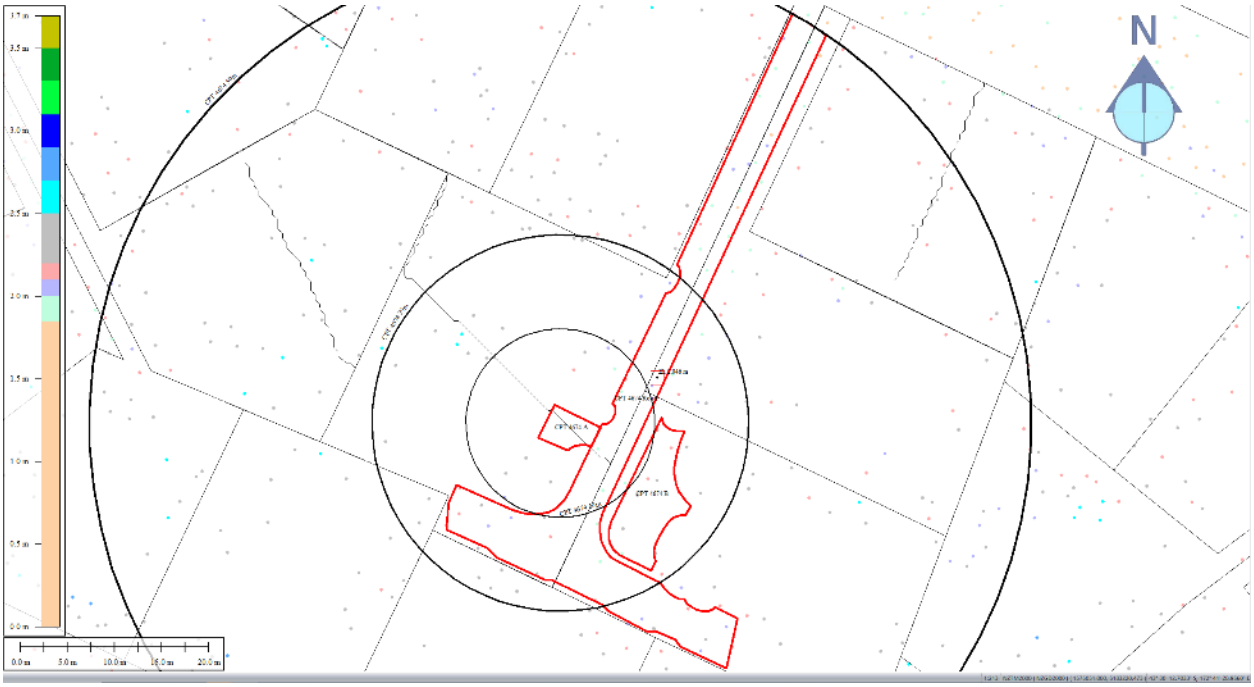

Figure 51: Ground surface elevation averaged over the 50-m buffer for Road for Jul 2003 LiDAR survey.

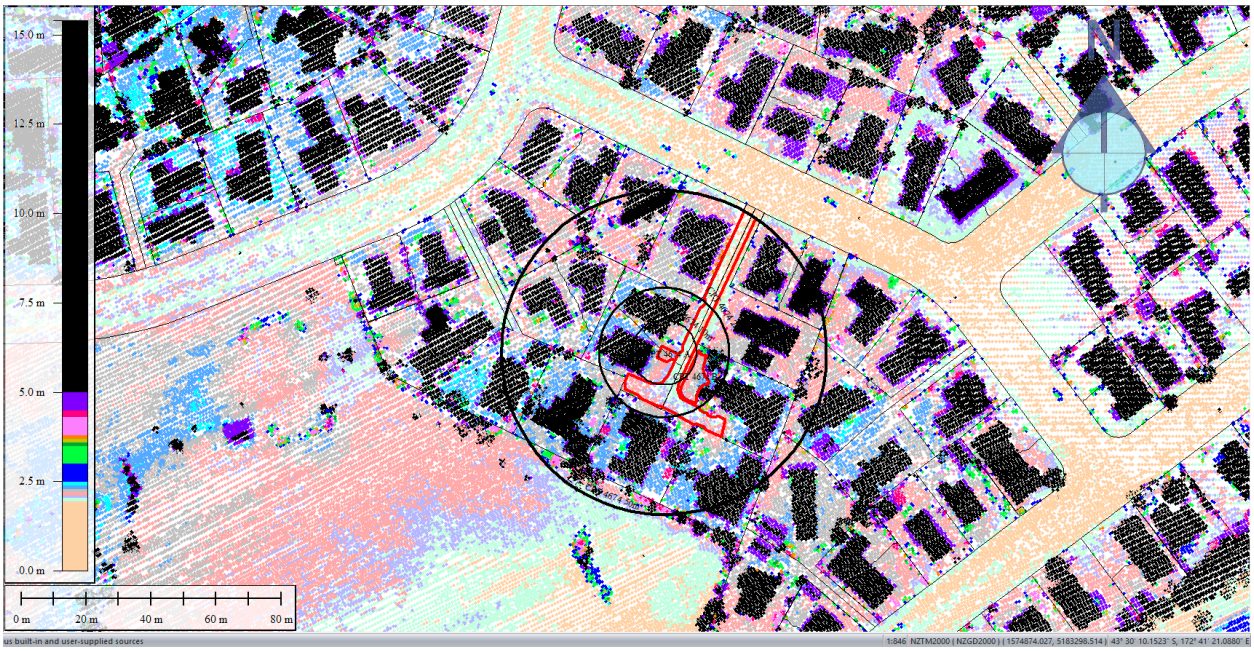

Figure 52: Sep 5, 2010 LiDAR survey.

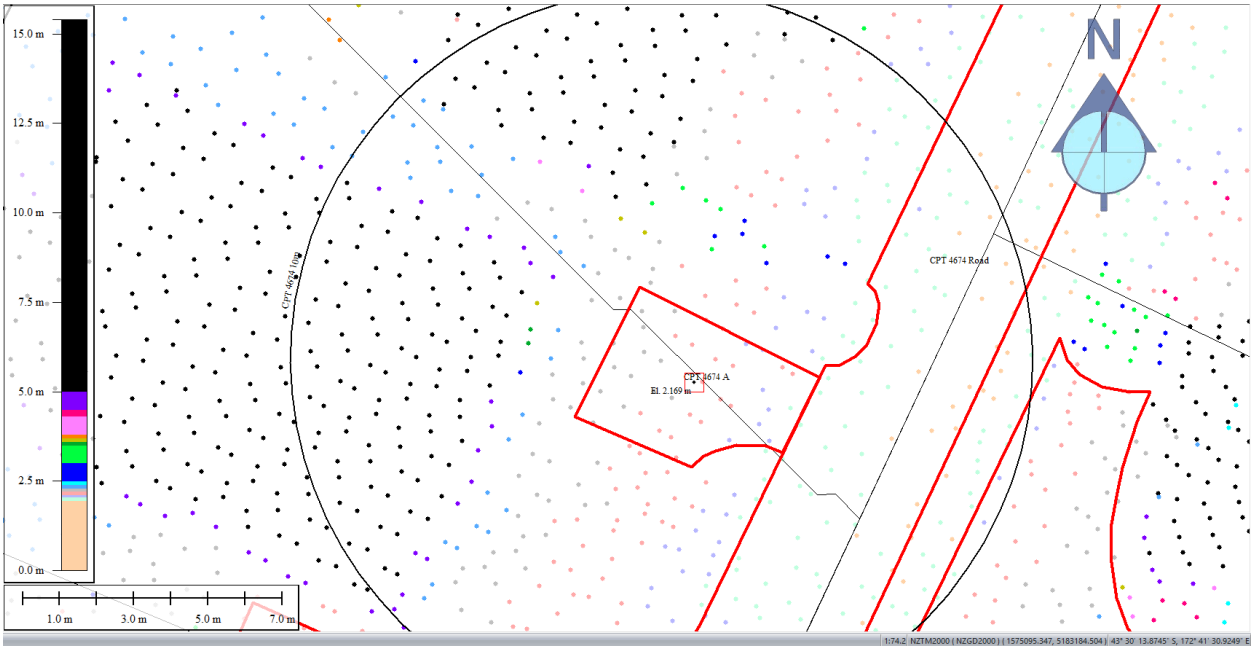

Figure 53: Ground surface elevation for Patch A for Sep 5, 2010 LiDAR survey.

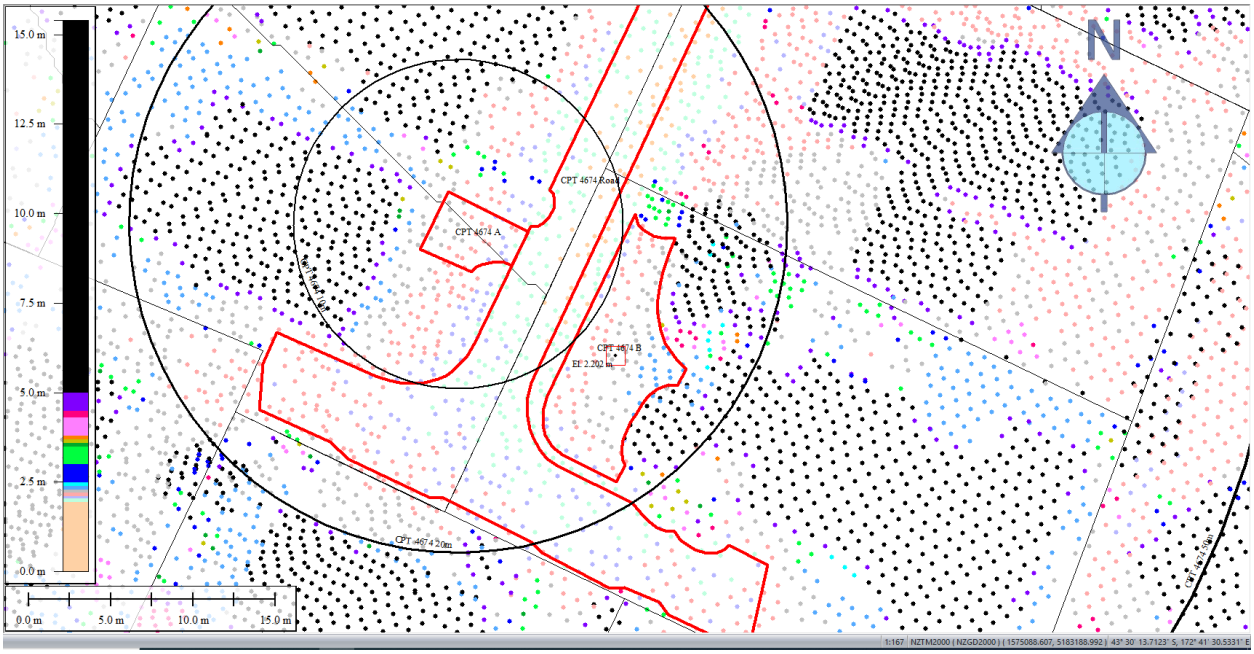

Figure 54: Ground surface elevation for Patch B for Sep 5, 2010 LiDAR survey.

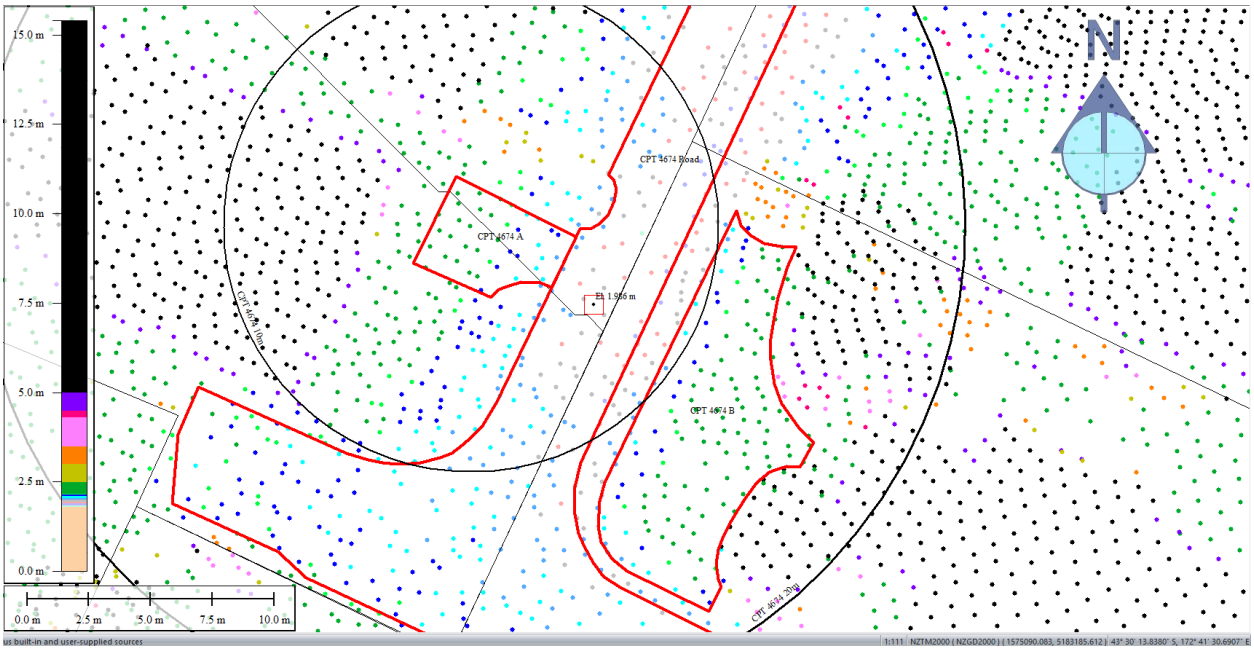

Figure 55: Ground surface elevation averaged over the 10-m buffer for Road for Sep 5, 2010 LiDAR survey.

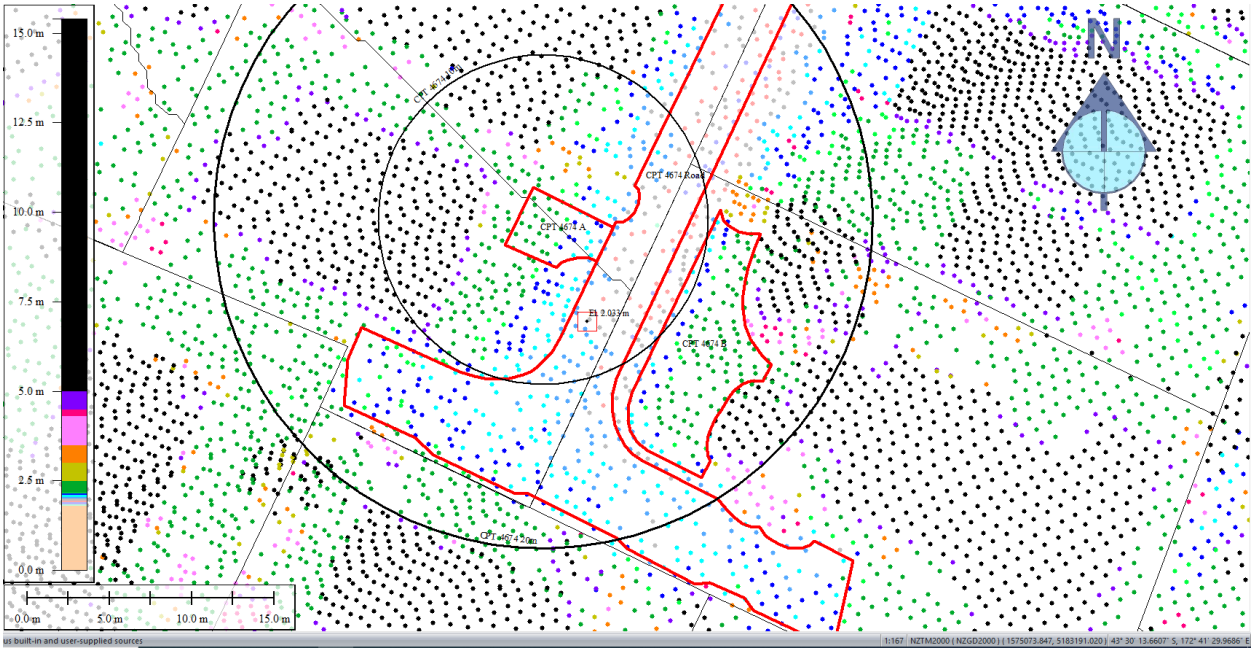

Figure 56: Ground surface elevation averaged over the 20-m buffer for Road for Sep 5, 2010 LiDAR survey.

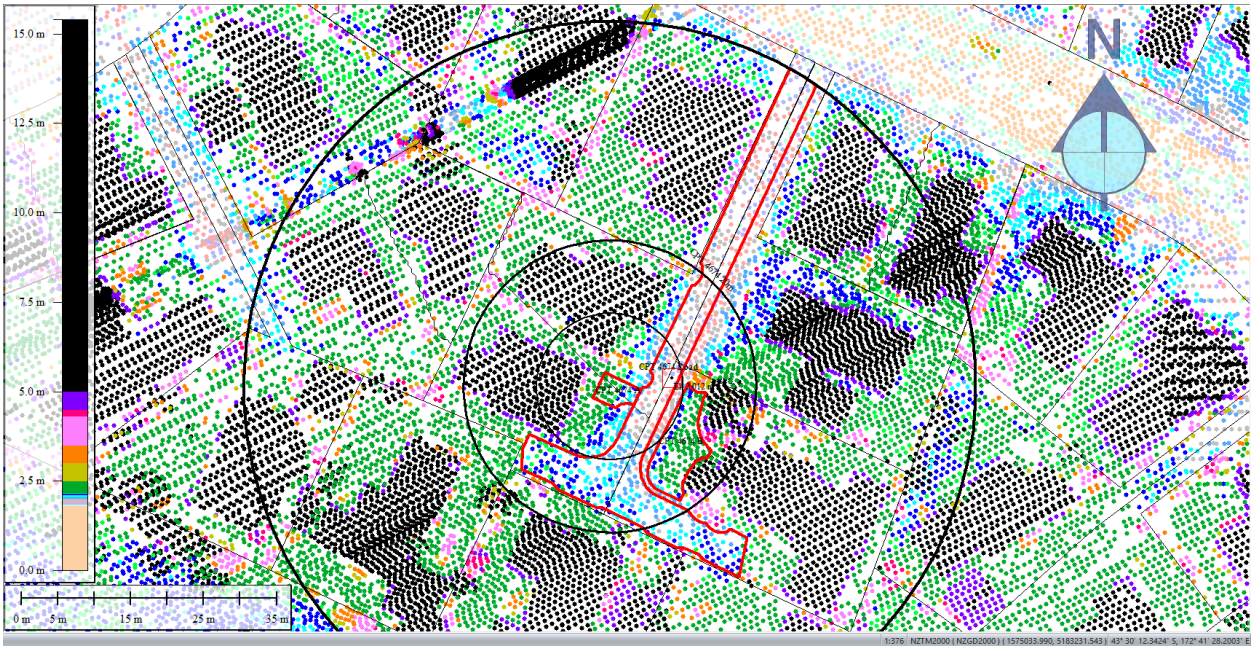

Figure 57: Ground surface elevation averaged over the 50-m buffer for Road for Sep 5, 2010 LiDAR survey.

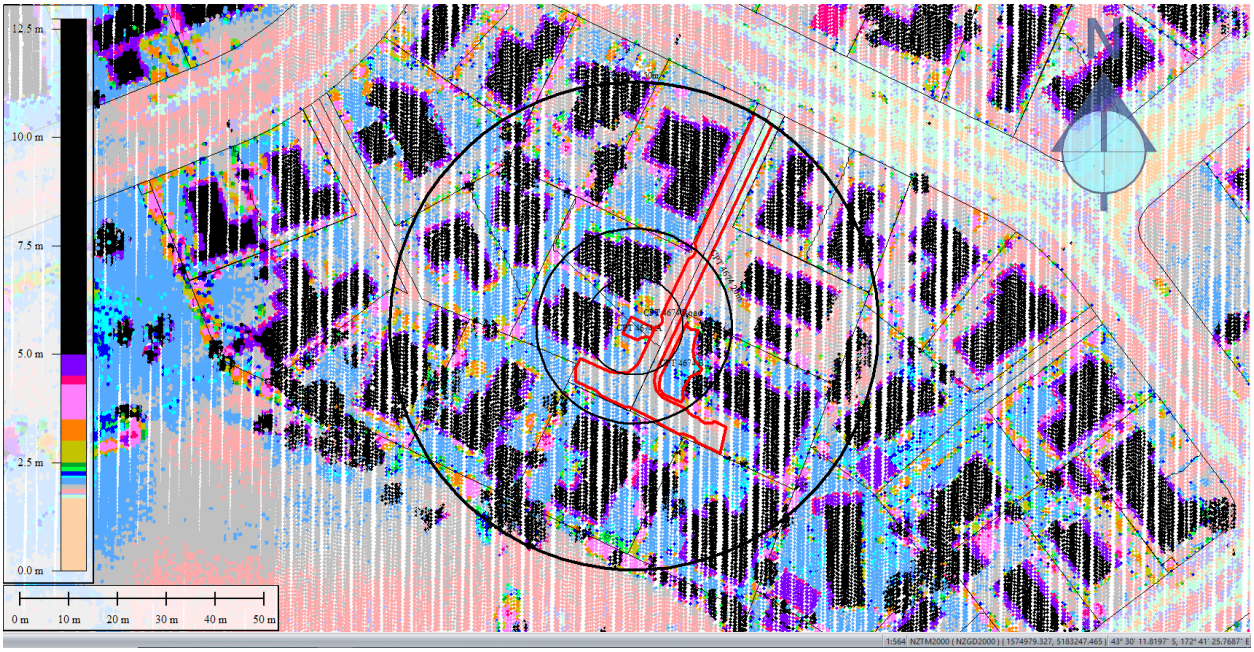

Figure 58: Mar 2011 LiDAR survey.

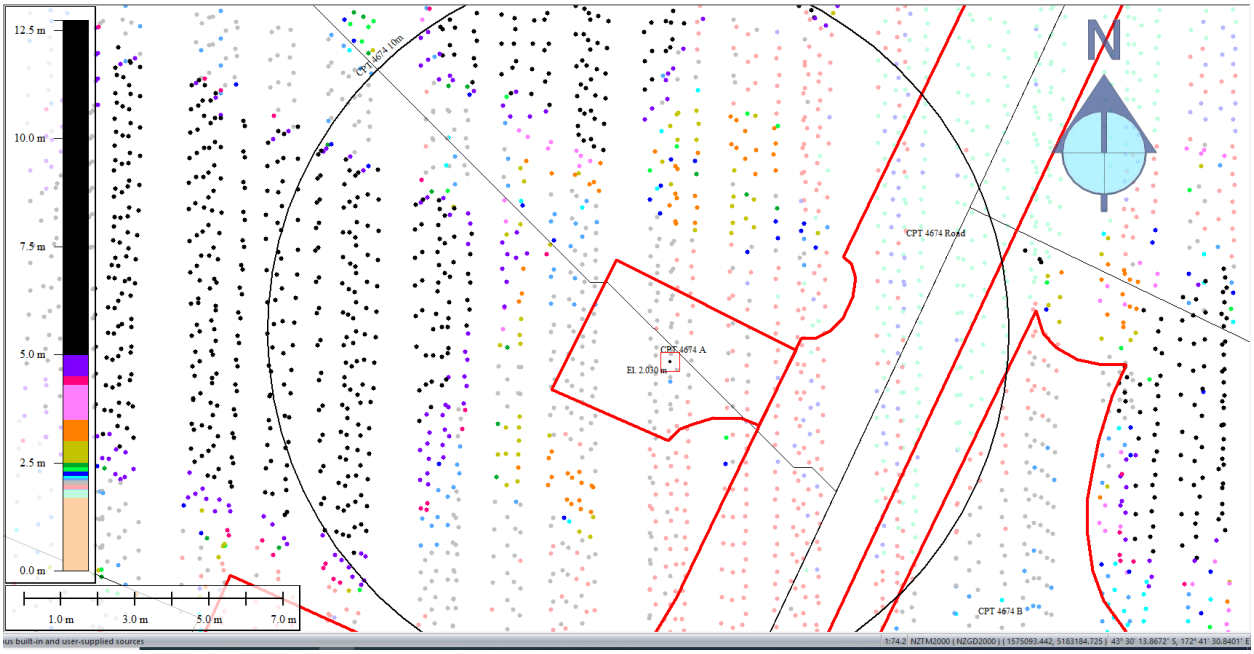

Figure 59: Ground surface elevation for Patch A for Mar 2011 LiDAR survey.

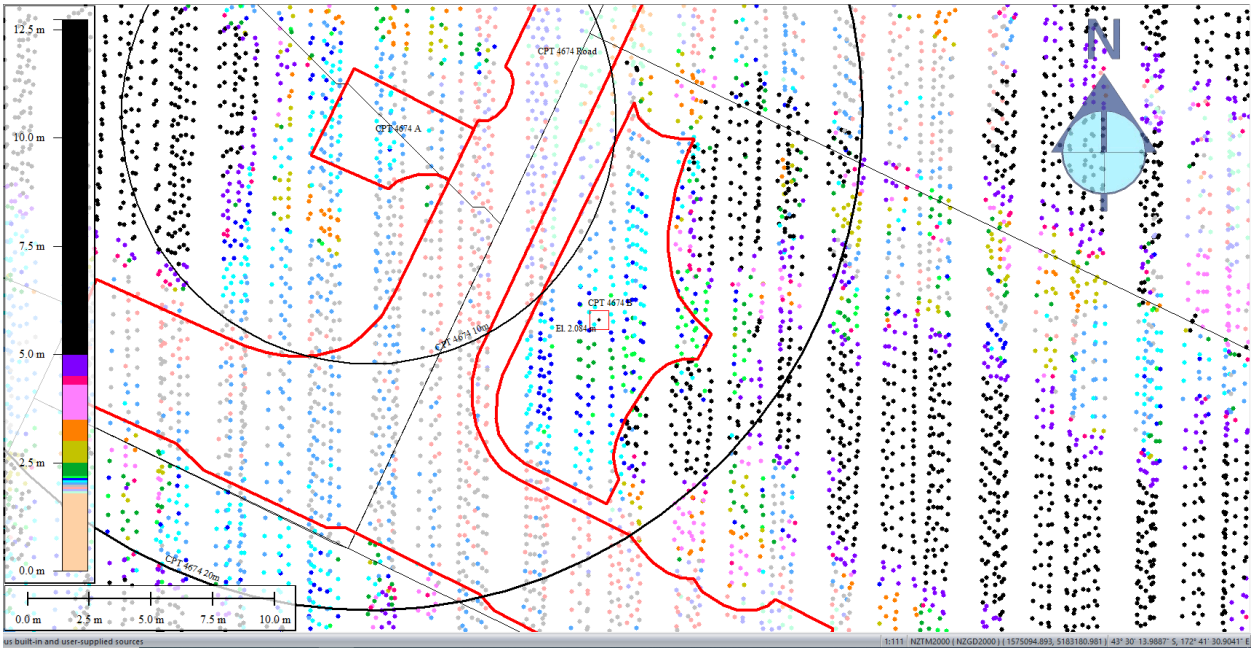

Figure 60: Ground surface elevation for Patch B for Mar 2011 LiDAR survey.

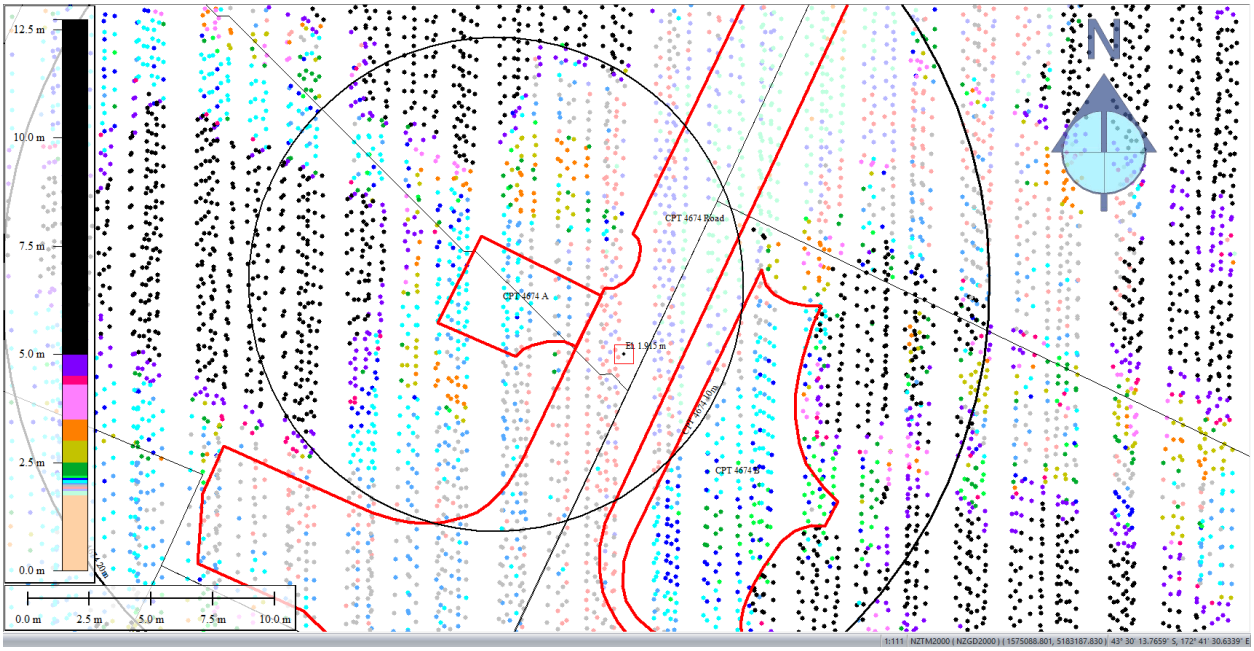

Figure 61: Ground surface elevation averaged over the 10-m buffer Road for Mar 2011 LiDAR survey.

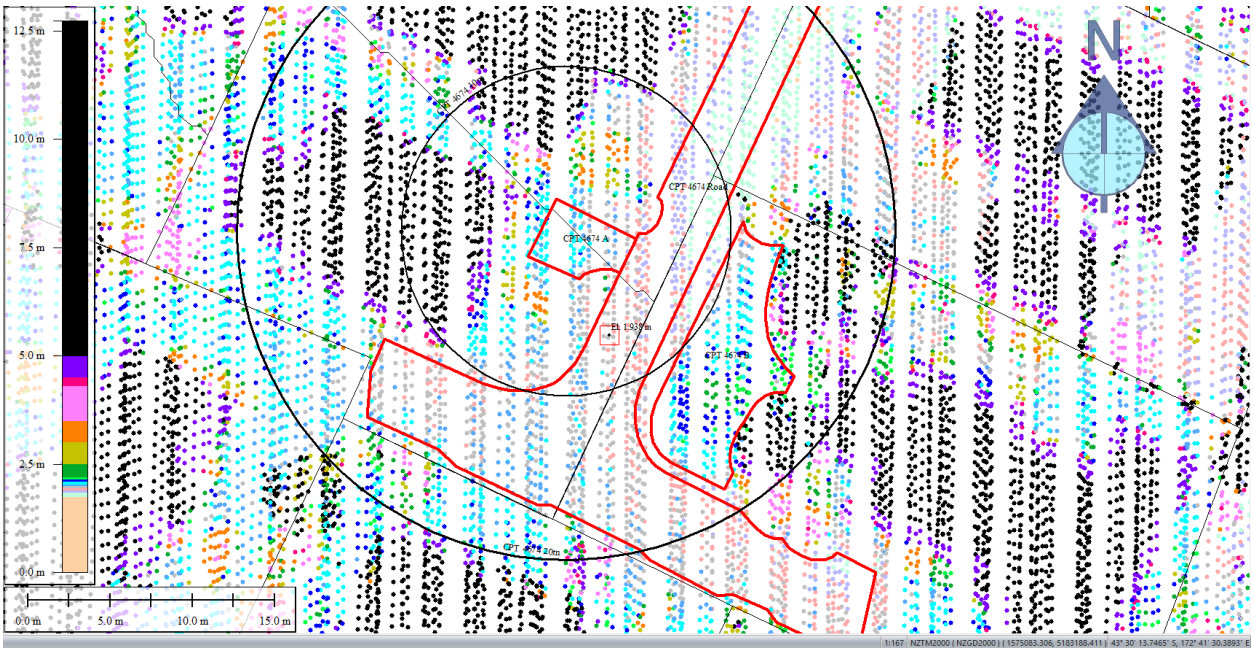

Figure 62: Ground surface elevation averaged over the 20-m buffer Road for Mar 2011 LiDAR survey.

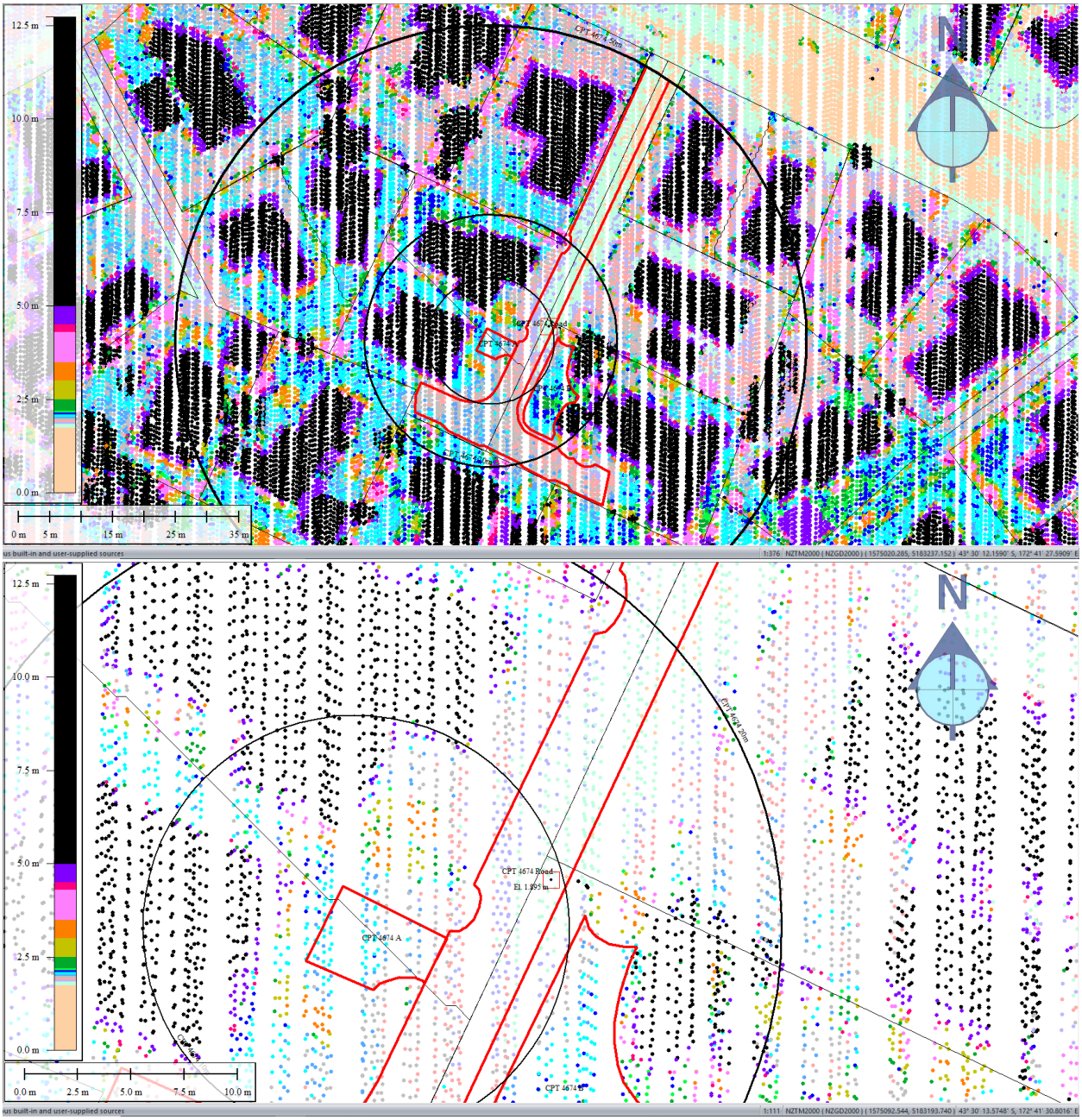

Figure 63: Ground surface elevation averaged over the 50-m buffer Road for Mar 2011 LiDAR survey.

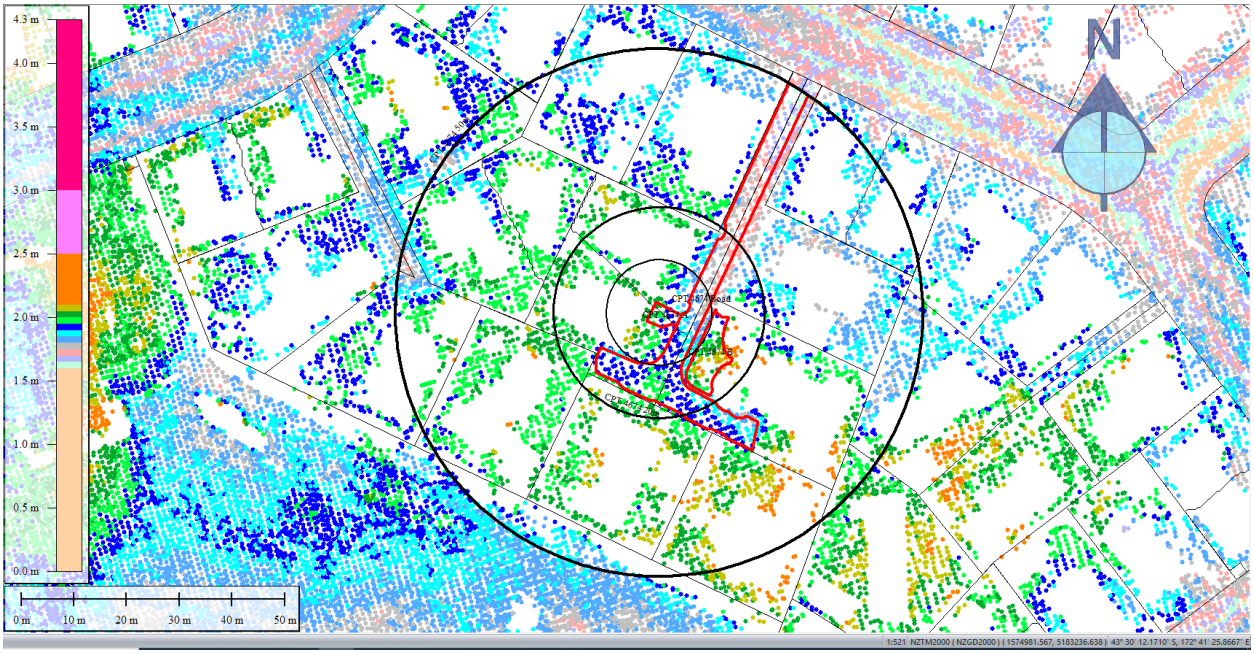

Figure 64: May 2011 LiDAR survey.

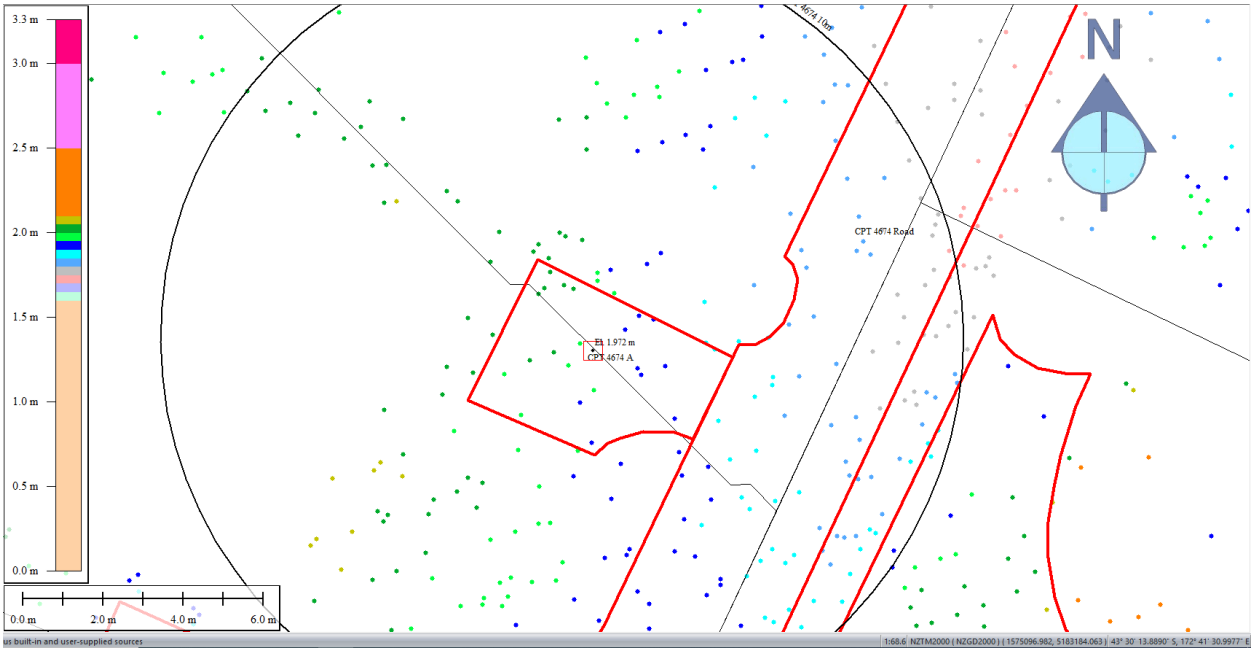

Figure 65: Ground surface elevation for Patch A for May 2011 LiDAR survey.

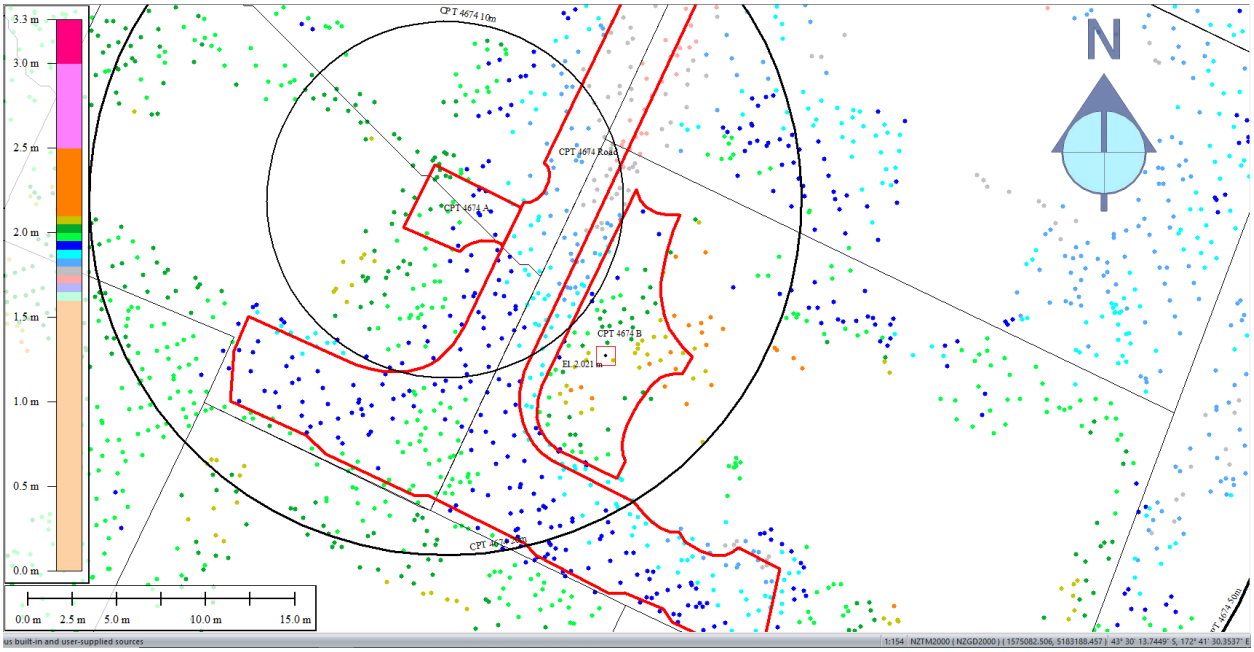

Figure 66: Ground surface elevation for Patch B for May 2011 LiDAR survey.

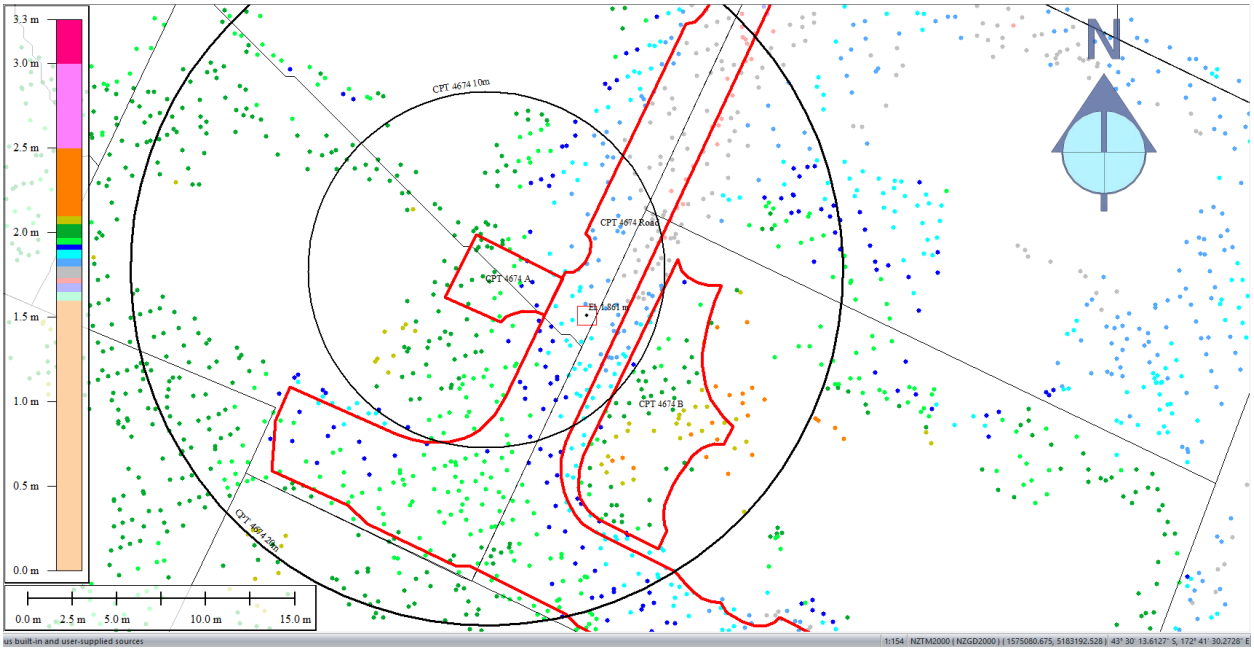

Figure 67: Ground surface elevation averaged over the 10-m buffer for Road for May 2011 LiDAR survey.

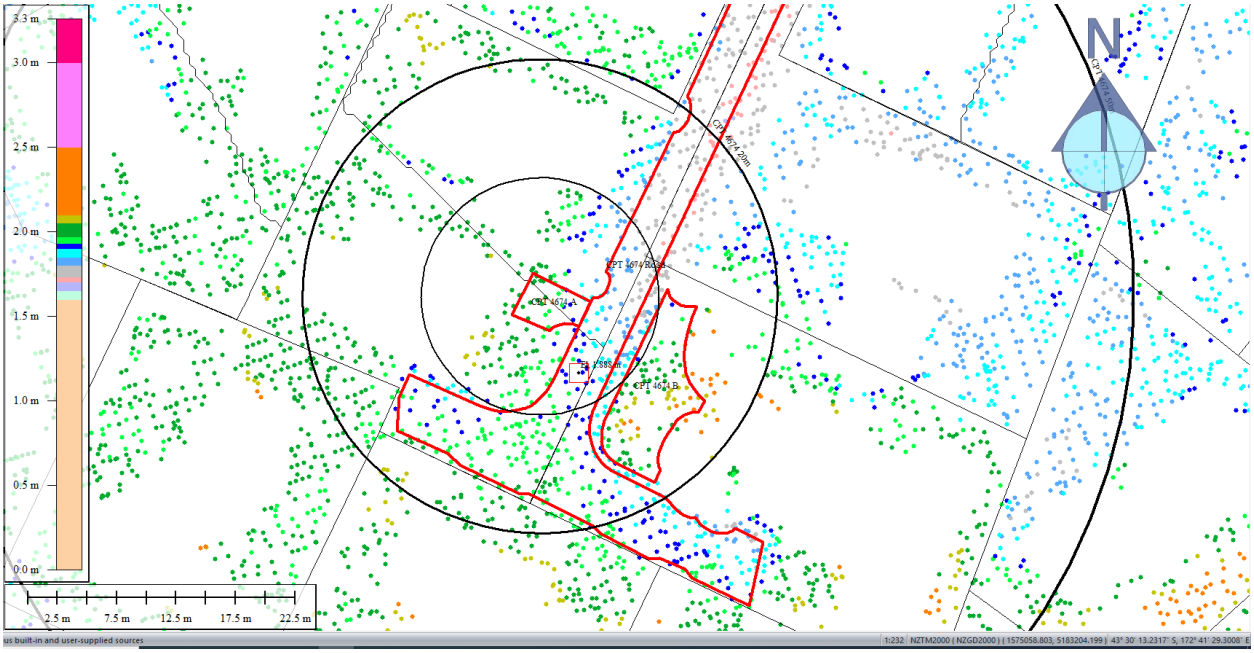

Figure 68: Ground surface elevation averaged over the 20-m buffer for Road for May 2011 LiDAR survey.

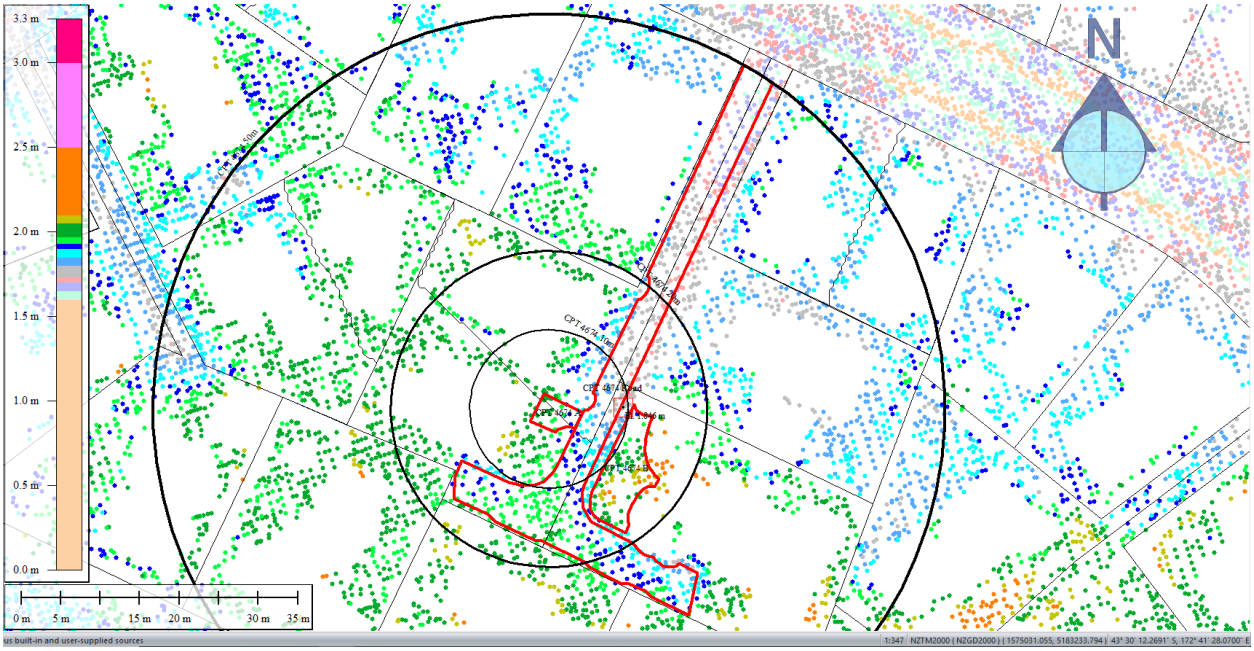

Figure 69: Ground surface elevation averaged over the 50-m buffer for Road for May 2011 LiDAR survey.

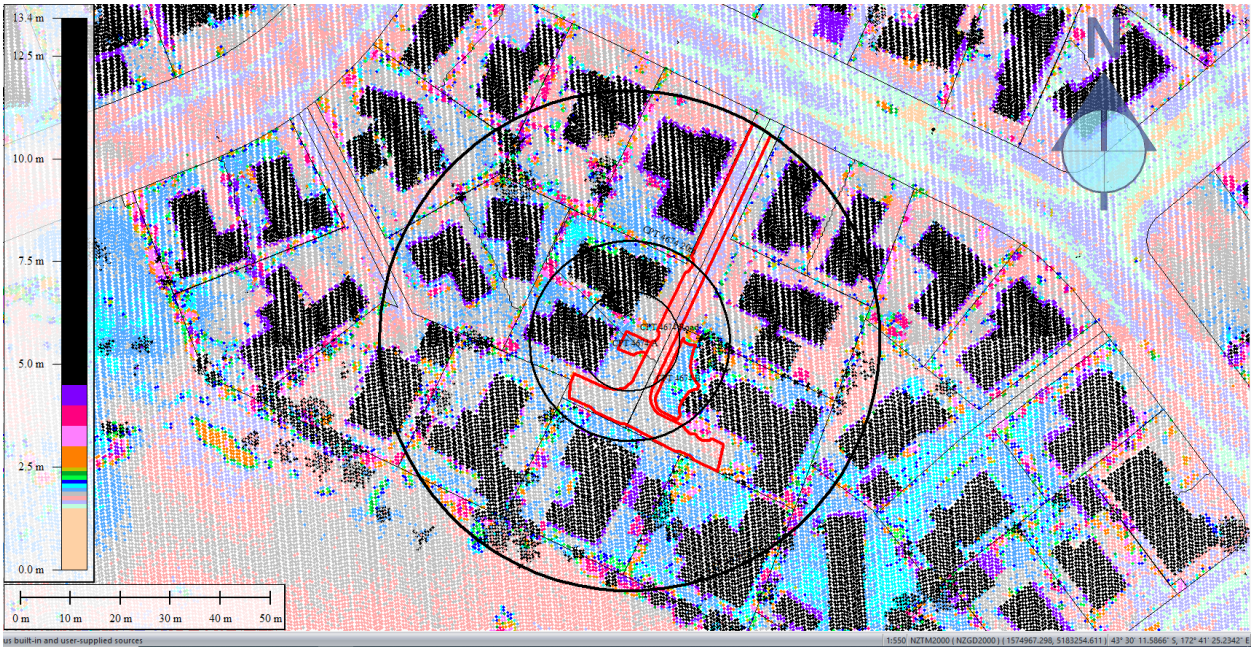

Figure 70: Sep 2011 LiDAR survey.

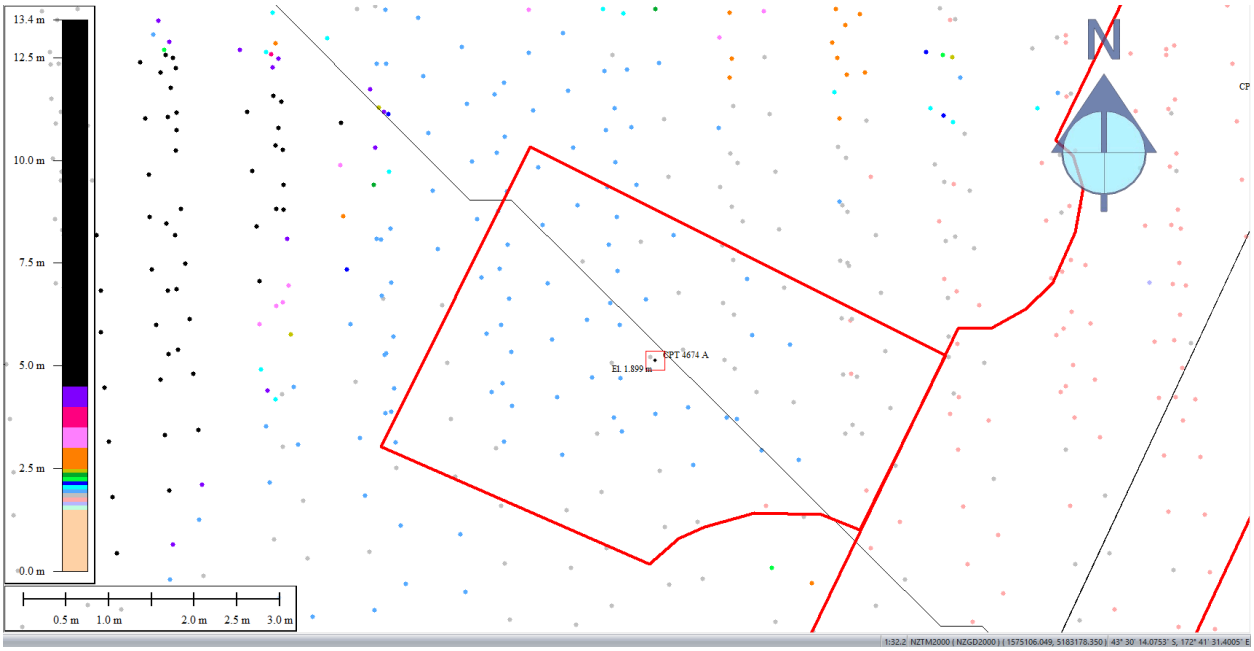

Figure 71: Ground surface elevation for Patch A for Sep 2011 LiDAR survey.

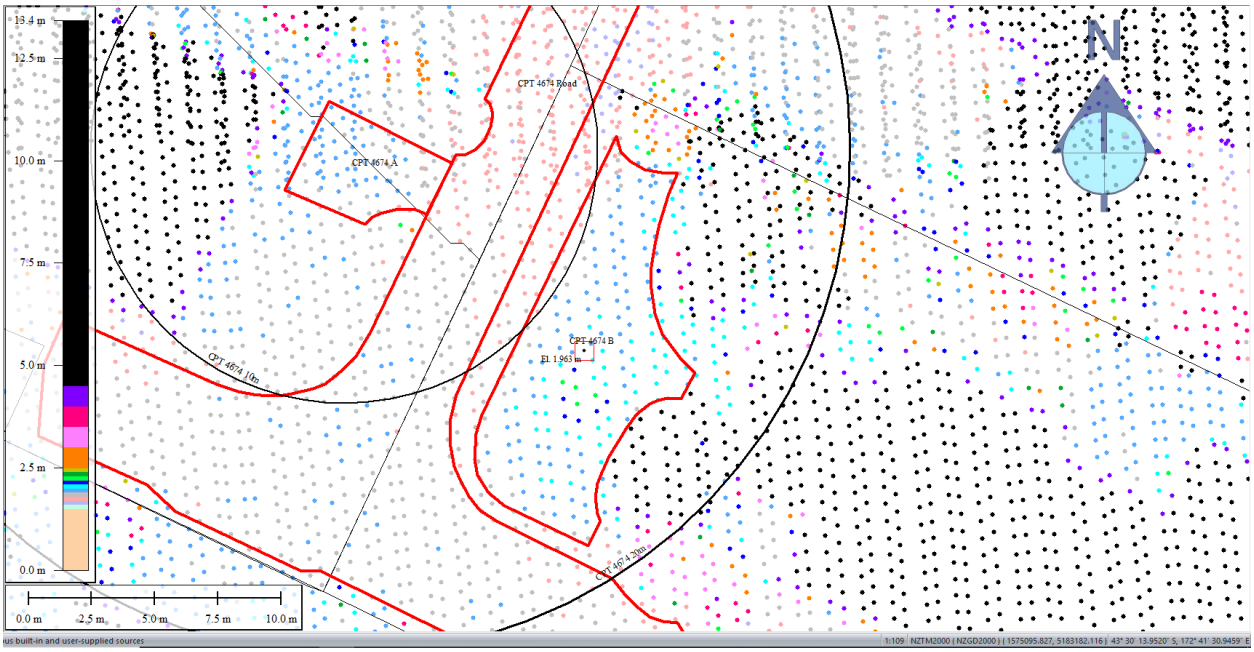

Figure 72: Ground surface elevation for Patch B for Sep 2011 LiDAR survey.

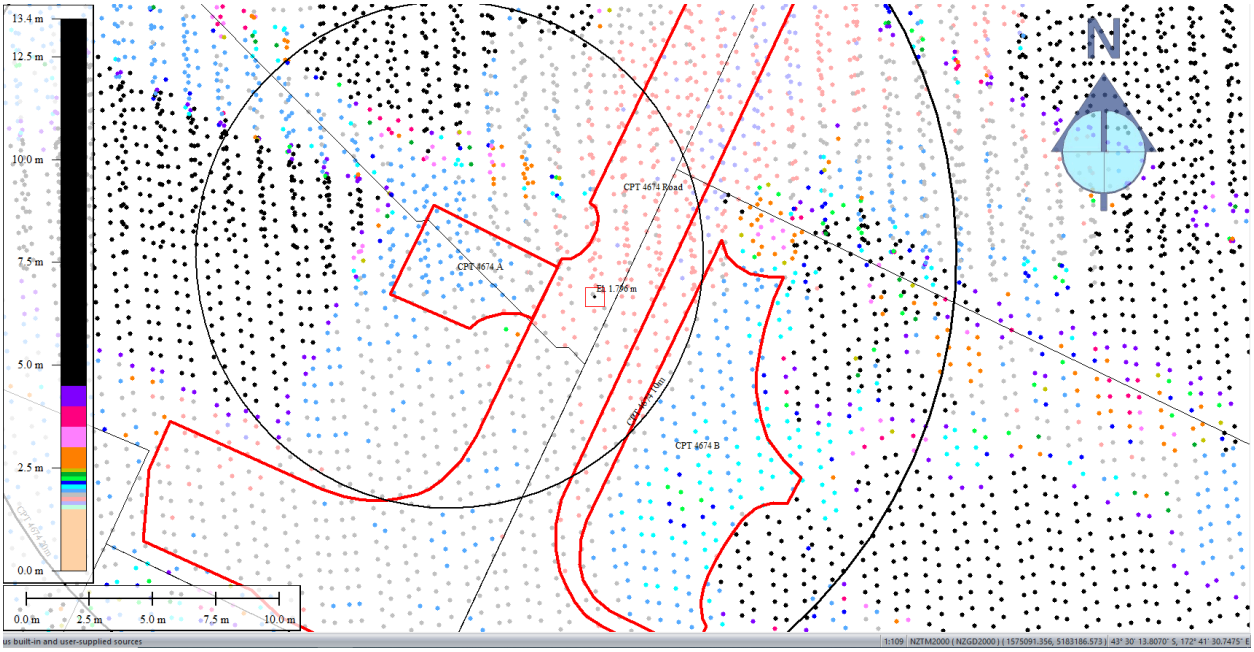

Figure 73: Ground surface elevation averaged over the 10-m buffer for Road for Sep 2011 LiDAR survey.

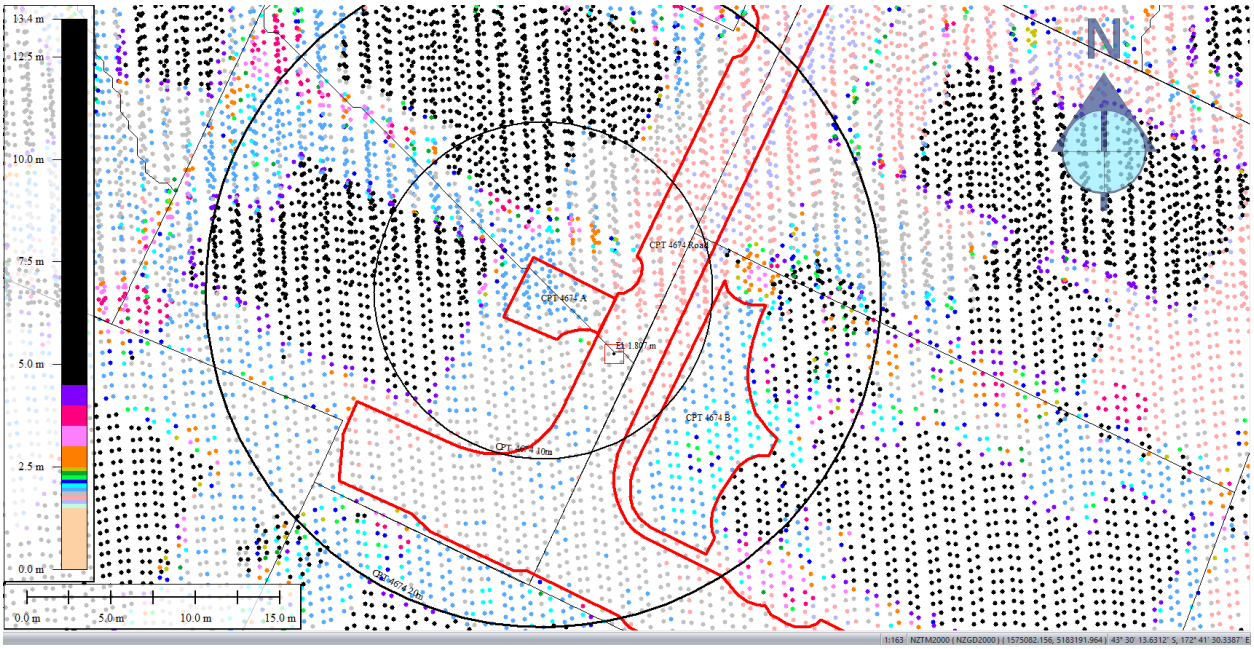

Figure 74: Ground surface elevation averaged over the 20-m buffer for Road for Sep 2011 LiDAR survey.

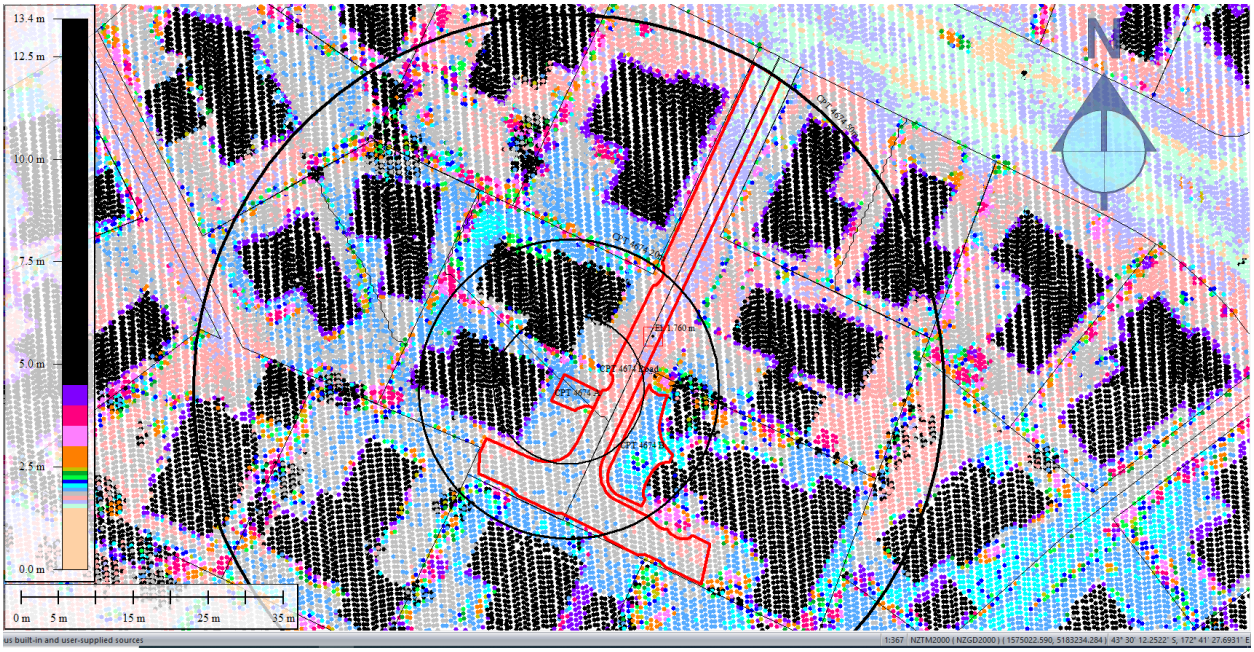

Figure 75: Ground surface elevation averaged over the 50-m buffer for Road for Sep 2011 LiDAR survey.

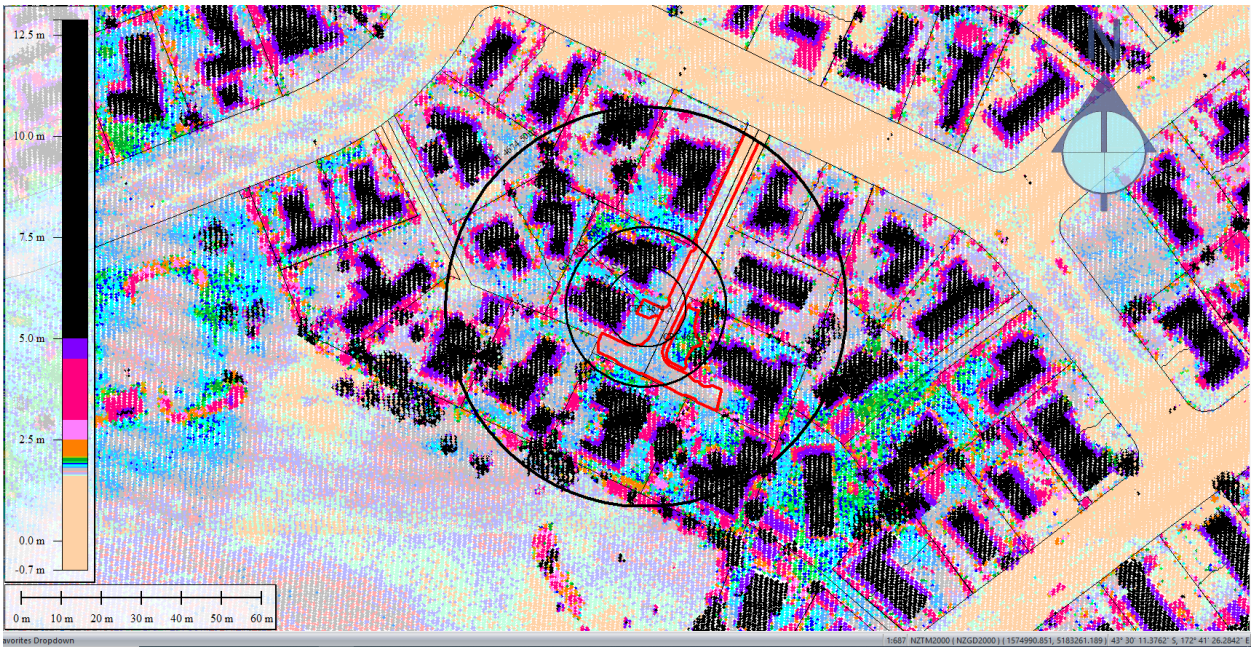

Figure 76: Feb 2012 LiDAR survey.

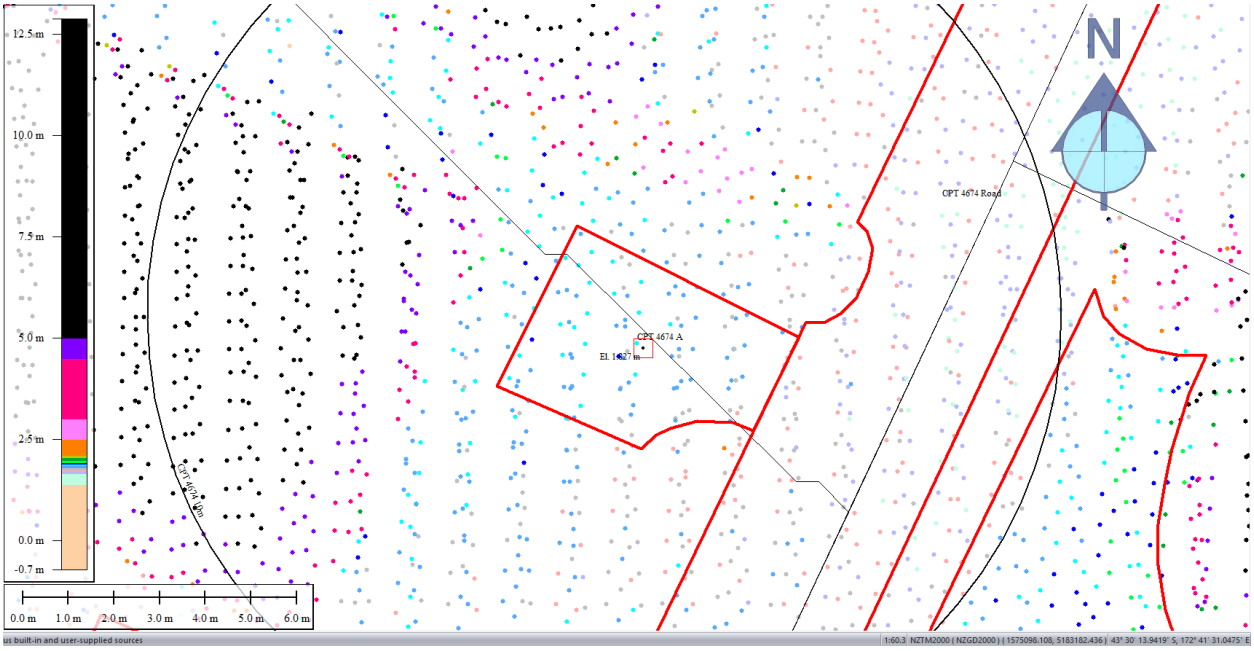

Figure 77: Ground surface elevation for Patch A for Feb 2012 LiDAR survey.

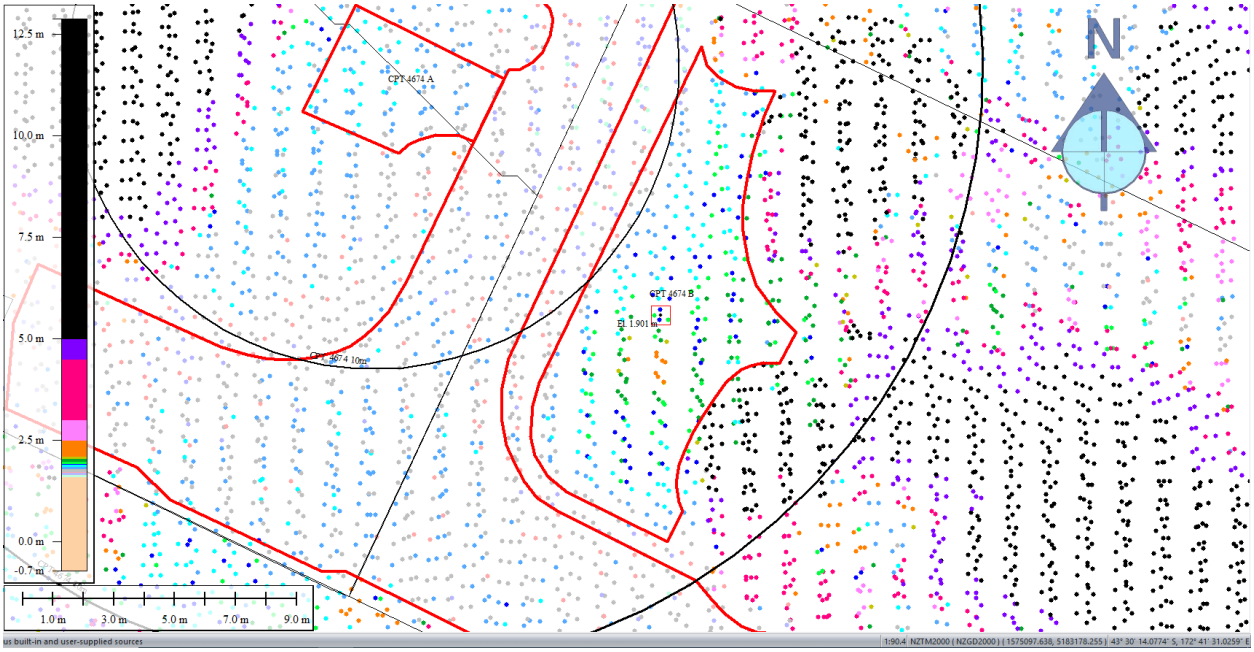

Figure 78: Ground surface elevation for Patch B for Feb 2012 LiDAR survey.

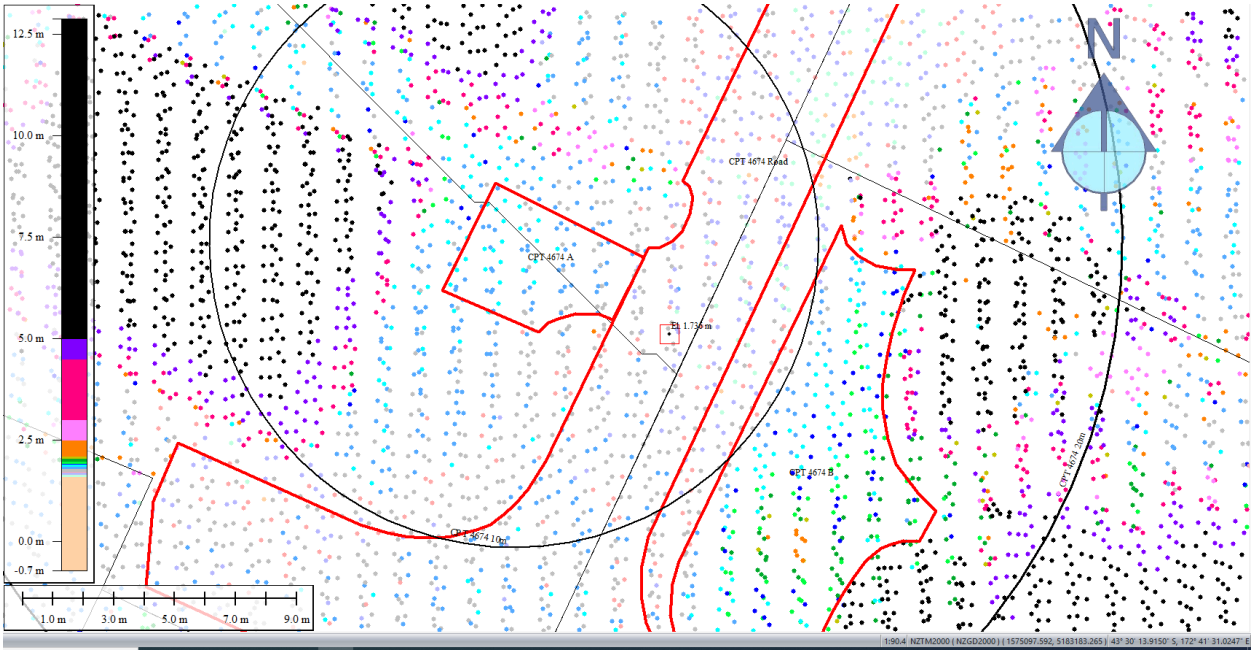

Figure 79: Ground surface elevation averaged over the 10-m buffer for Road for Feb 2012 LiDAR survey.

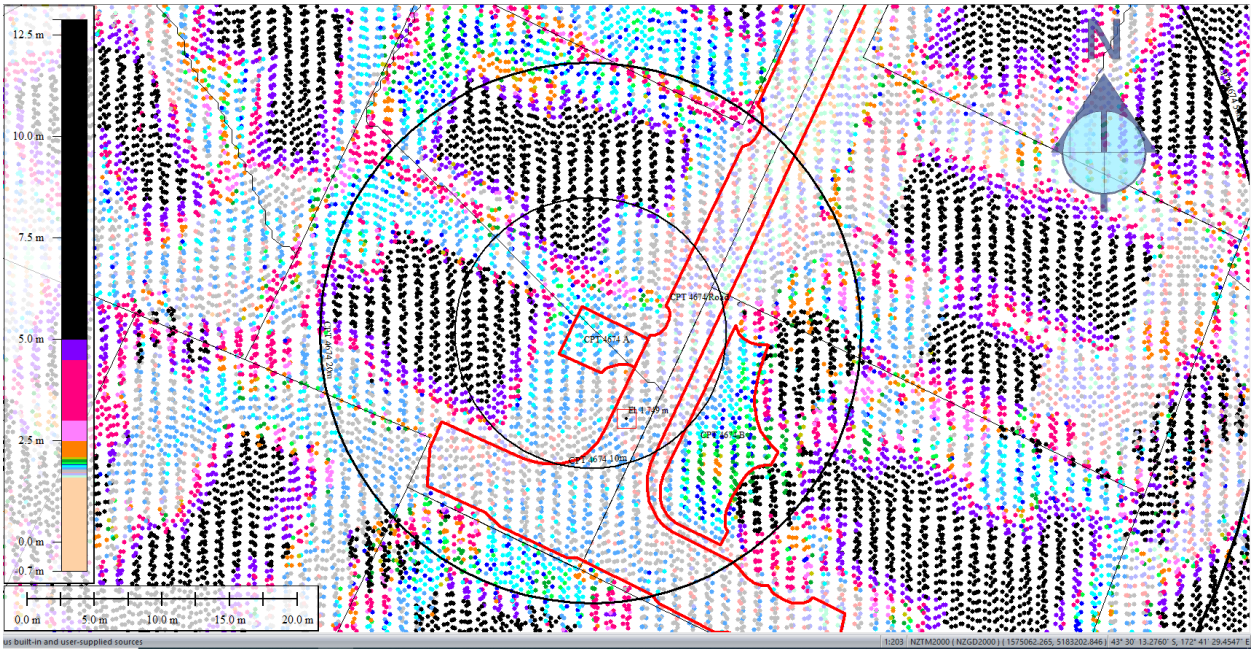

Figure 80: Ground surface elevation averaged over the 20-m buffer for Road for Feb 2012 LiDAR survey.

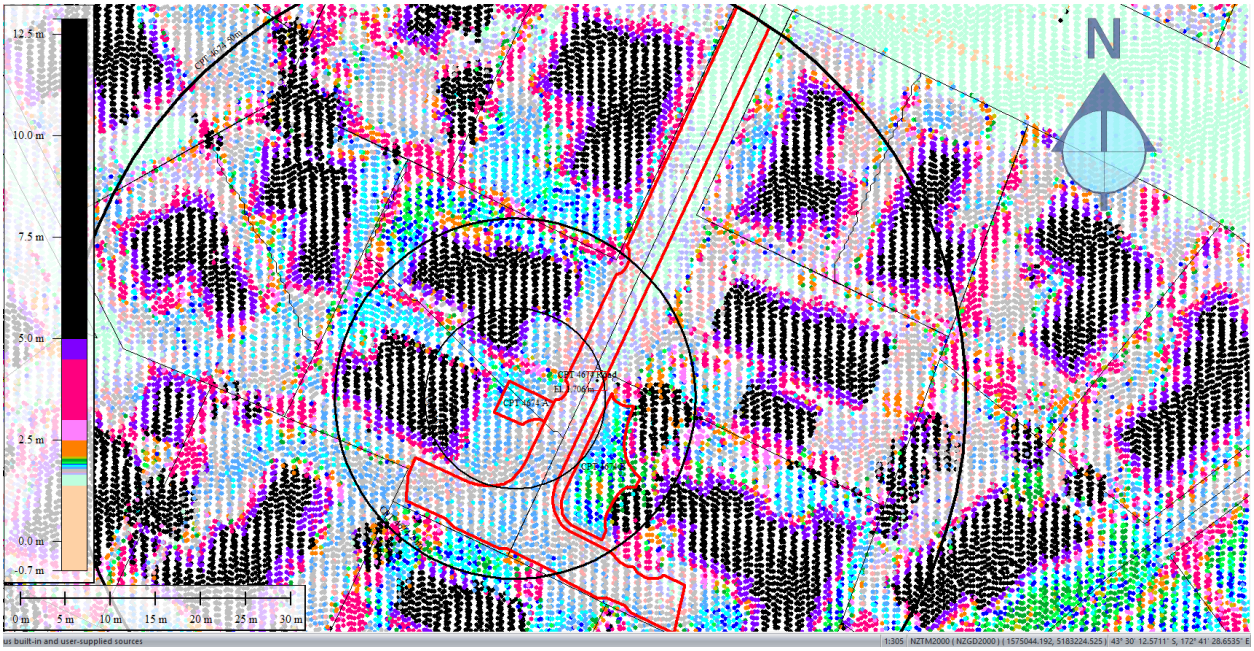

Figure 81: Ground surface elevation averaged over the 50-m buffer for Road for Feb 2012 LiDAR survey.

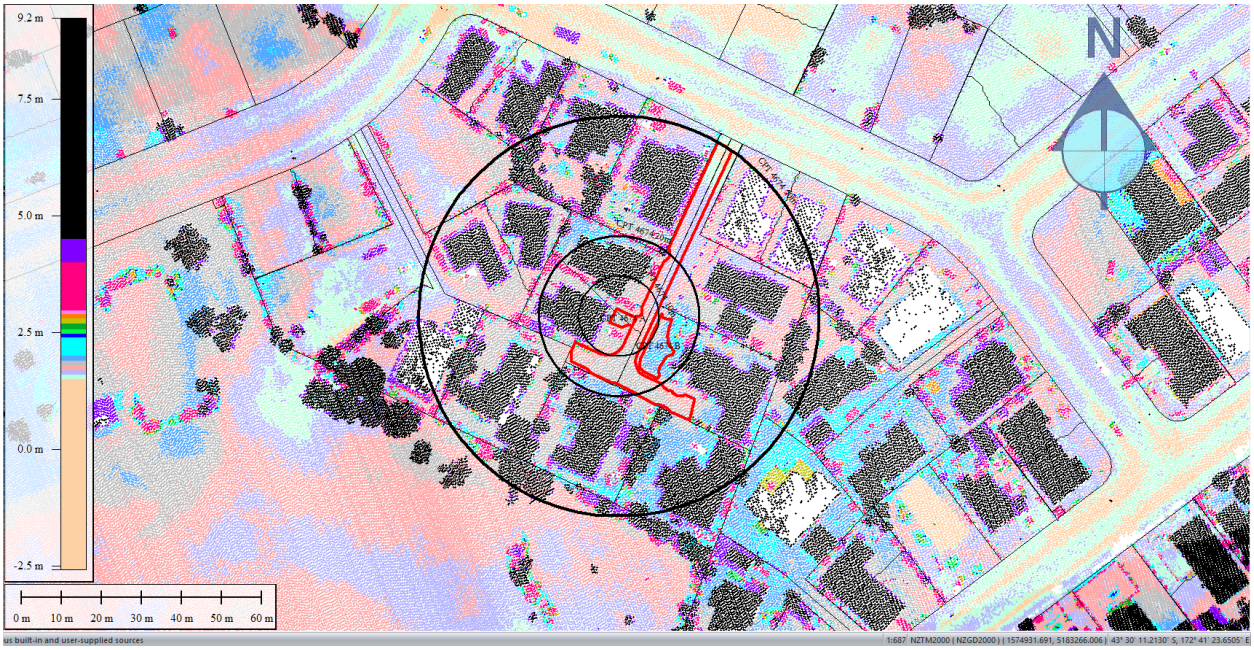

Figure 82: Oct 2015 LiDAR survey.

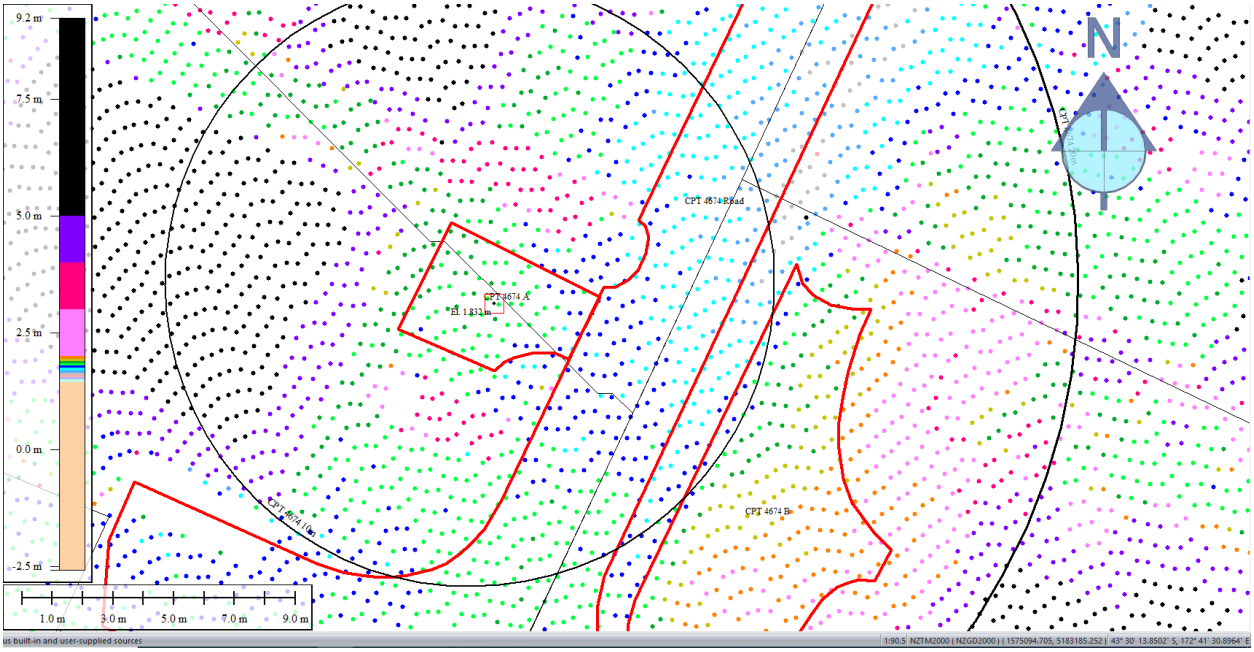

Figure 83: Ground surface elevation for Patch A for Oct 2015 LiDAR survey.

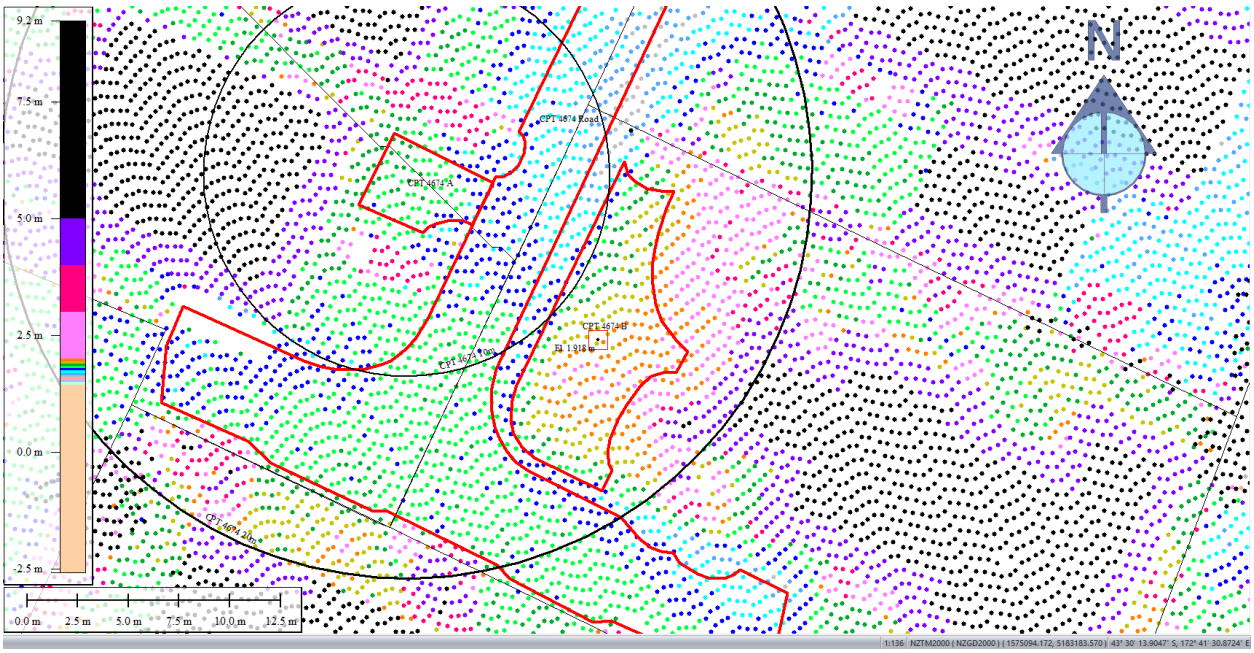

Figure 84: Ground surface elevation for Patch B for Oct 2015 LiDAR survey.

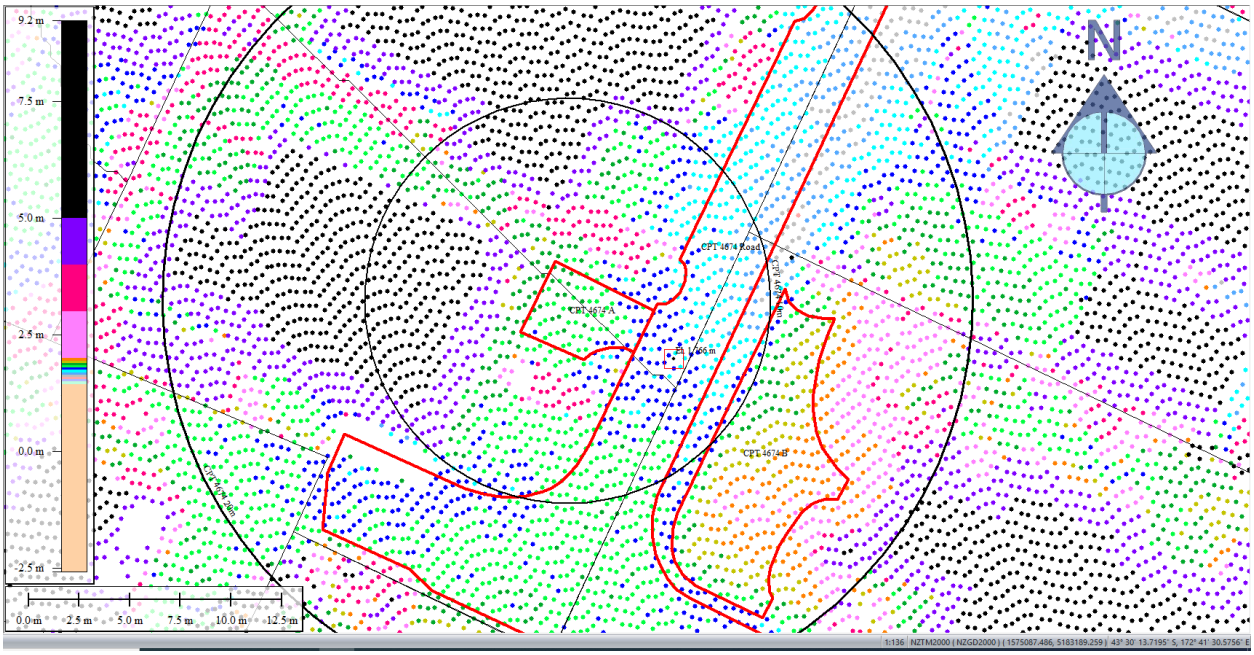

Figure 85: Ground surface elevation averaged over the 10-m buffer for Road for Oct 2015 LiDAR survey.

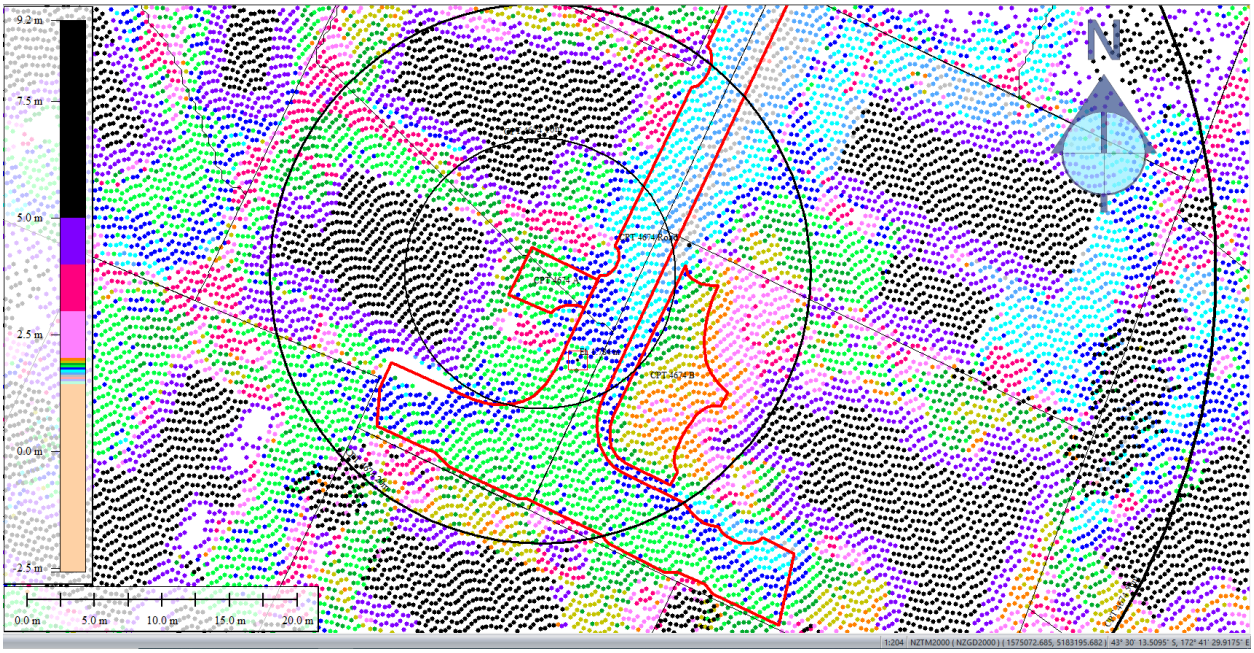

Figure 86: Ground surface elevation averaged over the 20-m buffer for Road for Oct 2015 LiDAR survey.

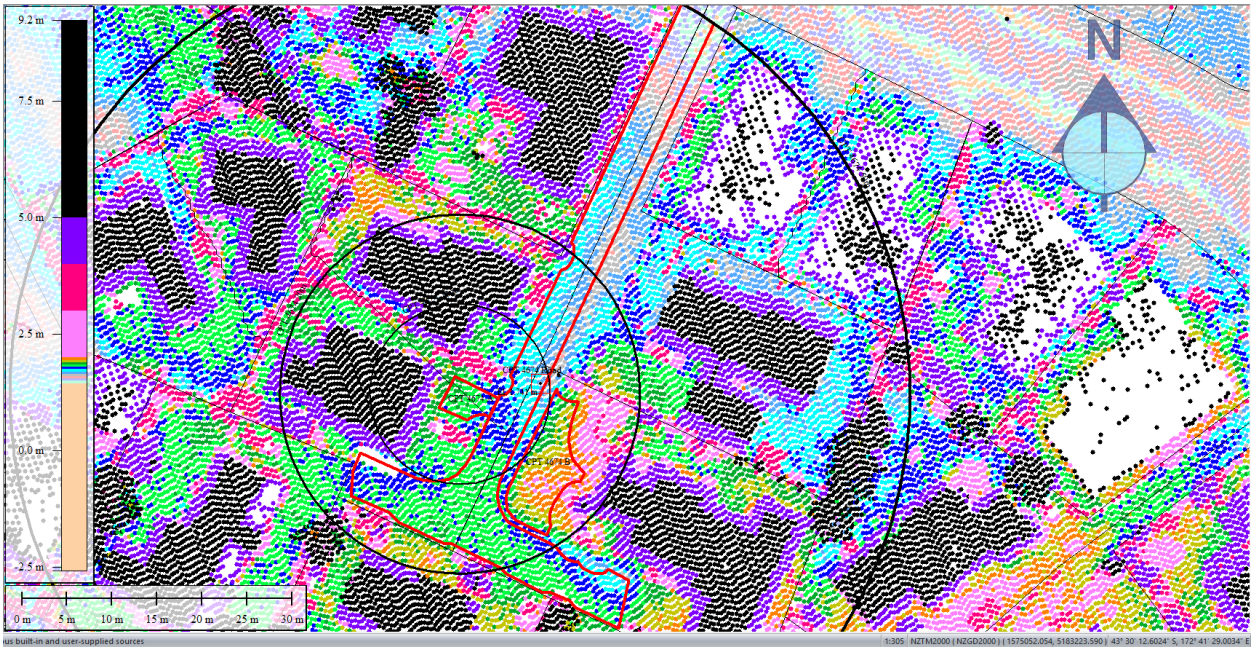

Figure 87: Ground surface elevation averaged over the 50-m buffer for Road for Oct 2015 LiDAR survey.

Figure 88: Aerial photograph showing absence of ejecta for Sep-10 EQ.

Figure 89: Satellite image from 23 Feb 2011 showing ejecta at the site.

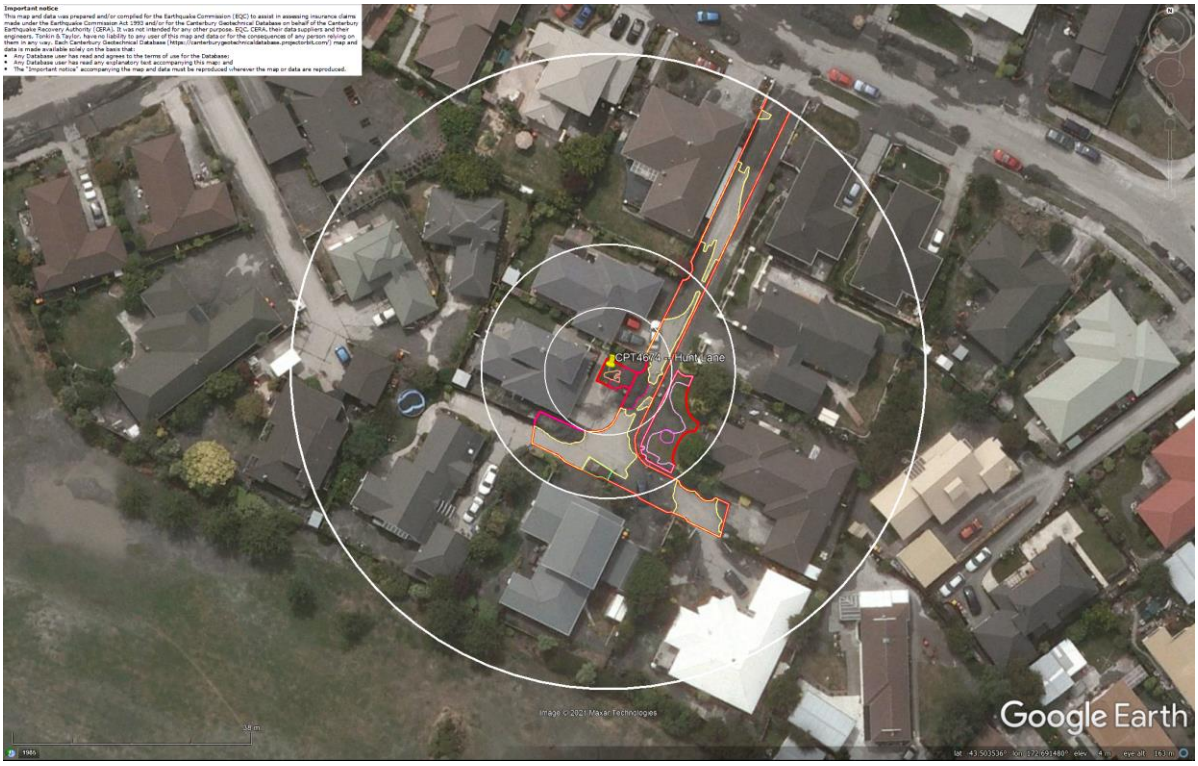

Figure 90: Ejecta outline for Feb-11 EQ.

Figure 91: Satellite image from 28 Mar 2011 showing no ejecta at the site (other than the blind sand boil within Patch B).

Figure 92: Aerial photograph from 14-15 Jun 2011 showing ejecta at the site.

Figure 93: Ejecta outline for Jun-11 EQ.

Figure 94: Ejecta outline for Dec-11 EQ.

Contents of this figure cannot be shared as doing so is restricted by a Non-Disclosure Agreement.

Figure 95: EQC LDAT property inspection notes for Patch A from Aug 2011.

Contents of this figure cannot be shared as doing so is restricted by a Non-Disclosure Agreement.

Figure 96: LDAT property inspection notes for Patch B (Aug 2011).

Contents of this figure cannot be shared as doing so is restricted by a Non-Disclosure Agreement.

Figure 97: LDAT property inspection notes for Road (Aug 2011).

Contents of this figure cannot be shared as doing so is restricted by a Non-Disclosure Agreement.

Figure 98: LDAT Property inspection notes for the property near Road (Aug 2011).

Contents of this figure cannot be shared as doing so is restricted by a Non-Disclosure Agreement.

Figure 99: LDAT Property inspection notes for the property near Road (Aug 2011).

Figure 100: Ground photograph of Patch B (Aug 2011).

Figure 101: Ground photographs of Road (Aug 2011).

Figure 102: PGA for Sep-10 EQ (st. dev. = 0.275-0.300 ln units).

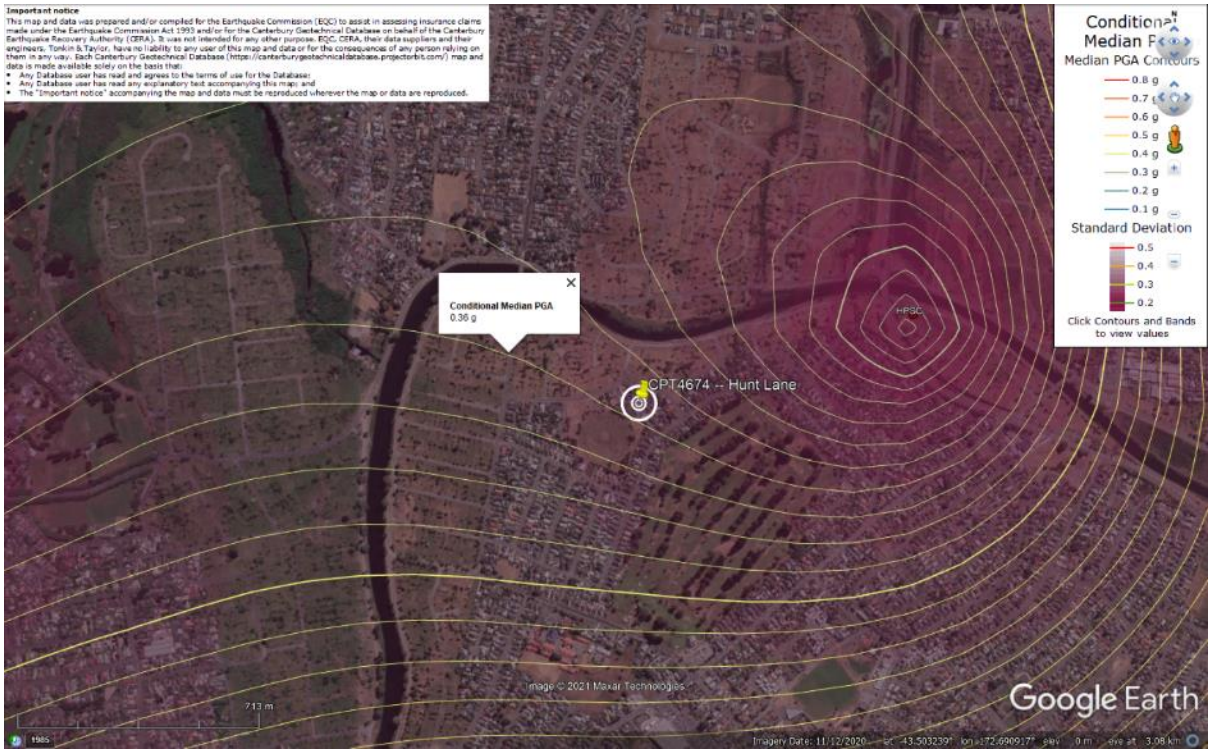

Figure 103: PGA for Feb-11 EQ (st. dev. = 0.300-0.325 ln units).

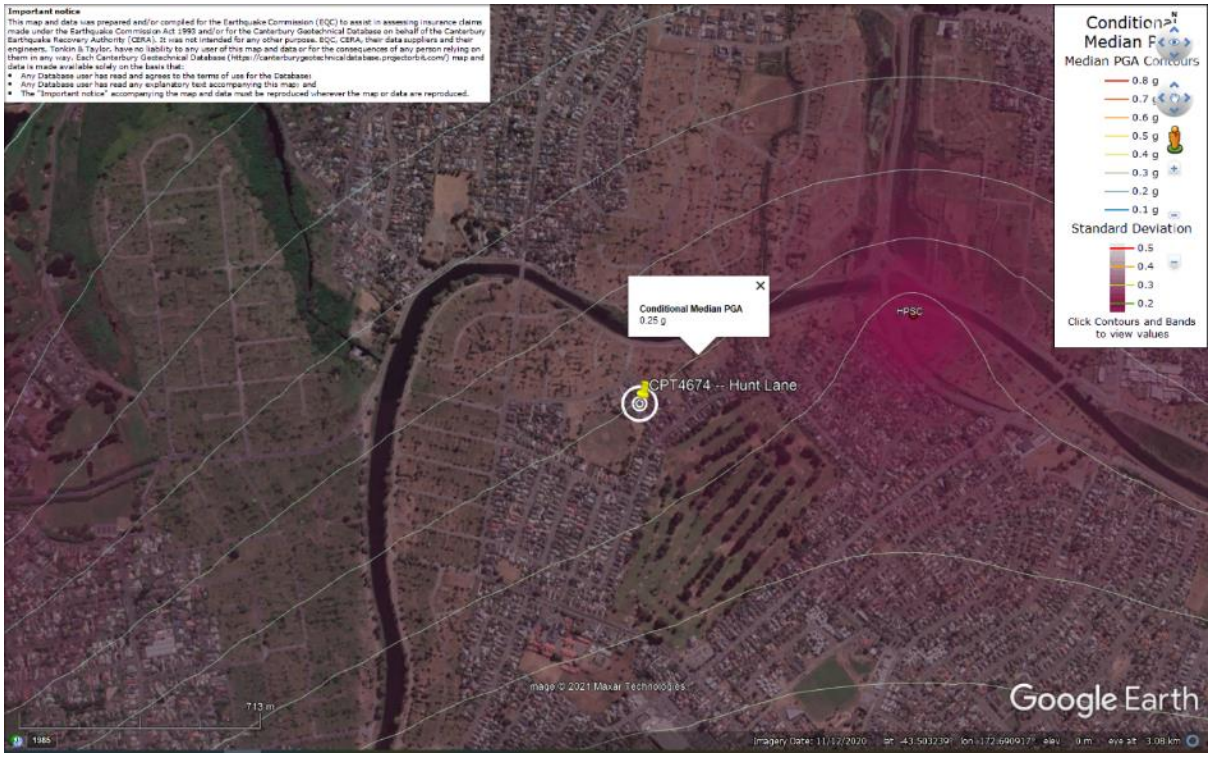

Figure 104: PGA for Jun-11 EQ (st. dev. = 0.300-0.350 ln units).

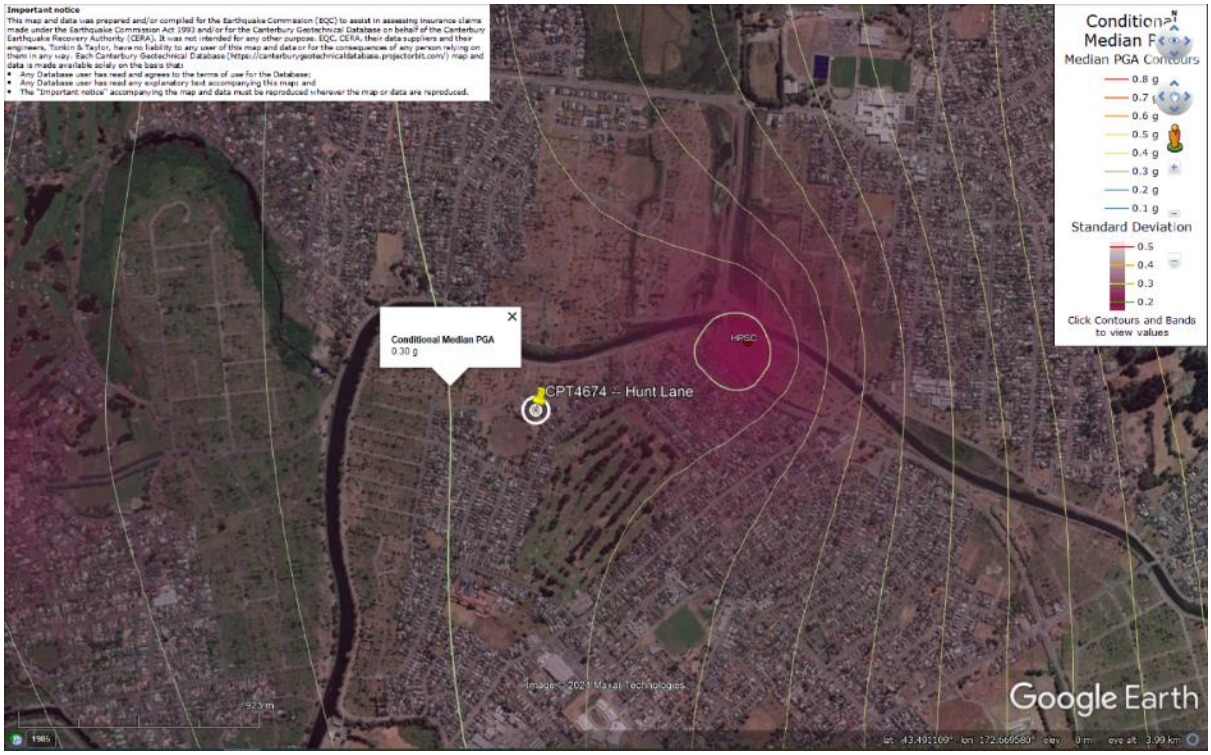

Figure 105: PGA for Dec-11 EQ (st. dev. = 0.325-0.350 ln units).

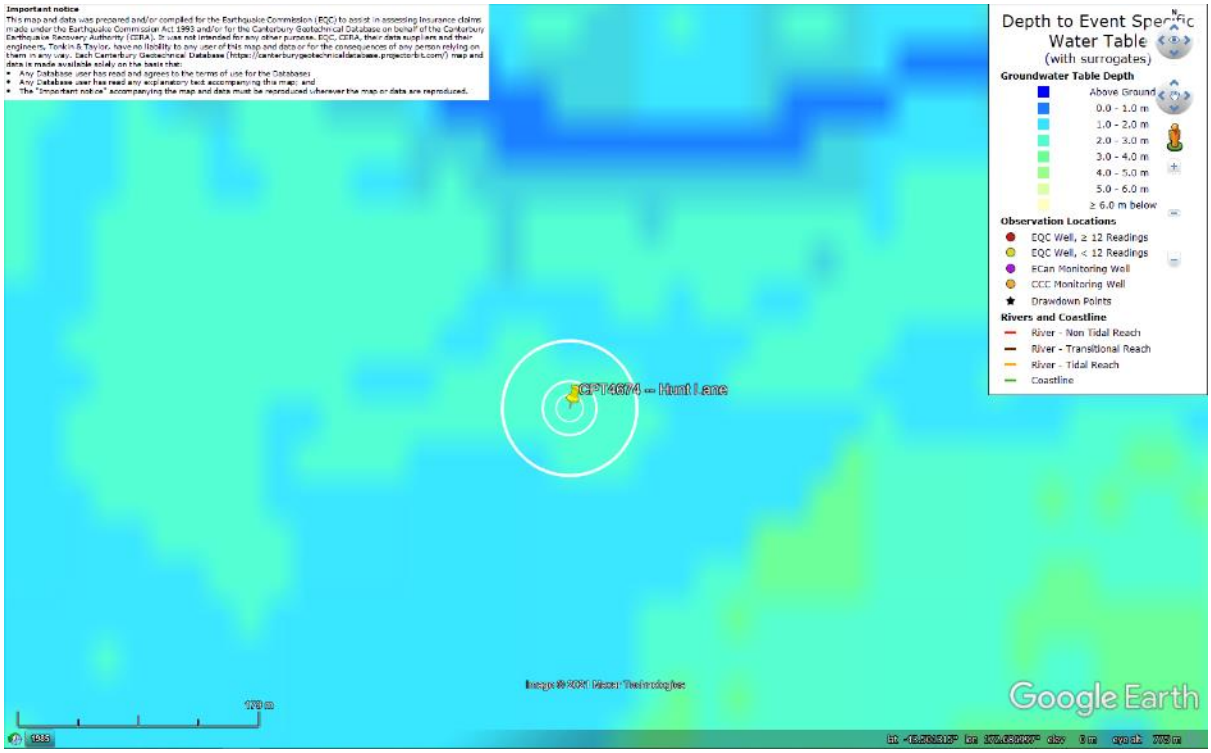

Figure 106: Depth to groundwater table for Sep-10 EQ.

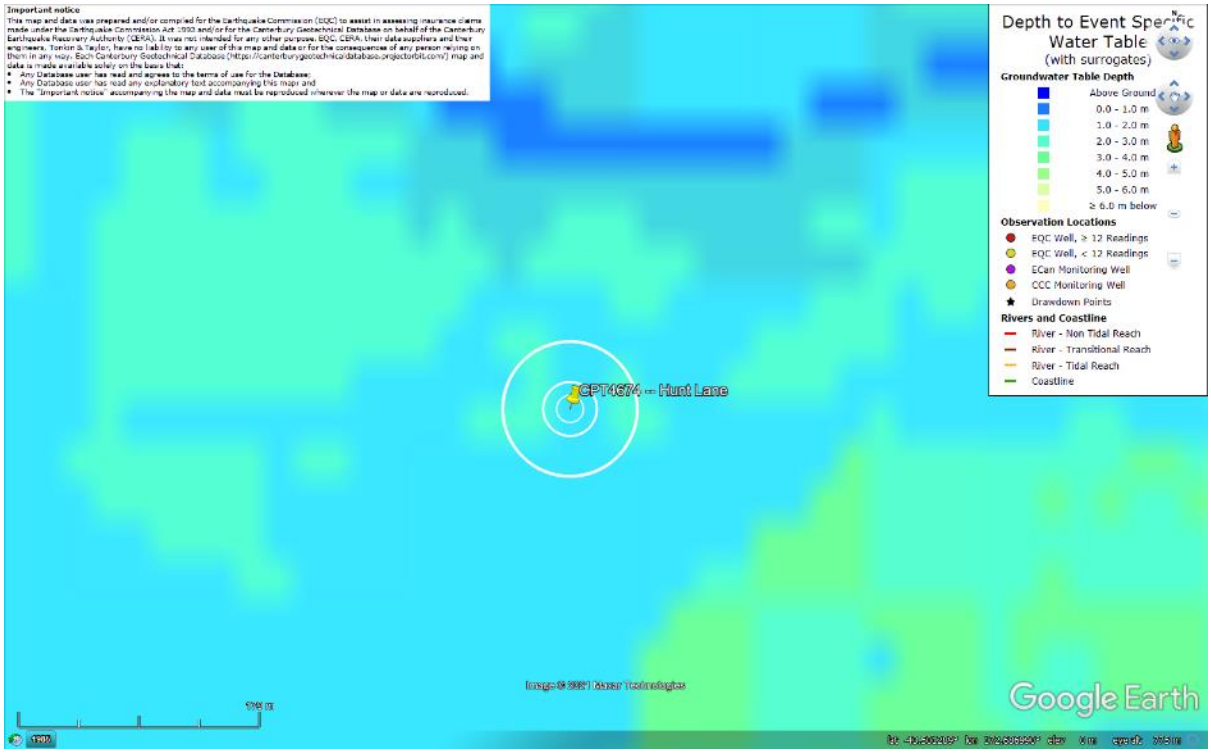

Figure 107: Depth to groundwater table for Feb-11 EQ.

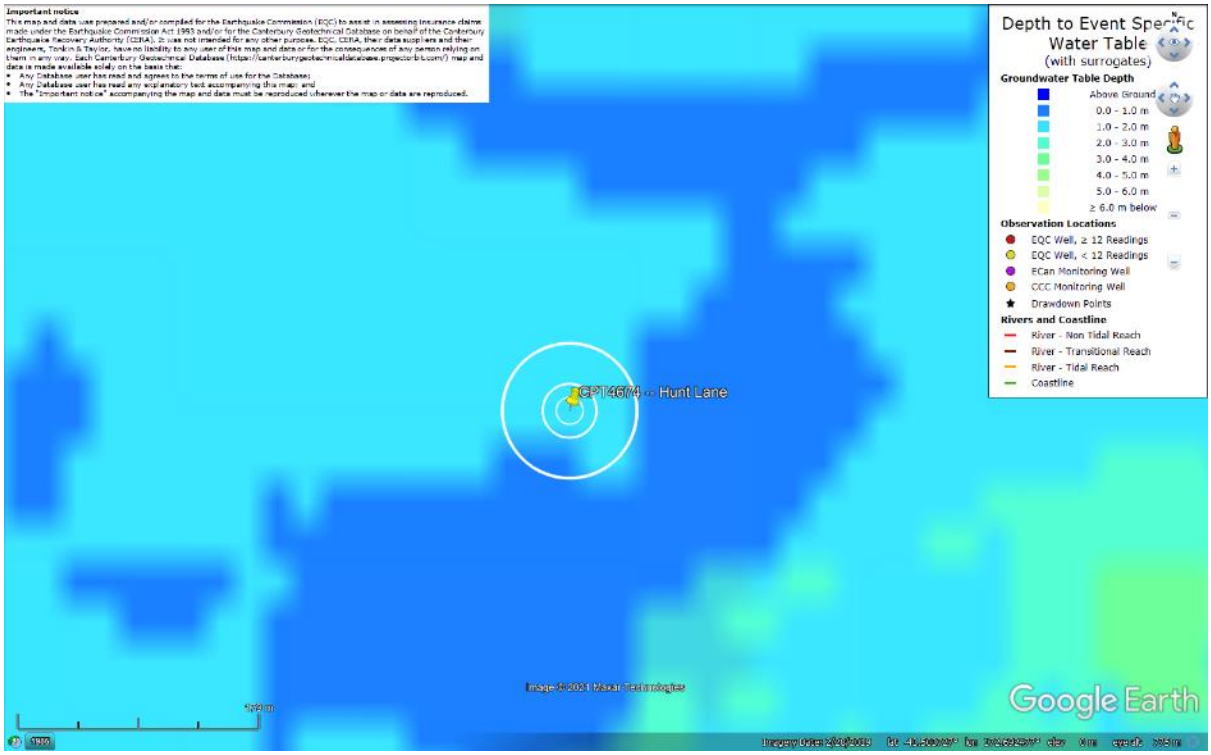

Figure 108: Depth to groundwater table for Jun-11 EQ.

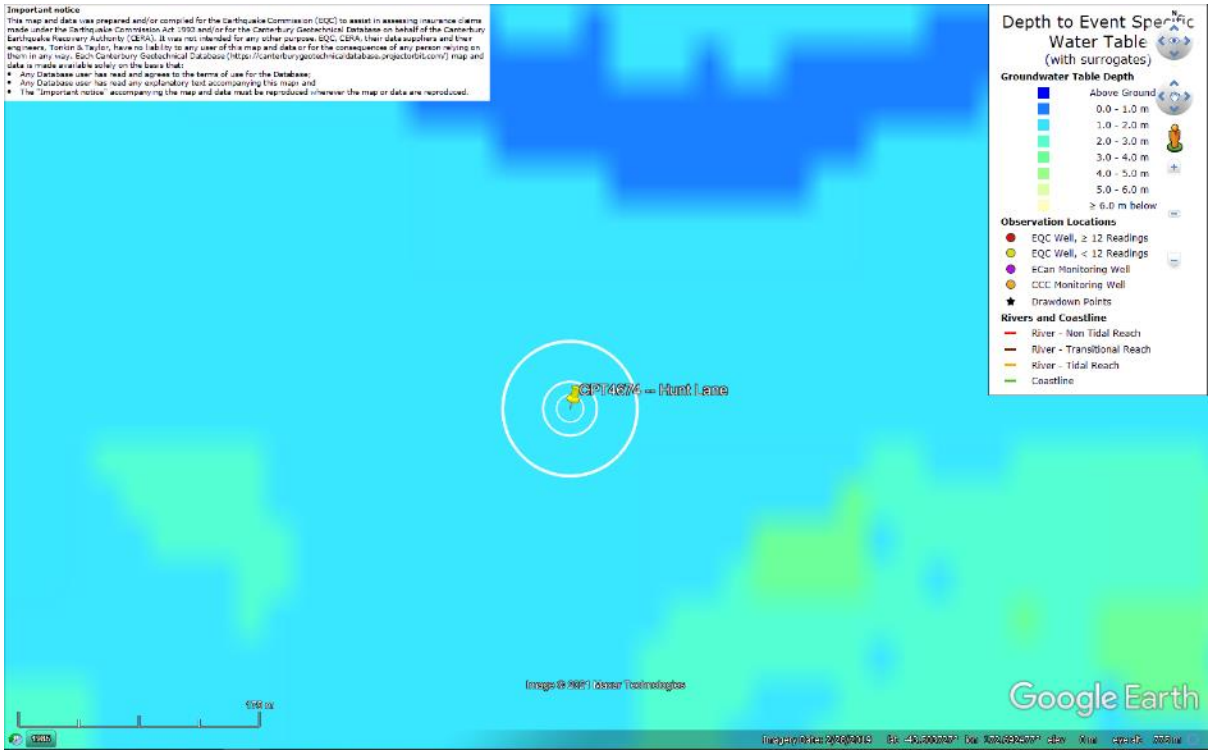

Figure 109: Depth to groundwater table for Dec-11 EQ.

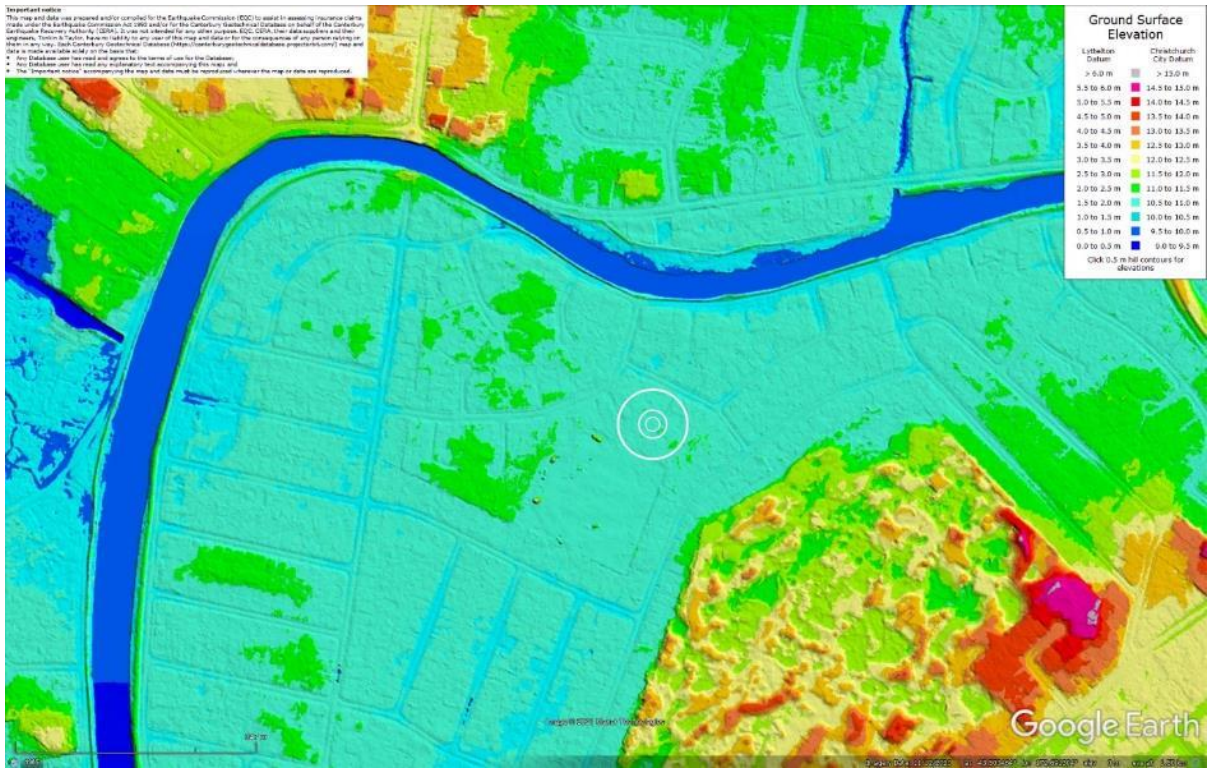

Figure 110: Ground surface elevation according to the Sep-11 LiDAR survey.

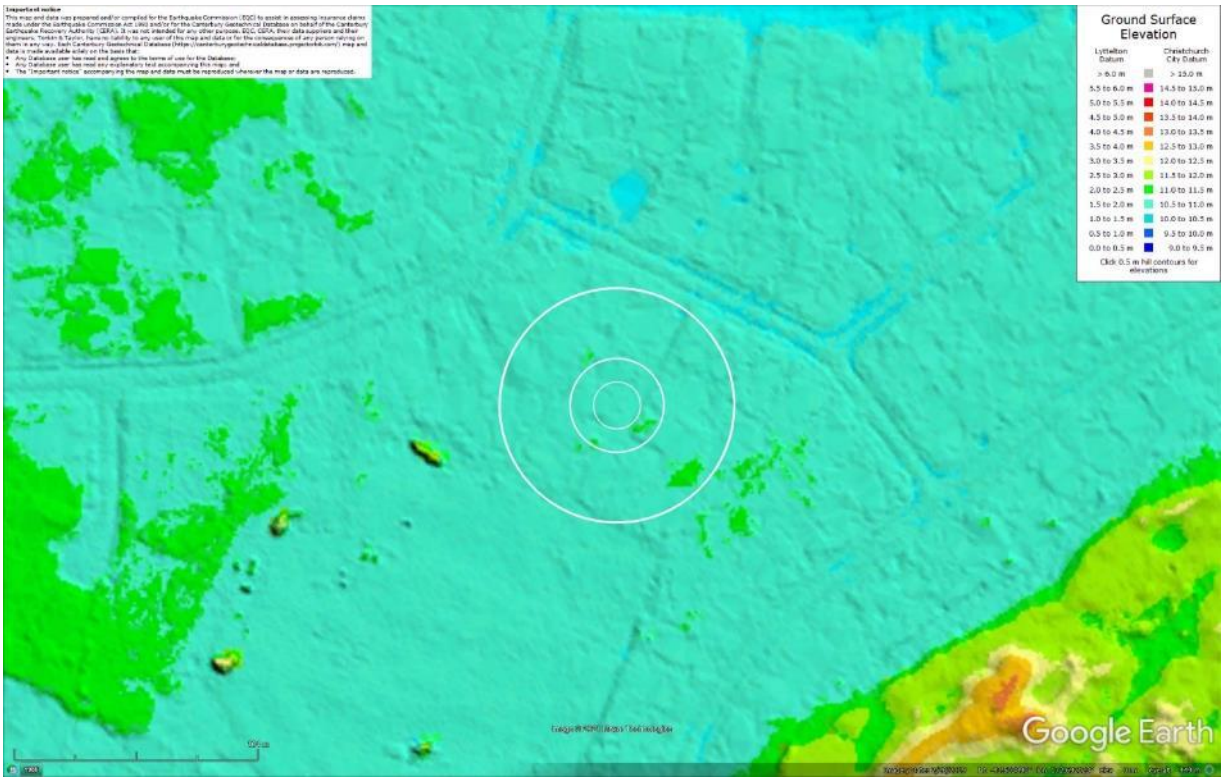

Figure 111: Ground surface elevation according to the Sep-11 LiDAR survey (enlarged).

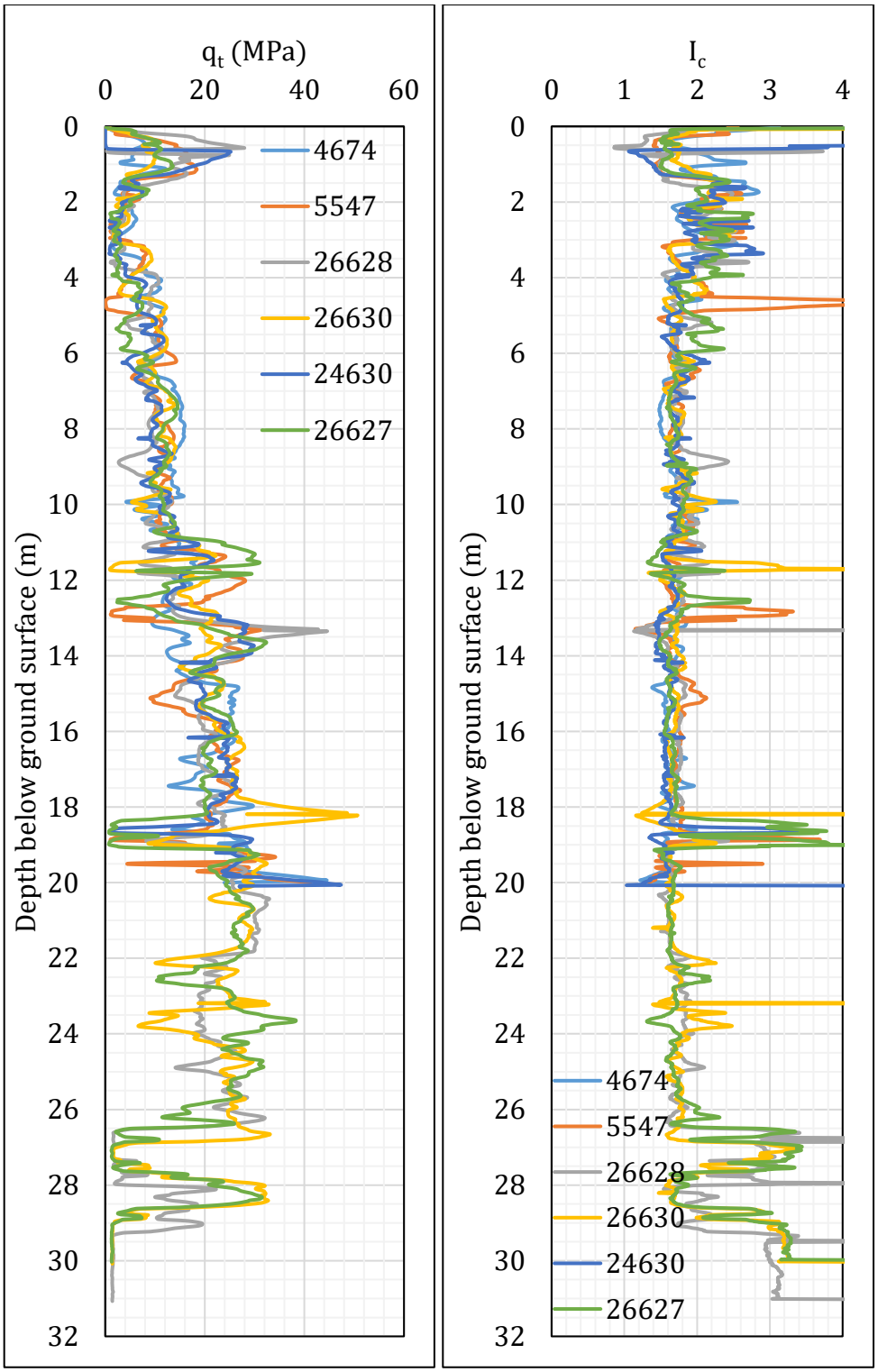

Figure 112: q_t and I_c profiles.

Note 7: The selection of CPTs for the area considered for settlement assessment (Figure 1) is based on the proximity of the CPTs to the considered areas. In accordance with that, the following table shows CPTs that were used for the volumetric settlement analysis in *Cliq v.3.0.3.2*, a CPT soil liquefaction software developed by GeoLogismiki. (The average volumetric settlements were reported in Table 8.)

Table 12: CPT profiles used in volumetric settlement analysis for areas selected for settlement assessment.

CPT ID No.	Patch A	Patch B	Road
4674	✓		✓
5547		✓	✓
26628			✓
26630			✓
24630			✓
26627			✓

Table 13: CPT-based results for the upper 20 m of the soil profile.

		CPT ID					
EQ Event	Parameter	4674	5547	26628	26630	24630	26627
Sep-10	S_{V1D} (mm)	8	9	16	6	13	14
	LSN	1	2	3	1	3	3
	LPI	0	0	0	0	0	0
	LPI_{ish}	0	0	0	0	0	0
	$D_{FS<1}$ (m)	undet.	undet.	8.79	undet.	undet.	undet.
Feb-11	S_{V1D} (mm)	105	74	121	73	140	114
	LSN	22	18	23	17	28	24
	LPI	6	6	10	5	12	10
	LPI_{ish}	4	5	5	3	8	6
	$D_{FS<1}$ (m)	1.90	2.17	2.36	2.01	2.08	2.44
Jun-11	S_{V1D} (mm)	46	43	68	37	78	70
	LSN	12	11	14	10	18	16
	LPI	2	2	3	2	4	4
	LPI_{ish}	1	1	1	0	0	0
	$D_{FS<1}$ (m)	2.04	2.26	2.57	2.67	2.69	2.46
Dec-11	S_{V1D} (mm)	68	55	90	51	104	90
	LSN	16	14	18	13	23	20
	LPI	3	4	6	3	7	6
	LPI_{ish}	1	2	3	1	3	3
	$D_{FS<1}$ (m)	2.00	2.24	2.42	2.04	2.13	2.44

Notes: $D_{FS<1}$ = Depth to the first liquefiable layer ($FS_L<1$) that is at least 200-mm thick, as determined by the Boulanger and Idriss (2016) liquefaction-triggering procedure (P_L=50%, C_{FC}=0.13, and $I_{c,cutoff}$ =2.6), and exported from *Cliq v.3.0.3.2*; undet. = the specified soil layer was not detected.

Note 8: Based on the borehole log (BH 13695, Figure 1), the groundwater table is at a depth of 3.0 m below the ground surface. The soil profile consists of (1) asphalt and gravelly fill to a depth of 0.4 m, (2) fine to medium sand, SP, the Yaldhurst member of the Springston formation to a depth of 1.5 m, (3) silt, ML, the Yaldhurst member of the Springston formation to a depth of 4.0 m, and (4) fine to medium sand, SP, of the Christchurch formation to a depth of 20 m.

Note 9: The ejecta-induced free-field settlement provided in Table 11 is an areal average settlement due to ejecta, which is based on the total settlement assessment area, A_T (provided in Table 9 and repeated in Table 14). However, the considered area was not always covered completely with ejecta; thus, it is important to provide the localized ejecta-induced settlement, too. The localized settlement due to ejecta is estimated using photographic evidence only as

$$S_{E,P\_localized} = \frac{V_E}{A_E}$$

where V_E is the total volume of ejecta within A_T and A_E is the total coverage area of ejecta within A_T. Please note that the areal ejecta-induced settlement provided in Table 14 as S_{E,P_areal} is the same as $S_{E,P}$ in Table 11, which was estimated as

$$S_{E,P\_areal} = S_{E,P} = \frac{V_E}{A_T}$$

where V_E is the total volume of ejecta within A_T and A_T is the total settlement assessment area.

Table 14a: Areal and localized ejecta-induced settlement estimates for Patch A (10-, 20-, and 50-m buffers) based on photographic evidence.

Earthquake Event	A_T (m^2)	A_E (m^2)	V_E (m^3)	S_{E,P_areal} (mm)	$S_{E,P\_localized}$ (mm)
Sep-10	18.5	0	0	0	0
Feb-11	18.5	10.7	1.7-2.6	115±25	200±40
Jun-11	18.5	NA	NA	NA	NA
Dec-11	18.5	4.3	0.04-0.1	5±5	20±10

Notes: $S_{E,P\_areal} = S_{E,P}$ reported in Table 11 = areal ejecta-induced settlement; $S_{E,P\_localized}$ = localized ejecta-induced settlement; A_T = total settlement assessment area; V_E = total volume of ejecta within A_T; A_E = total area of ejecta within A_T; The estimates of both areal and localized ejecta-induced settlement are rounded to the nearest 5; Final plus/minus values are also rounded to the nearest 5; NA = Not available.

Table 14b: Areal and localized ejecta-induced settlement estimates for Patch B (20-m and 50-m buffers) based on photographic evidence.

Earthquake Event	A_T (m^2)	A_E (m^2)	V_E (m^3)	S_{E,P_areal} (mm)	$S_{E,P\_localized}$ (mm)
Sep-10	69.4	0	0	0	0
Feb-11	69.4	32.5	1.3-2.0	25±5	50±10
Jun-11	69.4	22.7	0.2-0.5	5±5	15±5
Dec-11	69.4	5.2	0.05-0.2	<5	20±10

Notes: S_{E,P_areal} = $S_{E,P}$ reported in Table 11 = areal ejecta-induced settlement; $S_{E,P\_localized}$ = localized ejecta-induced settlement; A_T = total settlement assessment area; V_E = total volume of ejecta within A_T; A_E = total area of ejecta within A_T; The estimates of both areal and localized ejecta-induced settlement are rounded to the nearest 5; Final plus/minus values are also rounded to the nearest 5.

Table 14c: Areal and localized ejecta-induced settlement estimates for Road (50-m buffer) based on photographic evidence.

Earthquake Event	A_T (m^2)	A_E (m^2)	V_E (m^3)	S_{E,P_areal} (mm)	$S_{E,P\_localized}$ (mm)
Sep-10	410	0	0	0	0
Feb-11	401	401	13.2-22.3	45±10	45±10
Jun-11	410	410	2.3-4.7	10±5	10±5
Dec-11	421	58.4	1.2-2.4	5±5	30±10

Notes: S_{E,P_areal} = $S_{E,P}$ reported in Table 11 = areal ejecta-induced settlement; $S_{E,P\_localized}$ = localized ejecta-induced settlement; A_T = total settlement assessment area; V_E = total volume of ejecta within A_T; A_E = total area of ejecta within A_T; The estimates of both areal and localized ejecta-induced settlement are rounded to the nearest 5; Final plus/minus values are also rounded to the nearest 5.

Summary 2:

- **The best estimate of the localized ejecta-induced free-field ground settlement at the Hunt Ln site for the SEP 2010, FEB 2011, JUN 2011, and DEC 2011 earthquake is 0 mm, 200±40 mm, 15±5 mm, and 20±10 mm, respectively.**
- **The best estimate of the localized ejecta-induced settlement of the road at the Hunt Ln site for the SEP 2010, FEB 2011, JUN 2011, and DEC 2011 earthquake is 0 mm, 45±10 mm, 10±5 mm, and 30±10 mm, respectively.**